Species Differences in the Metabolism and Toxicity of 4-Ipomeanol

Oliver Thomas Parkinson

A dissertation

submitted in partial fulfillment of the

requirements for the degree of

Doctor of Philosophy

University of Washington
2012

Reading Committee:

Allan E. Rettie, Chair

Edward J. Kelly

Kent L. Kunze

Program Authorized to Offer Degree:

Pharmacy – Medicinal Chemistry

University of Washington

Abstract

Species Differences in the Metabolism and Toxicity of 4-Ipomeanol

Oliver Thomas Parkinson

Chair of the Supervisory Committee:
Professor Allan E. Rettie
Department of Medicinal Chemistry

The studies presented in this dissertation investigate the enzymatic basis for the species differences in target organ toxicity of the pro-toxin, 4-ipomeanol (IPO). In vitro studies that monitored the production of a pyrrole-based IPO adduct formed from the reactive ene-dial reactive intermediate, establish a dominant role for CYP4B1 in the *in vitro* bioactivation of IPO in lung and kidney tissues from toxicity-susceptible animal species. Antibodies against CYP4B1 and HET0016, a CYP4-specific chemical inhibitor, eliminated IPO adduct formation in lung microsomes from mice, dogs, rats and rabbits, and in kidney from male mice, indicating that IPO activation in these tissues is catalyzed predominantly, if not exclusively, by CYP4B1. Furthermore, despite the fact that IPO toxicosis is agriculturally relevant due to the relatively frequent occurrence of cattle poisoning, these studies are the first to identify a CYP4B1 ortholog in cow lung and establish a role for this enzyme in IPO-mediated pneumotoxicity in cattle. We also detail the characterization of a *Cyp4b1* null mouse strain and demonstrate that disruption of CYP4B1 expression is protective against IPO poisoning *in vivo* in mice, thereby definitively establishing CYP4B1

as the enzyme responsible for bioactivating IPO. We have shown further that IPO is glucuronidated readily in liver microsomes from all species examined, with the exception of humans. An IPO-glucuronide conjugate was also detected in the urine of IPO-treated mice, the first evidence for UGT-mediated phase II metabolism of IPO beyond that reported for the rat. Cell-based studies with the Ser207 variant of human CYP4B1 demonstrate further that human *CYP4B1* in all of its known splice variant forms does not encode a functional protein. Attempts to identify the causative IPO bioactivating enzyme in human liver implicated human CYP1A2, in part, but several other recombinant P450 forms were also capable of catalyzing this reaction. The lack of evidence from *in vitro* studies for a dominant role for human CYP1A2 in the human hepatotoxicity of IPO was complemented by *in vivo* experiments conducted with transgenic mice that expressed human CYP1A enzymes on a null murine CYP1A2 background. Therefore, the lack of pulmonary toxicity and the prevalent hepatotoxicity observed in humans exposed to IPO is not due to increased rates of IPO activation in human liver or by human liver CYP1A2, but more likely to decreased rates of IPO activation in lung, possibly coupled to a lack of UGT-mediated phase II metabolism of IPO in human liver.

Table of Contents

LIST OF ABBREVIATIONS

3MC	3-methylcholanthrene
3MI	3-methylindole
3MEI	2,3-epoxy-3-methylindoline
AhR	aryl hydrocarbon receptor
AFB1	aflatoxin b1
ALT	alanine aminotransferase
ALP	alkaline phosphatase
AST	aspartate aminotransferase
BUN	blood urea nitrogen
DMSO	dimethyl sulfoxide
EDTA	ethylenediaminetetraacetic acid
ESI	electrospray ionization
GGT	gamma-glutamyl transpeptidase
GST	glutathione *S*-transferase
IACUC	institutional animal care and use committee
IPO	4-ipomeanol
LC/MS	liquid chromatography/mass spectrometry
NAC	*N*-acetyl cysteine
NADPH	nicotinamide adenine dinucleotide phosphate
NAL	*N*-acetyl lysine
PCR	polymerase chain reaction
PK	perilla ketone
SDS PAGE	sodium dodecyl sulfate polyacrylamide gel electrophoresis
UGT	UDP glucuronosyltransferase
UDPGA	uridine 5-diphospho-glucuronic acid

List of Figures

List of Tables

Acknowledgements

The author wishes to express his sincere appreciation to those individuals who help make this possible:

To Dr. Allan Rettie for his good humor and patience and for his excellent insight and guidance throughout this project;

To Dr. Ed Kelly for developing the Cyp4b1 knockout nice, for his company during the in vivo studies and for serving on the reading and supervisory committees;

To Dr. Kent Kunze for his insight and enthusiasm and for serving on the reading and supervisory committees;

To Drs. Sid Nelson, Dave Eaton and Ken Thummel for serving on the supervisory committee;

To Kayte Edson for her synthetic skills, but more importantly for her company and friendship and for brightening the lab every day;

To Dr. Erin Peck, Dale Whittington and Dr. Denny Liggitt for their assistance and input which was integral to the completion of this project;

To Meg Running, Jeanine Kanov, Lois Haupt and Caryl Lynch for making the department a friendly and welcoming place;

To fellow students and lab-mates Dr. Clara Hsia, Dr. Matt McDonald, Nick Au, Amanda Johnson, Dr. Mariko Nakano, Caleb Woods, Dr. Jed Lampe, Dr. Shawna Hengel, Dr. Brooke Vandenbrink and Dr. Brendan Stamper for your help and friendship;

To Stephanie, Aimee, Diana, Betsy, Cory, Kelly and Boss for their love and support. They helped make the hours both inside and outside of work far more enjoyable;

Finally, to my parents Andrew and Kay for their love and encouragement and for setting such a superb example.

Dedication

To Bandit

Chapter 1

Introduction

1.1 Metabolic Bioactivation

Bioactivation refers to the process of converting essentially inert chemical compounds into biologically active species. This is a widely exploited phenomenon in drug development, as evidenced by the multitude of pro-drugs that have been developed and marketed to become important therapeutics. Pro-drugs are pharmacologically inactive compounds that require activation, usually involving metabolism, to generate the active drug. For example, the commonly prescribed analgesic, codeine, is a low affinity μ-opiod receptor agonist. Codeine has ~200-fold lower affinity for its biological target than morphine (1). However, up to 20% of the administered dose of codeine is *O*-dealkylated to morphine by CYP2D6 (2) in the liver (Figure 1). Therefore, the majority of the analgesic effect of codeine is due to P450-dependent bioactivation to a much more pharmacologically active metabolite (3).

Genetic polymorphisms often cause differential responses to P450-activated pro-drugs. Roughly 20% of Caucasians have one of several polymorphisms in the CYP2D6 gene that result in inactive enzyme (4). In this subset of poor metabolizers (PM), codeine will be a far less effective analgesic than in extensive metabolizers (EM) (5). Furthermore, up to 5% of Caucasians have a CYP2D6 gene duplication that results in ultra-rapid CYP2D6 metabolism. Ultra-rapid metabolizers (UMs) produce roughly 50% more morphine from

codeine than EMs (6). The pharmacological effects of pro-drugs (and pro-toxins) are influenced by inter-individual (and also inter-species) differences in the rates of bioactivation.

Unlike the activation of pro-drugs, which results in the intended pharmacological activity of the drug, activation of pro-toxins results in deleterious effects. Pro-toxins are compounds that are not inherently cytotoxic, but undergo metabolic activation to a reactive metabolite that can directly cause cellular damage. Similar to the bioactivation of pro-drugs, this activation step often involves P450-mediated oxidation of the pro-toxin, but in this case an electrophilic metabolite is often produced that can adduct to cellular nucleophiles. The extent to which pro-toxins cause toxicity generally reflects the balance between bioactivation to reactive metabolites, (non-activating) metabolism of the parent compound and/or reactive metabolite that leads to elimination and cellular repair mechanisms. Differences among species in their susceptibility to various pro-toxins can be due to differences in any of these processes, with those involving metabolic bioactivation and elimination being best understood. Several examples of species differences in metabolism-dependent toxicity are discussed below.

1.2 Aflatoxin B1: A Liver Toxicant

Aflatoxin B1 (AFB1) toxicity was first reported in 1960 when over 100,000 turkeys and other poultry in Great Britain suffered from a lethal hepatotoxicity that was originally dubbed Turkey X Disease. All affected animals were eventually found to have been fed

contaminated peanut feed (7, 8). The toxic species was later found to be a mycotoxin produced by *Aspergillus flavus* that infects a wide variety of nuts and grains both pre- and post-harvest (9, 10).

AFB1 is a heterocyclic pro-toxin that is activated by P450-mediated epoxidation (11). AFB1 epoxide can directly adduct to DNA (12), or be hydrolyzed to the dihydrodiol which has been shown to adduct cellular proteins (13). Apart from the hepatotoxicity prominent in avian exposure to AFB1, AFB1 is highly carcinogenic. Binding of the 8,9-*exo*-epoxide to DNA leads to N7-guanine adducts which undergo rapid ring opening to form the formamidopyridine moiety that is resistant to cellular DNA repair mechanisms (14). Indeed, AFB1 is one of the most potent carcinogenic substances, causing hepatic tumors in rats at levels as low as 15 parts per billion (ppb) in the diet (15).

Interestingly, AFB1 is non-carcinogenic in mice at levels as high as 100,000 ppb (16). The lack of tumor development in mice is not due to lack of activation since mice activate AFB1 to the 8,9-*exo*-epoxide at slightly higher rates than rats (17). Mice constitutively express a hepatic α-class GST enzyme (mGSTA3-3) that is adept (k_{cat} $2x10^3$ $M^{-1}s^{01}$) at catalyzing the conjugation of glutathione to the *exo*-epoxide of AFB1 (Figure 1.2). This conjugation leads to deactivation and metabolic elimination of the ultimate toxin of AFB1 (18-21). Rats lack constitutive hepatic expression of the orthologous AFB1 epoxide detoxifying GST enzyme (21), so the species difference in hepatic tumor formation between rats and mice exposed to AFB1 is based upon murine expression of a relatively specific Phase II detoxifying enzyme.

1.3 Respiratory and Pulmonary Pro-toxins

1.3.1 3-Methylindole

3-Methylindole (3MI) is a breakdown product of tryptophan metabolism and a constituent of cigarette smoke. 3MI is a known pulmonary pro-toxin in mice and cattle that causes necrosis in the terminal bronchioles which are lined with Clara cells, the primary pulmonary site of P450 expression and P450-mediated oxidation (22). Toxicity of 3MI is mediated by P450 catalyzed dehydrogenation to 3-methyleneidolinenine and oxidation to 2,3-epoxy-3-methylindoline (Figure 1.3) (23). Pulmonary toxicity in mice seems to be linked to activation of 3MI by CYP2F2 (24).

3MI is a purported pulmonary toxin and possible mutagen in humans based on the observations that 3MI forms covalent adducts in human pulmonary microsomes (25, 26) and causes cytotoxicity in bronchial epithelial cells *ex vivo (27)*. However, expression of CYP2F1 (the human ortholog of murine CYP2F2) resulted in an inactive protein that did not bind heme, suggesting that humans may be immune to toxicity from pro-toxins that are activated by this enzyme (28).

1.3.2 Naphthalene

Naphthalene is an environmental toxin that, like 3MI, is found in cigarette smoke, as well as exhaust fumes. It is extensively used in the production of PVC and as an insect repellant (mothballs). Inhalation of naphthalene leads to bronchial tumors in mice (29), but olfactory tumors in rats (30). Naphthalene is activated to an arene oxide *via* P450 mediated metabolism by CYP2F enzymes (Figure 1.4). The species difference in response to respiratory naphthalene exposure is likely due to differential expression of CYP2F enzymes in that CYP2F2 is highly expressed in murine lung, but expressed at low levels in olfactory epithelia. However, in rats, CYP2F4 is highly expressed in olfactory epithelia and poorly expressed in lung (31). Similar to 3MI, humans may not be susceptible to pulmonary toxicity of naphthalene if toxicity is mediated by CYP2F catalyzed activation.

1.3.3 Furan

Furan is a heterocyclic aromatic pro-toxin widely used in production of drugs, insecticides and industrial chemicals. Due to its high volatility and low boiling point (31^{o}C), the primary route of large-scale human exposure to furan has historically been occupational exposure via inhalation (32, 33). However, since 1991 the EPA has required that all industrial use of furan occur in closed systems to minimize exposure risk. Recently, the FDA has begun to assess human exposure to furan in food and found that in certain heat-processed canned foods, furan is present up to 125 ppb (34, 35) although these levels are not thought to be hazardous.

Furan has been shown to be carcinogenic in test species causing both hepatocellular adenoma and hepatocellular carcinoma in rats and mice as well as mononuclear cell leukemia and cholangiocarcinoma in rats (33, 36). While there is no direct evidence that furan is carcinogenic in humans, based on evidence in other species, the NIH currently characterizes furan as "reasonably anticipated to be a human carcinogen" (32).

Activation of furan in mammals occurs *via* P450-mediated epoxidation followed by ring-opening to form the reactive cis-2-butene 1,4 dial (37) (Figure 1.5). Epoxides are susceptible to nucleophilic attack and may be reasonably assumed to be ultimate toxins, however, Chen et al. were able to verify NADPH-dependent production of the dial by trapping with semicarbazide to form the cis-2-butene semicarbazone. This reactive dialdehyde is the ultimate toxin that is susceptible to reaction with cellular nucleophiles such as glutathione, amino acids and DNA (38-42) and is known to be mutagenic in the Ames assay (43).

1.3.4 Ipomeanol

Spoiled sweet potatoes have been known for nearly 80 years to be toxic to livestock (44, 45). Sweet potatoes (*Ipomoea batatas*) produce the furanosesquiterpenes, ipomeamarone and ipomeamarol, following fungal infection by *F. solani* and *C. fimbriata*, but also in response to larval infection or challenge with toxic chemicals (Figure 1.6). Following multiple instances of cattle in Japan experiencing toxicity resulting from consumption of mold-infested sweet potatoes, an extensive analysis of extracts from

spoiled sweet potatoes resulted in the isolation and identification of ipomeamarone, the first phytoalexin (an anti-pathogen compound synthesized by plants) (46, 47). Both ipomeamarone and ipomeamarol cause hepatotoxicity, in contrast to the pulmonary toxicity and edema prevalent in cattle after ingestion of moldy sweet potatoes. Cattle that ingest infected sweet potatoes can develop interstitial pneumonia that is characterized by pulmonary edema and emphysema. Moldy sweet potatoes have been linked to the death of livestock in cases spanning the last century from the 1920s (44), 1950s (48), to recent cases (2011) in Wisconsin where 200 steer died (49) and England, where six cows died in what is believed to be the first case of sweet potato induced pulmonary toxicity in the UK (50).

4-Ipomeanol (IPO; 1-(3-Furyl)-4-hydroxy-1-pentanone) is the most widely studied furanoterpenoid pro-toxin. IPO is found specifically in extracts of sweet potatoes that have been infected by the molds of the *Fusarium* genus (51, 52) (Figure 1.6). Whereas ipomeamarone is produced by sweet potatoes in response to various fungal infections or chemical challenge by $HgCl_2$ (53), IPO is only found in extracts from sweet potatoes infected with *F. solani, F. oxysporum* or *F.javanicum (51-53)*. Furthermore, Burka et al. demonstrated that *F. solani*, but not *C. fimbriata*, could produce IPO following incubation with purified ipomeamarone (53). These data suggest that IPO is a product of ipomeamarone metabolism within *Fusarium* molds.

Originally termed lung oedema factor, IPO was shown to be the agent responsible for pulmonary toxicity when purified IPO given intra-peritoneally (IP) caused pulmonary

edema and pleural effusion in mice similar to the toxicity observed in mice treated with infected sweet potato extracts (51). IPO is an order of magnitude more toxic in mice - LD_{50} of 20 mg/kg-, than the hepatotoxic ipomeamarone - LD_{50} of 200 mg/kg (54). IPO is lethal to cattle in doses as low as 7.5 mg/kg which can be achieved by ingesting as little as 6 kg of spoiled sweet potatoes (55).

Pulmonary toxicity of IPO is localized to the Clara cells of the terminal bronchioles. *Ex vivo* studies comparing IPO activation as a measure of covalent binding of radiolabeled IPO in Clara cells and alveolar type II cells isolated from rabbit lung showed that binding occurred at a ~10 fold higher rate (135 pmol/10^6 cells/min versus 13 pmol/10^6 cells/min) in Clara cells (56). In addition, binding of labeled IPO to rabbit pulmonary microsomal protein was inhibited by 50% with antibodies to rabbit pulmonary P450 enzymes, and up to 90% by antibodies against cytochrome P450 reductase (57). These data suggest that activation of IPO occurs following P450-mediated oxidation, according to the scheme proposed in Figure 1.7 (58).

Further evidence to support lung P450-mediated activation of IPO is seen in the IPO-induced toxicity towards avian species. Birds lack terminal bronchioles as they they have a continuous airway and, therefore, lack the Clara cells that provide a concentrated site of pulmonary P450 expression in most mammals (59). When treated with IPO, birds suffer from hepatotoxicity, with no adverse effects evident in the lung (60), and lethal doses are up to 5 fold higher in birds than in other animal species.

The specific and pronounced pulmonary toxicity observed in all land species exposed to IPO resulted in the National Cancer Institute (NCI) initiating studies with IPO as a potential anti-lung cancer agent in humans. In accordance with the a morphological similarity to Clara cells, IPO was shown to be toxic to human non-small cell cancer cells (NSCLC) lines and xenografts (61, 62). which lead to a Phase I studies of IPO in patients with NSCLC (63, 64). According to the NCI:

> "4-Ipomeanol (IPO) is the first agent to undergo preclinical development at the National Cancer Institute (NCI) based principally on a specific biochemical-biological rationale for clinical investigation as an antineoplastic agent targeted against lung cancer (65)."

Somewhat surprisingly, not only did IPO show no significant anti-tumor activity, patients experienced no adverse effects in the lung, but were subject to dose-limiting hepatotoxicity - albeit at doses roughly ~20 fold higher than the equivalent lethal animal doses. The specificity of liver damage in humans treated with IPO lead to a Phase II study for treatment of patients with hepatocellular carcinoma. Once again, IPO was inactive as an anti-tumor agent and patients experienced dose-limiting liver toxicity (66). Interestingly, mice treated with IPO and polycyclic aromatic hydrocarbons, which characteristically induce the CYP1A family of P450s, develop liver toxicity (67, 68). Additionally, there are several indications that human CYP1A2 is an highly effective enzyme for bioactivating IPO (58, 69).

Whereas the lack of lung toxicity in birds (and possibly resultant hepatotoxicity) might have been predicted based on the anatomical differences between avian and mammalian lung, the architecture of the terminal bronchioles in humans is similar to

rodents and includes Clara cells with high levels of P450 expression (70). What then accounts for the species difference in IPO-induced pulmonary toxicity in common experimental animals and humans?

In both rabbits and rats, activation of IPO occurs *via* oxidation that has been shown to be mediated readily by pulmonary cytochrome P450 4B1 (CYP4B1) (71). Furthermore, there is indirect evidence for a role of CYP4B1 in the activation of IPO in mice. IPO causes pulmonary toxicity in female mice, whereas, it causes pulmonary and renal toxicity in male mice (67, 72). Whereas, CYP4B1 is highly expressed in the lung of both male and female mice, *Cyp4b1* gene expression in mouse kidney is androgen regulated, which leads to high expression in male kidney, but not female kidney (73, 74). Toxicity of IPO in the mouse occurs only in tissues with high levels of *Cyp4b1* gene expression, suggesting that IPO activation is catalyzed by CYP4B1. Indeed, the lung toxicity observed in most experimental animals species may be adequately accounted for by high pulmonary CYP4B1 expression.

While a lack of CYP4B1 expression in female mouse kidney may plausibly account for the gender difference in IPO-mediated renal toxicity in mice, the pattern of CYP4B1 expression is otherwise similar between humans and other mammalian species. In humans (as well as most preclinical test species) *CYP4B1* mRNA is highly expressed in the lung. Therefore, the species differences in target organ toxicity IPO between animals and humans is not due to a differential tissue distribution of CYP4B1.

The lack of pulmonary toxicity observed in humans treated with IPO as well as the lack of IPO activation in human pulmonary microsomes may be due to a 'variant' *CYP4B1* that encodes a serine in the meander region at amino acid 427 that interferes with heme incorporation (75). This amino acid is an evolutionarily conserved proline in a host of other species (Figure 1.8). Furthermore, this meander proline is conserved in all other human P450 enzymes (Figure 1.9). Introducing a P427S mutation into rabbit *CYP4B1* interferes with heme incorporation, and reverting the meander serine to the conserved proline in human CYP4B1 yields a functional enzyme that incorporates heme (Figure 1.10) (75, 76). This could explain why attempts to express human CYP4B1 in a recombinant system have yielded inactive enzyme lacking heme. Therefore, the species difference between test species and humans in response to IPO is likely due, at least in part, to human CYP4B1 being catalytically inactive despite high expression at the message level.

Inactive CYP4B1 does not result from polymorphisms in humans; wild-type CYP4B1 appears to be inactive. There are several theories that might explain a lack of functional CYP4B1 in humans. Firstly, unique among animals, humans utilize fire for warmth and to cook food. This means that throughout history we have been exposed to potential pulmonary toxins through regular inhalation of smoke as well as toxic species that potentially arise within food as a result of the cooking process. The exposure to fire-related toxic species is unique to humans, even compared to animals with similar territories and diets. If smoke or charred food contained a pro-toxic species activated by CYP4B1, this would select for individuals with inactive CYP4B1. It is also possible that at some point humans were forced to rely on a food source that contained dangerous levels of a CYP4B1-

activated pro-toxin (like Fusarium infected sweet potatoes). Either of these hypothetical scenarios might account for inactive CYP4B1 by selecting CYP4B1 deficient individuals as our founder population.

Finally, IPO is known to undergo glucuronidation in the rat. Up to 50% of the dose administered can be recovered in rat urine as a glucuronide conjugate (77). Unfortunately, it is not known if glucuronidation of IPO occurs in other test species or in humans, so the impact on the species differences observed with regard to the sites of toxicity is due to differences in glucuronidation/elimination rates.

1.4 Scope of project work

Given the questions raised above about species differences in target organ toxicity of IPO, the goals of this thesis were set to first determine which enzyme(s) is/are responsible for catalyzing IPO activation *in vitro* in various experimental animal species (Chapter 2) and *in vivo* in the mouse (Chapter 3). Secondly, I will probe the basis for the unexpected lack of pulmonary toxicity in humans and prevalence of hepatic toxicity observed in clinical trials with IPO by assessing bioactivation and phase II metabolism in human tissue microsomes, recombinant enzymes and CYP1A humanized mice (Chapters 2, 4 and 5).

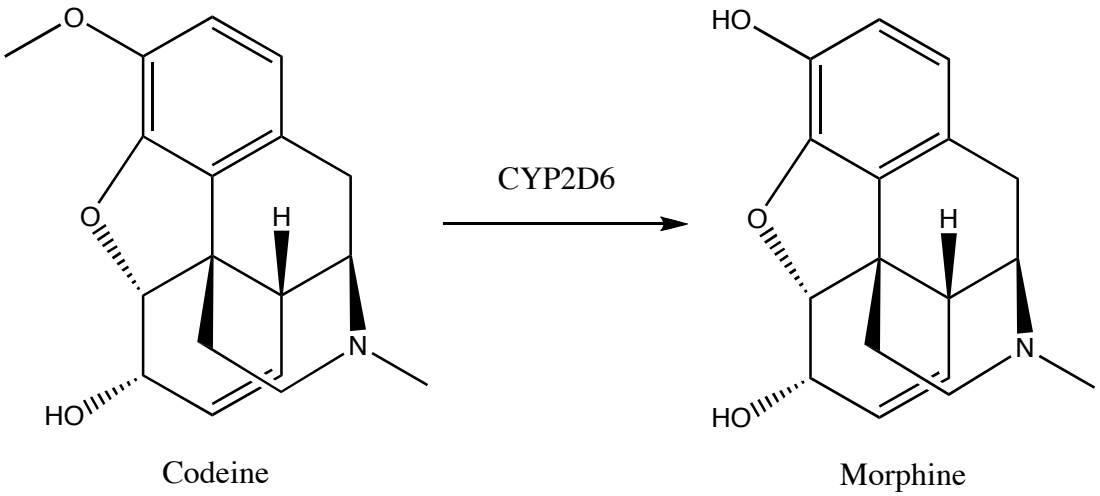

Codeine Morphine

Figure 1.1: Codeine is *O*-demethylated by CYP2D6 in human liver to morphine, a ~200-fold more potent μ-opiod receptor ligand. Much of the analgesic effect of codeine is due to bioactivation of the parent drug to morphine.

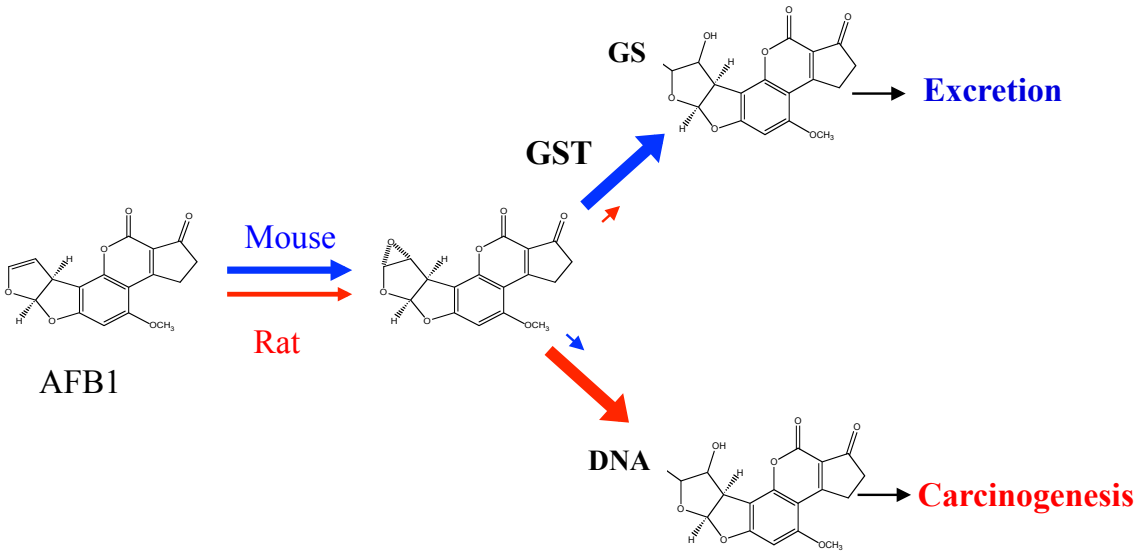

Figure 1.2: Metabolic scheme for activation of aflatoxin B1 (AFB1) in rats and mice. AFB1 is extensively activated to the 8,9-*exo*-epoxide in both rats and mice. This activation leads to carcinogenesis only in rats because mice readily deactivated the activated species via GST-mediated glutathione conjugation to the epoxide.

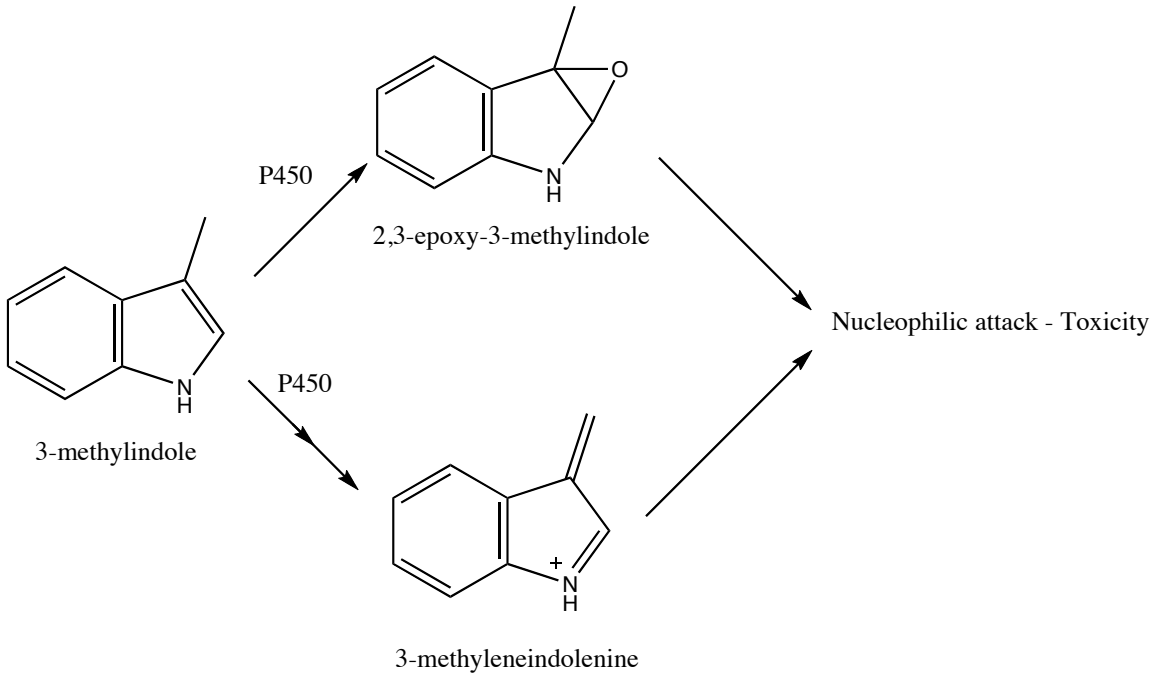

Figure 1.3: Metabolic scheme for activation of 3-methylindole *via* P450-mediated oxidation. Both 3-methyleneindolenine and 2,3-epoxy-3-methylindol can react with cellular nucleophiles including glutathione as well as covalently binding cellular proteins leading to toxicity (adapted from *Zhou et al. 2012*).

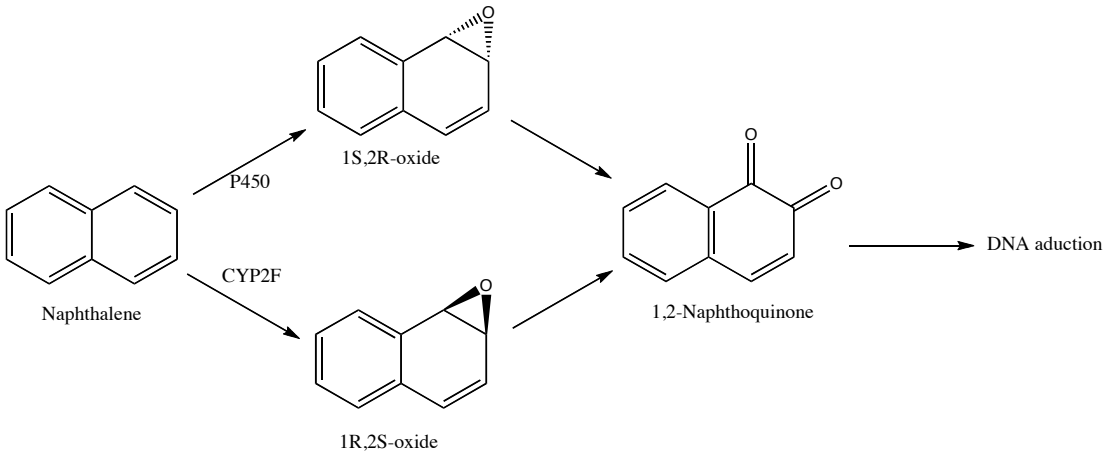

Figure 1.4: Naphthalene is oxidized by P450 to arene oxides. CYP2F enzymes selectively produces the 1R,2S-oxide that can undergo further metabolism to the mutagenic 1,2-napthoquinone which can directly adduct to DNA leading to carcinogenesis.

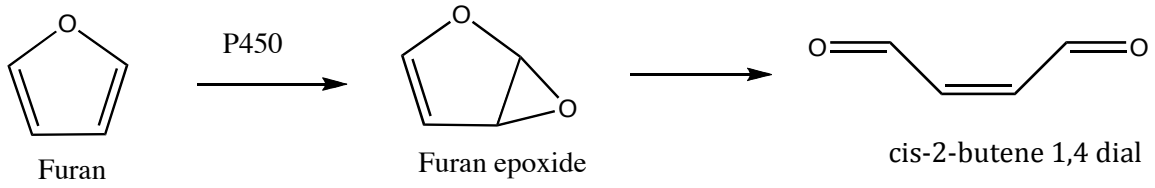

Figure 1.5: Putative scheme for the metabolic activation of furan. Furan is activated to an epoxide via P450-mediated oxidation. The epoxide ring opens to the reactive and toxic cis-2-butene 1,4 dial that can adduct to cellular nucleophiles like DNA leading to carcinogenesis (adapted from *Chen et al. 1995*).

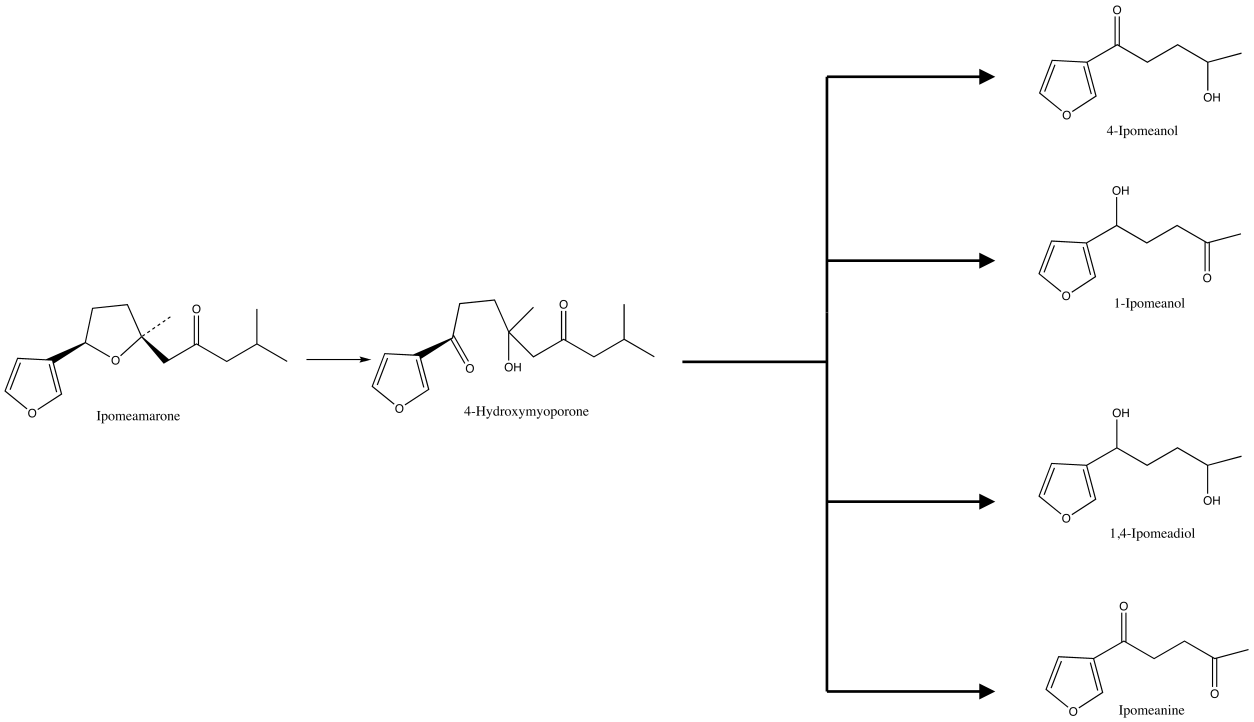

Figure 1.6: Biosynthesis of pulmonary toxic 3-furyl ketones and 3-furyl diol by *Fusarium* molds from the phytoalexin ipomeamarone. Infection or chemical damage results in production of ipomeamarone by sweet potatoes. Several different mold species produce 4-hydroxymyoporone however only *Fusarium* molds produce IPO and its structural analogs. Adapted from *Schneider et al. 1984.*

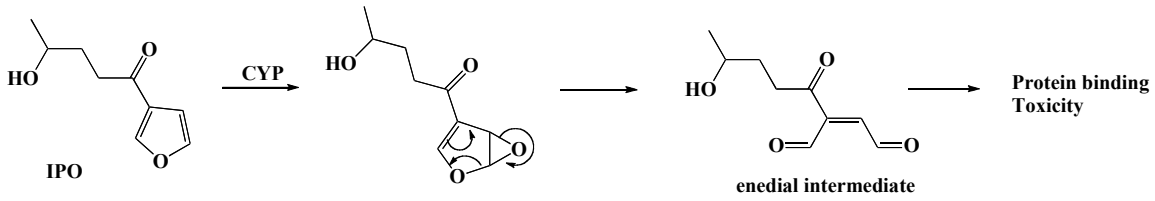

Figure 1.7: Putative mechanism of IPO toxicity. IPO is activated via P450-mediated oxidation of the furan ring to an epoxide, which undergoes sigmatropic rearrangement and ring-opening to the reactive enedial. The enedial intermediate can directly adduct cellular nucleophiles leading to cytotoxicity (*adapted from Baer et al. 2004*).

	Meander region
Rat CYP4B1	**P E V F D ^{427}P L R F**
Mouse CYP4B1	**P E V F D ^{427}P L R F**
Goat CYP4B2	**P E V F D ^{427}P L R F**
Rabbit CYP4B1	**P E V F D ^{427}P L R F**
Human CYP4B1	**P E V F D ^{427}S L R F**

Figure 1.8: Conservation of the meander proline in CYP4B1 in different species. CYP4B1 genes in all species except human encode for a proline, which results in a characteristic kink in the peptide change. Loss of proline leads to pronounced changes in the tertiary structure of the protein and may account for lack of hCYP4B1 function.

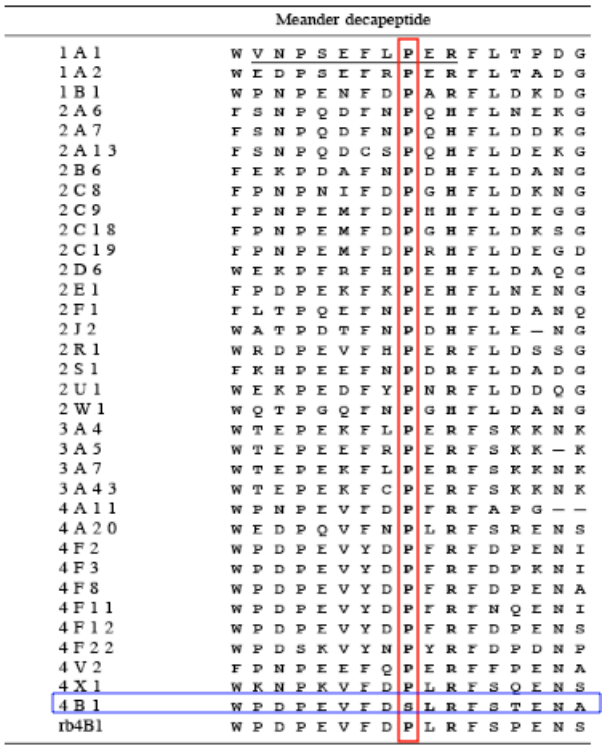

Figure 1.9: Conservation of meander proline across human P450 enzymes. The meander proline is conserved in every known P450 enzyme except CYP4B1. This suggests that the meander proline is essential for P450 function.

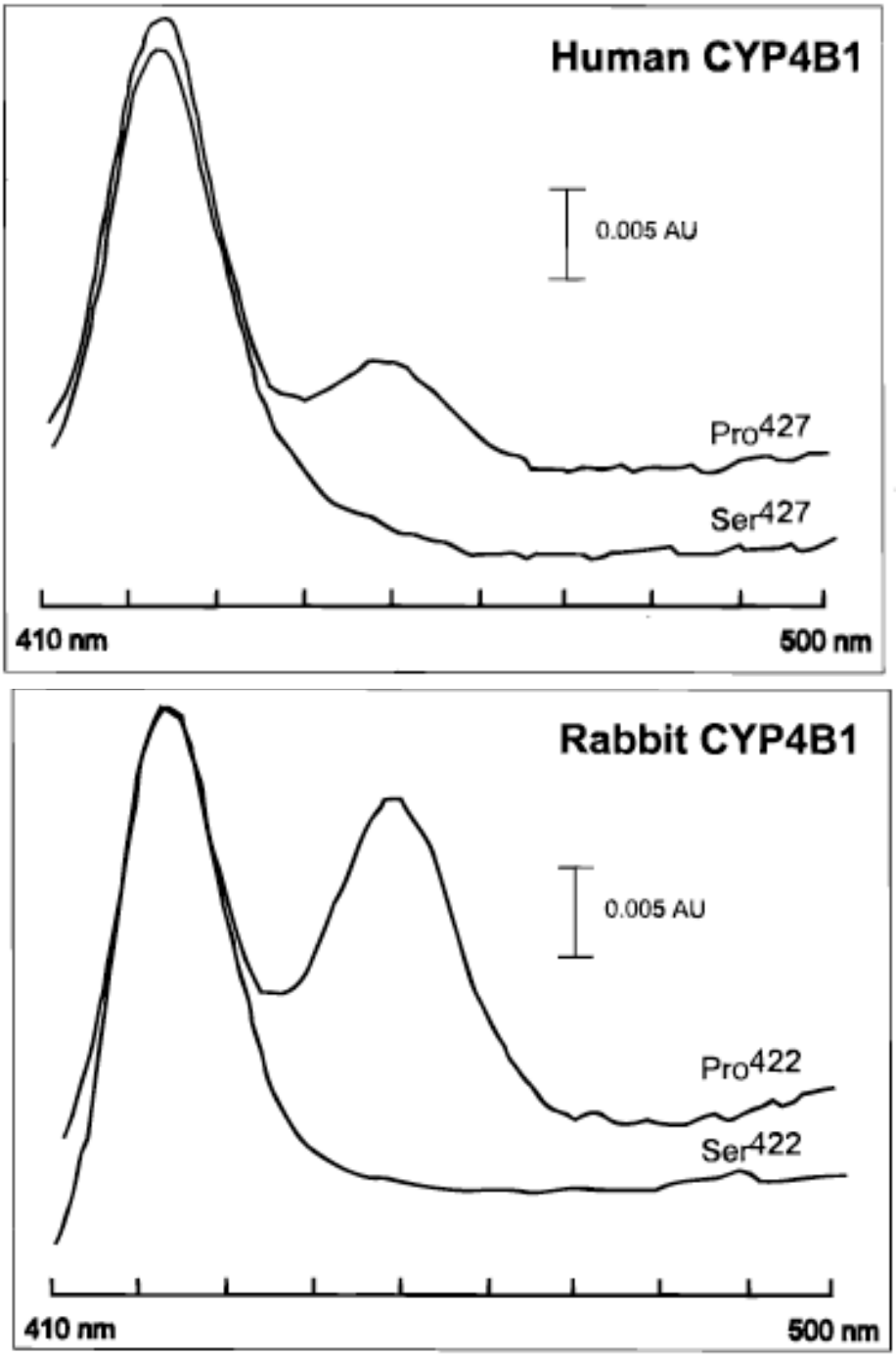

Figure 1.10: A. Lack of incorporation of heme in wild-type human CYP4B1. The human enzyme that lacks the conserved meander proline does not encode a functional enzyme that binds heme. B. When the meander proline is mutated to a serine in functionally active rabbit CYP4B1 it encodes an inactive enzyme that doesn't bind heme. This suggests that the meander proline is essential for heme incorporation and that wild-type human CYP4B1 encodes an inactive enzyme (Zheng et al. 1998).

1.5 Notes to Chapter 1

1. Chen ZR, Somogyi AA, Reynolds G, Bochner F. Disposition and metabolism of codeine after single and chronic doses in one poor and seven extensive metabolisers. Br J Clin Pharmacol. 1991;31(4):381-90. PMCID: 1368322.

2. Yue QY, Svensson JO, Sjoqvist F, Sawe J. A comparison of the pharmacokinetics of codeine and its metabolites in healthy Chinese and Caucasian extensive hydroxylators of debrisoquine. Br J Clin Pharmacol. 1991;31(6):643-7. PMCID: 1368573.

3. Yue QY, Hasselstrom J, Svensson JO, Sawe J. Pharmacokinetics of codeine and its metabolites in Caucasian healthy volunteers: comparisons between extensive and poor hydroxylators of debrisoquine. Br J Clin Pharmacol. 1991;31(6):635-42. PMCID: 1368572.

4. Ingelman-Sundberg M. Genetic polymorphisms of cytochrome P450 2D6 (CYP2D6): clinical consequences, evolutionary aspects and functional diversity. Pharmacogenomics J. 2005;5(1):6-13.

5. Desmeules J, Gascon MP, Dayer P, Magistris M. Impact of environmental and genetic factors on codeine analgesia. Eur J Clin Pharmacol. 1991;41(1):23-6.

6. Kirchheiner J, Schmidt H, Tzvetkov M, Keulen JT, Lotsch J, Roots I, et al. Pharmacokinetics of codeine and its metabolite morphine in ultra-rapid metabolizers due to CYP2D6 duplication. Pharmacogenomics J. 2007;7(4):257-65.

7. Lancaster MC, Jenkins FP, Philp JM. Toxicity associated with Certain Samples of Groundnuts. Nature. 1961;192(4807):1095-6.

8. Sargeant K, Sheridan ANN, O'Kelly J, Carnaghan RBA. Toxicity associated with Certain Samples of Groundnuts. Nature. 1961;192(4807):1096-7.

9. Asao T, Buechi G, Abdel-Kader MM, Chang SB, Wick EL, Wogan GN. The Structures of Aflatoxins B and G. J Am Chem Soc. 1965;87:882-6.

10. Armbrecht BH, Hodges FA, Smith HR, Nelson AA. Mycotoxins. I. Studies on aflatoxin derived from contaminated peanut meal and certain strains of Aspergillus flavus. J Assoc Offic Agr Chemists. 1963;16:13.

11. Swenson DH, Lin JK, Miller EC, Miller JA. Aflatoxin B1-2,3-oxide as a probable intermediate in the covalent binding of aflatoxins B1 and B2 to rat liver DNA and ribosomal RNA in vivo. Cancer Res. 1977;37(1):172-81.

12. Fahmy MJ, Fahmy OG, Swenson DH. Aflatoxin B1-2,3-dichloride as a model of the active metabolite of aflatoxin B1 in mutagenesis and carcinogenesis. Cancer Res. 1978;38(8):2608-16.

13. Sabbioni G, Skipper PL, Buchi G, Tannenbaum SR. Isolation and characterization of the major serum albumin adduct formed by aflatoxin B1 in vivo in rats. Carcinogenesis. 1987;8(6):819-24.

14. Martin CN, Garner RC. Aflatoxin B -oxide generated by chemical or enzymic oxidation of aflatoxin B1 causes guanine substitution in nucleic acids. Nature. 1977;267(5614):863-5.

15. Newberne PM, Wogan GN. Sequential morphologic changes in aflatoxin B carcinogenesis in the rat. Cancer Res. 1968;28(4):770-81.

16. Wogan GN, Newberne PM. Dose-response characteristics of aflatoxin B1 carcinogenesis in the rat. Cancer Res. 1967;27(12):2370-6.

17. Ramsdell HS, Eaton DL. Species susceptibility to aflatoxin B1 carcinogenesis: comparative kinetics of microsomal biotransformation. Cancer Res. 1990;50(3):615-20.

18. Roebuck BD, Wogan GN. Species comparison of in vitro metabolism of aflatoxin B1. Cancer Res. 1977;37(6):1649-56.

19. O'Brien K, Moss E, Judah D, Neal G. Metabolic basis of the species difference to aflatoxin B1 induced hepatotoxicity. Biochem Biophys Res Commun. 1983;114(2):813-21.

20. Degen GH, Neumann HG. Differences in aflatoxin B1-susceptibility of rat and mouse are correlated with the capability in vitro to inactivate aflatoxin B1-epoxide. Carcinogenesis. 1981;2(4):299-306.

21. Monroe DH, Eaton DL. Effects of modulation of hepatic glutathione on biotransformation and covalent binding of aflatoxin B1 to DNA in the mouse. Toxicol Appl Pharmacol. 1988;94(1):118-27.

22. Boyd MR. Evidence for the Clara cell as a site of cytochrome P450-dependent mixed-function oxidase activity in lung. Nature. 1977;269(5630):713-5.

23. Regal KA, Laws GM, Yuan C, Yost GS, Skiles GL. Detection and characterization of DNA adducts of 3-methylindole. Chem Res Toxicol. 2001;14(8):1014-24.

24. Zhou X, D'Agostino J, Li L, Moore CD, Yost GS, Ding X. Respective roles of CYP2A5 and CYP2F2 in the bioactivation of 3-methylindole in mouse olfactory mucosa and lung: studies using Cyp2a5-null and Cyp2f2-null mouse models. Drug Metab Dispos. 2012;40(4):642-7. PMCID: 3310420.

25. Weems JM, Lamb JG, D'Agostino J, Ding X, Yost GS. Potent mutagenicity of 3-methylindole requires pulmonary cytochrome P450-mediated bioactivation: a comparison to the prototype cigarette smoke mutagens B(a)P and NNK. Chem Res Toxicol. 2010;23(11):1682-90. PMCID: 2981624.

26. Weems JM, Cutler NS, Moore C, Nichols WK, Martin D, Makin E, et al. 3-Methylindole is mutagenic and a possible pulmonary carcinogen. Toxicol Sci. 2009;112(1):59-67. PMCID: 2769061.

27. Nichols WK, Mehta R, Skordos K, Mace K, Pfeifer AM, Carr BA, et al. 3-methylindole-induced toxicity to human bronchial epithelial cell lines. Toxicol Sci. 2003;71(2):229-36.

28. Baldwin RM, Shultz MA, Buckpitt AR. Bioactivation of the pulmonary toxicants naphthalene and 1-nitronaphthalene by rat CYP2F4. J Pharmacol Exp Ther. 2005;312(2):857-65.

29. Toxicology and Carcinogenesis Studies of Naphthalene (CAS No. 91-20-3) in B6C3F1 Mice (Inhalation Studies). Natl Toxicol Program Tech Rep Ser. 1992;410:1-172.

30. Toxicology and carcinogenesis studies of naphthalene (cas no. 91-20-3) in F344/N rats (inhalation studies). Natl Toxicol Program Tech Rep Ser. 2000(500):1-173.

31. Baldwin RM, Jewell WT, Fanucchi MV, Plopper CG, Buckpitt AR. Comparison of pulmonary/nasal CYP2F expression levels in rodents and rhesus macaque. J Pharmacol Exp Ther. 2004;309(1):127-36.

32. Furan. Rep Carcinog. 2011;12:205-7.

33. Furan. Rep Carcinog. 2002;10:130-1.

34. Morehouse KM, Nyman PJ, McNeal TP, Dinovi MJ, Perfetti GA. Survey of furan in heat processed foods by headspace gas chromatography/mass spectrometry and estimated adult exposure. Food Addit Contam Part A Chem Anal Control Expo Risk Assess. 2008;25(3):259-64.

35. Heppner CW, Schlatter JR. Data requirements for risk assessment of furan in food. Food Addit Contam. 2007;24 Suppl 1:114-21.

36. Toxicology and Carcinogenesis Studies of Furan (CAS No. 110-00-9) in F344 Rats and B6C3F1 Mice(Gavage Studies). Natl Toxicol Program Tech Rep Ser. 1993;402:1-286.

37. Chen LJ, Hecht SS, Peterson LA. Identification of cis-2-butene-1,4-dial as a microsomal metabolite of furan. Chem Res Toxicol. 1995;8(7):903-6.

38. Chen LJ, Hecht SS, Peterson LA. Characterization of amino acid and glutathione adducts of cis-2-butene-1,4-dial, a reactive metabolite of furan. Chem Res Toxicol. 1997;10(8):866-74.

39. Burka LT, Washburn KD, Irwin RD. Disposition of [14C]furan in the male F344 rat. J Toxicol Environ Health. 1991;34(2):245-57.

40. Byrns MC, Vu CC, Neidigh JW, Abad JL, Jones RA, Peterson LA. Detection of DNA adducts derived from the reactive metabolite of furan, cis-2-butene-1,4-dial. Chem Res Toxicol. 2006;19(3):414-20. PMCID: 2530910.

41. Byrns MC, Vu CC, Peterson LA. The formation of substituted 1,N6-etheno-2'-deoxyadenosine and 1,N2-etheno-2'-deoxyguanosine adducts by cis-2-butene-1,4-dial, a reactive metabolite of furan. Chem Res Toxicol. 2004;17(12):1607-13.

42. Byrns MC, Predecki DP, Peterson LA. Characterization of nucleoside adducts of cis-2-butene-1,4-dial, a reactive metabolite of furan. Chem Res Toxicol. 2002;15(3):373-9.

43. Peterson LA, Naruko KC, Predecki DP. A reactive metabolite of furan, cis-2-butene-1,4-dial, is mutagenic in the Ames assay. Chem Res Toxicol. 2000;13(7):531-4.

44. Hansen AA. Two Fatal Cases of Potato Poisoning. Science. 1925;61(1578):340-1.

45. Hansen AA. Potato poisoning. N Am Vet. 1928;9:4.

46. Hiura M. Studies on storage and rot of sweet potato. Rep Gifu Agric Coll. 1943;50:5.

47. Kubota M, Matsuura T. J Chem Soc Japan. 1952;74.

48. Monlux W, Fitte J, Kendrick G, Dubuisson H. Progressive Pulmonary Adenomatosis in Cattle. The Southwestern Veterinarian. 1953;6.

49. Spoto C. Moldy Sweet Potatoes Caused 200 Steer Deaths. Wausau Daily Herald. 2011 Jan. 28, 2011.

50. Steckel L, Rhodes N. Perilla Mint. University of Tennessee Agricultural Extension Publication w1352007.

51. Wilson BJ, Boyd MR, Harris TM, Yang DT. A lung oedema factor from mouldy sweet potatoes (Ipomoea batatas). Nature. 1971;231(5297):52-3.

52. Wilson BJ, Yang DT, Boyd MR. Toxicity of mould-damaged sweet potatoes (Ipomoea batatas). Nature. 1970;227(5257):521-2.

53. Burka LT, Kuhnert L, Wilson BJ, Harris TM. Biogenesis of lung-toxic furans produced during microbial infection of sweet potatoes (Ipomoea batatas). J Am Chem Soc. 1977;99(7):2302-5.

54. Wilson BJ, Burka LT. Toxicity of novel sequiterpenoids from the stressed sweet potato (Ipomoea batatas). Food Cosmet Toxicol. 1979;17(4):353-5.

55. Doster AR, Mitchell FE, Farrell RL, Wilson BJ. Effects of 4-ipomeanol, a product from mold-damaged sweet potatoes, on the bovine lung. Vet Pathol. 1978;15(3):367-75.

56. Devereux TR, Jones KG, Bend JR, Fouts JR, Statham CN, Boyd MR. In vitro metabolic activation of the pulmonary toxin, 4-ipomeanol, in nonciliated bronchiolar epithelial (Clara) and alveolar type II cells isolated from rabbit lung. J Pharmacol Exp Ther. 1982;220(1):223-7.

57. Slaughter SR, Statham CN, Philpot RM, Boyd MR. Covalent binding of metabolites of 4-ipomeanol to rabbit pulmonary and hepatic microsomal proteins and to the enzymes of the pulmonary cytochrome P-450-dependent monooxygenase system. J Pharmacol Exp Ther. 1983;224(1):252-7.

58. Baer BR, Rettie AE, Henne KR. Bioactivation of 4-Ipomeanol by CYP4B1: Adduct Characterization and Evidence for an Enedial Intermediate. Chem Res Toxicol. 2004;18:855-64.

59. Buckpitt AR, Boyd MR. Xenobiotic metabolism in birds, species lacking pulmonary Clara cells. Pharmacologist. 1978;20.

60. Buckpitt AR, Statham CN, Boyd MR. In vivo studies on the target tissue metabolism, covalent binding, glutathione depletion, and toxicity of 4-ipomeanol in birds, species deficient in pulmonary enzymes for metabolic activation. Toxicol Appl Pharmacol. 1982;65(1):38-52.

61. Falzon M, McMahon JB, Schuller HM, Boyd MR. Metabolic activation and cytotoxicity of 4-ipomeanol in human non-small cell lung cancer lines. Cancer Res. 1986;46(7):3484-9.

62. McLemore TL, Litterst CL, Coudert BP, Liu MC, Hubbard WC, Adelberg S, et al. Metabolic activation of 4-ipomeanol in human lung, primary pulmonary carcinomas, and established human pulmonary carcinoma cell lines. J Natl Cancer Inst. 1990;82(17):1420-6.

63. Rowinsky EK, Noe DA, Ettinger DS, Christian MC, Lubejko BG, Fishman EK, et al. Phase I and pharmacological study of the pulmonary cytotoxin 4-ipomeanol on a single dose schedule in lung cancer patients: hepatotoxicity is dose limiting in humans. Cancer Res. 1993;53(8):1794-801.

64. Kasturi VK, Dearing MP, Piscitelli SC, Russell EK, Sladek GG, O'Neil K, et al. Phase I study of a five-day dose schedule of 4-Ipomeanol in patients with non-small cell lung cancer. Clin Cancer Res. 1998;4(9):2095-102.

65. Christian MC, Wittes RE, Leyland-Jones B, McLemore TL, Smith AC, Grieshaber CK, et al. 4-Ipomeanol: a novel investigational new drug for lung cancer. J Natl Cancer Inst. 1989;81(15):1133-43.

66. Lakhanpal S, Donehower RC, Rowinsky EK. Phase II study of 4-ipomeanol, a naturally occurring alkylating furan, in patients with advanced hepatocellular carcinoma. Invest New Drugs. 2001;19(1):69-76.

67. Boyd MR, Burka LT. In vivo studies on the relationship between target organ alkylation and the pulmonary toxicity of a chemically reactive metabolite of 4-ipomeanol. J Pharmacol Exp Ther. 1978;207(3):687-97.

68. Boyd MR, Dutcher JS. Renal toxicity due to reactive metabolites formed in situ in the kidney: investigations with 4-ipomeanol in the mouse. J Pharmacol Exp Ther. 1981;216(3):640-6.

69. Czerwinski M, McLemore TL, Philpot RM, Nhamburo PT, Korzekwa K, Gelboin HV, et al. Metabolic activation of 4-ipomeanol by complementary DNA-expressed human cytochromes P-450: evidence for species-specific metabolism. Cancer Res. 1991;51(17):4636-8.

70. Hukkanen J, Pelkonen O, Hakkola J, Raunio H. Expression and regulation of xenobiotic-metabolizing cytochrome P450 (CYP) enzymes in human lung. Crit Rev Toxicol. 2002;32(5):391-411.

71. Verschoyle RD, Philpot RM, Wolf CR, Dinsdale D. CYP4B1 Activates 4-Ipomeanol in Rat Lung. Toxicol Appl Pharmacol. 1993;123:193-8.

72. Boyd MR, Burka LT, Wilson BJ, Sasame HA. In vitro studies on the metabolic activation of the pulmonary toxin, 4-ipomeanol, by rat lung and liver microsomes. J Pharmacol Exp Ther. 1978;207(3):677-86.

73. Degawa M, Miura S, Hashimoto Y. Androgen-dependent renal microsomal cytochrome P-450 responsible for N-hydroxylation and mutagenic activation of 3-methoxy-4-aminoazobenzene in the BALB/c mouse. Cancer Res. 1990;50(9):2729-33.

74. Isern J, Meseguer A. Hormonal regulation and characterisation of the mouse Cyp4b1 gene 5'-flanking region. Biochem Biophys Res Commun. 2003;307(1):139-47.

75. Zheng YM, Fisher MB, Yokotani N, Fujii-Kuriyama Y, Rettie AE. Identification of a meander region proline residue critical for heme binding to cytochrome P450: implications for the catalytic function of human CYP4B1. Biochemistry. 1998;37(37):12847-51.

76. Zheng YM, Henne KR, Charmley P, Kim RB, McCarver DG, Cabacungan ET, et al. Genotyping and site-directed mutagenesis of a cytochrome P450 meander Pro-X-Arg motif critical to CYP4B1 catalysis. Toxicol Appl Pharmacol. 2003;186(2):119-26.

77. Statham CN, Dutcher JS, Kim SH, Boyd MR. Ipomeanol 4-glucuronide, a major urinary metabolite of 4-ipomeanol in the rat. Drug Metab Dispos. 1982;10(3):264-7.

Chapter 2

In vitro Metabolism of 4-Ipomeanol by Lung, Liver and Kidney Microsomes from Toxicity-Susceptible Animals

2.1 Introduction

4-Ipomeanol (IPO; 1-(3-Furyl)-4-hydroxy-1-pentanone) is a furanoterpenoid toxin produced by sweet potatoes (*Ipomoea batatas*) in response to infection by the mold *Fusariam solani* (1). Cattle that ingest infected sweet potatoes can develop interstitial pneumonia that is characterized by pulmonary edema and emphysema. Moldy sweet potatoes have been linked to the death of livestock since 1952 (2), including recent cases in Wisconsin where 200 cattle died (3) and England, where six cows died in what is believed to be the first case of IPO toxicity in the UK (4). IPO is lethal to cattle in doses as low as 7.5 mg/kg which can be achieved by ingesting as little as 6 kg of spoiled sweet potatoes (1). Despite the relatively common occurrence of cattle being poisoned by IPO, no attempt has been made to determine the enzymology of the bioactivation process in bovine lung.

Beyond cattle poisoning, IPO is a pulmonary pro-toxin in all known non-primate mammalian species which are known to bioactivate the compound in a reaction that has been shown to be mediated readily by rat pulmonary cytochrome P450 4B1 (CYP4B1) (5). In certain circumstances, IPO is also a renal toxin in mice. Whereas, CYP4B1 is highly expressed in the lung of both male and female mice, CYP4B1 expression in mouse kidney is androgen regulated, which leads to high expression in male kidney, but not female kidney (6, 7). This pattern of expression mimics the pattern of IPO toxicity in that IPO causes

pulmonary toxicity in female mice whereas it causes pulmonary and renal toxicity in male mice (8, 9).

The present study was undertaken, firstly to determine the ability of bovine lung microsomes to bioactivate IPO to potentially pneumotoxic species and secondly to assess involvement of bovine CYP4B1 in the process. Previous studies to assess in vitro activation of IPO have relied on the use of radiolabeled substrate and the detection of protein-bound adducts (10). Here, we use a recently developed in vitro bioactivation assay for IPO which employs the nucleophilic amino acid derivatives N-acetyl-cysteine (NAC) and N-acetyl-lysine (NAL) to trap a reactive ene-dial intermediate (Figure 2.1) generating a stable IPO adduct (NAC/NAL) that can be detected by LC/MS (11). CYP4 involvement in bovine lung bioactivation was evaluated with the selective CYP4 ligand HET0016 (12), an N-aryl formamidoxime that is known to be a potent inhibitor of CYP4A (13), CYP4F (14) and CYP4V (15) enzymes and an anti-CYP4B1 antibody (16).

Next, we extended analysis of IPO bioactivation to lung, liver and kidney microsomes from a wide variety of toxicity-susceptible species (mouse, rat, rabbit, and dog) in an attempt to correlate species- and organ-selective toxicity with in vitro bioactivation rates to the NAC/NAL adduct. Finally, because IPO has previously been shown to be subject to phase II metabolism via glucuronidation in the rat (17). We also developed an *in vitro* IPO-glucuronidation assay to assess the ability of tissue microsomes from various species to glucuronidate IPO. We tested the hypothesis that that the target organ toxicity of IPO in various species will correlate positively with the relative extent of

in vitro bioactivation to the NAC/NAL adduct and correlate negatively with *in vitro* inactivation via glucuronidation.

2.2 Experimental Procedures

Materials.

IPO was a gift from the National Cancer Institute (Bethesda, MD). N-acetylcysteine, N-acetyllysine, CHAPS, β-glucuronidase and 3-methylumbelliferone glucuronide, were purchased from Sigma Aldrich (St. Louis, MO). A/J mice, BALB mice, C57/BL6 mice, DBA mice, and C3H mice were obtained from Jackson Laboratories (Bar Harbor, ME). NIH/Swiss mice were obtained from Harlan Laboratories (Indianapolis, IN). HET0016 was purchased from Cayman Chemical (Ann Arbor, MI). Bovine tissue was purchased from Pel-Freez Biologicals (Rogers, AR). Rabbit tissue was purchased from R&R Research (Stanwood, WA).

Microsomes were prepared by differential centrifugation according to previously published protocols (18). Microsomal experiments were conducted in triplicate using pooled lung and liver microsomes from frozen tissue from 5 animals for mouse or single animals for rabbit and cow. Beagle dog, Sprague-Dawley rat and cynomolgus monkey microsomes were obtained from XenoTech LLC (Lenexa, KS).

Bioactivation of IPO

In vitro bioactivation of IPO was assessed by incubating microsomal preparations in triplicate with IPO (50 μM), potassium phosphate buffer (100 mM pH 7.4), NADPH (1 mM), EDTA (1 mM), MgCL2 (3 mM) and NAC and NAL (20 mM each). All metabolic incubations were allowed to proceed for 20 minutes at 37^{o}C in a shaking water bath with a final incubation volume of 200 μL and final protein concentration of 0.2 mg/mL. Reactions were terminated by the addition of an equal volume of ice-cold methanol containing the internal standard, furafylline, and centrifuged for 10 min at 4000 rpm to remove protein. Activation rates were assessed by monitoring fragmentation of the NAC/NAL adduct shown in Figure 1 at *m/z* 353 by LC/MS/MS on a Micromass Quattro II tandem quadrupole mass spectrometer operating in electrospray + mode. The mass spectrometer was coupled to a Shimadzu LC system equipped with a 3 micron particle size Thermo Hypersil gold 100x2.1 mm column. Samples were eluted with 10 mM formic acid in water (aqueous phase, A) and 10 mM formic acid in methanol (organic phase, B) at a flow rate of 300 μL per minute. The initial conditions were 70% solvent A and 30% solvent B, which increased to 100% solvent B between 2 and 4 minutes and remained at 100% solvent B until the end of the run at 5 minutes. IPO eluted at 4.4 min and was monitored at *m/z* 191 (sodiated IPO) with a cone voltage of 65 V and collision energy of 30 V. The NAC/NAL-IPO adduct eluted at 4.7 minutes and was monitored by fragmentation at *m/z* 482➔352, which represents loss of water from the M+H ion (11). The internal standard, furafylline, eluted at 4.55 minutes and was monitored by fragmentation of the parent *m/z* 261.3➔80.5 at a cone voltage of 35 V and collision energy of 25 V.

CYP4 involvement in bioactivation was evaluated with the selective CYP4 ligand, HET0016 (12). Incubations containing HET0016 were conducted at a final organic (DMSO) concentration of ≤ 1% and compared to control incubations containing DMSO with no inhibitor present. To further determine the contribution of CYP4B1 specifically, towards the activation of IPO, microsomal incubations were conducted in the presence of goat anti-CYP4B1 IgG (raised against rabbit CYP4B1) or goat IgG control at 5 mg IgG per mg microsomal protein as previously described (16). The antibody was also used to visualize the presence of CYP4B protein(s) in bovine pulmonary microsomes by western blotting at a dilution of 1:5000 and visualized using a donkey anti-goat IRDye® 800CW secondary antibody from LI-COR Biosciences (Lincoln, NE).

Glucuronidation of IPO

In vitro glucuronidation of IPO was assessed by incubating microsomal preparations in triplicate with IPO (50 μM), Tris buffer (100 mM pH 8.4), UDPGA (5 mM), CHAPS (0.5 mg/mL) and MgCl2 (10 mM) in a final incubation volume of 250 μL. All metabolic incubations were allowed to proceed for 60 minutes at 37^{o}C, terminated by the addition of an equal volume of ice-cold methanol containing the internal standard, 4-methylumbelliferone glucuronide (4-MBG), and centrifuged for 10 min at 4000 rpm to remove precipitated protein. Inactivation rates were assessed by monitoring fragmentation of the glucuronide shown in Figure 2.1 at *m/z* 191 by LC/MS/MS using similar detection and separation conditions described above for the NAC/NAL adduct. Samples were eluted with 10 mM formic acid in water (aqueous phase, A) and 10 mM formic acid in methanol (organic phase, B) at a flow rate of 300 μL per minute. The initial

conditions were 90% solvent A and 10% solvent B, which increased to 100% solvent B between 2 and 4 minutes and remained at 100% solvent B until the end of the run at 8 minutes. As noted above, IPO elutes at 4.4 min and is monitored by m/z 191 (sodiated IPO) at a cone voltage of 65 V and collision energy of 30 V. Under these conditions, IPO-glucuronide eluted at 4.8 minutes and was monitored by fragmentation of the parent sodiated glucuronide *m/z* 367➔191 at a cone voltage of 35 V and collision energy of 22 V. The internal standard 3-MBG eluted at 4.7 minutes and was monitored by fragmentation of the parent *m/z* 375➔199 at a cone voltage of 30 V and collision energy of 15 V.

To substantiate the identity of the IPO-glucuronide peak, microsomal incubations were treated with equal volumes of potassium phosphate buffer (100 mM) pH 6.0 to adjust the pH of the incubation to ~6.8, 50 units of E. coli β–glucuronidase from Sigma-Aldrich (St. Louis, MO) added and the mixture incubated for 60 minutes at 37^{o}C in a shaking water bath in a final reaction volume of 500 μL. Reactions were terminated, spiked with internal standard and analyzed as described above.

2.3 Results

To identify the P450 enzyme responsible for IPO toxicity in cattle, we examined the ability of both HET0016 and an anti-rabbit CYP4B1 antibody to inhibit IPO bioactivation in bovine pulmonary microsomes. Parallel experiments were performed with rabbit pulmonary microsomes, which are known to contain high levels of CYP4B1 (19, 20). P450 spectral content in cow lung microsomes was 0.09 nmol/mg protein, similar to the levels

observed in rabbit lung of 0.11 nmol/mg. To help put these values in context and to assess the viability of frozen, stored tissue, we also measured P450 specific contents in our bovine and rabbit liver microsomes. These latter values of 0.34 nmol/mg and 0.98 nmol/mg, respectively, were ~50% lower than literature data describing freshly prepared liver microsomes from cattle (21) and rabbits (22). Despite the relatively low lung P450 content, cow and rabbit lung microsomes formed the NAC/NAL-IPO adduct at higher rates than the respective liver microsomes.

Formation of the NAC/NAL adduct was NADPH-dependent in all microsomal preparations (not shown), which is consistent with P450 involvement in the bioactivation process. Figure 2.3 depicts inhibition by HET0016 of the NAC/NAL-IPO adduct generated from reconstituted, purified rabbit CYP4B1. HET0016 shows roughly equal potency of inhibition towards CYP4B1 as it does towards CYP4A enzymes and slightly higher levels of inhibition towards CYP4B1 compared to CYP4F enzymes (12-14). HET0016 was found to be a potent inhibitor of IPO activation with IC_{50} values of 37 nM and 23 nM in purified rabbit CYP4B1 and bovine lung microsomes, respectively. NAC/NAL-IPO adduct formation in both bovine lung and rabbit lung microsomes was decreased by more than 90% when metabolic reactions contained 300 nM HET0016 (Figure 2.4). This concentration of HET0016 was chosen to maintain CYP4 selectivity, because it is approximately ten times the IC50 value in bovine or rabbit lung, but is still ten-fold lower than the IC_{50} towards any mammalian non-CYP4 family enzyme (12).

To further probe for bovine CYP4B involvement in IPO bioactivation, we employed a polyclonal antibody raised against rabbit CYP4B1. This antibody is monospecific for rabbit lung CYP4B1 and maximally inhibits lung microsomal CYP4B1-dependent catalysis at a concentration of 4 mg IgG/mg microsomal protein (16, 23). Moreover, the antibody is known to cross-react with pulmonary CYP4B1 from numerous other animal species including rats, hamsters, mice, guinea pigs and monkeys (24). The protein sequences of bovine CYP4B1 and rabbit CYP4B1 are also highly related (>80% identical); therefore the polyclonal antibody raised against rabbit CYP4B1 would be expected to immunochemically cross-react with the bovine ortholog. NAC/NAL-IPO adduct formation was reduced by 70% and 85%, respectively in bovine and rabbit lung microsomes when reactions were pre-incubated with anti-CYP4B1 IgG compared to control IgG (Figure 2.4). The lower degree of immunoinhibition in bovine lung presumably reflects the fact that the antibody was raised specifically against the rabbit enzyme. However residual activity in both rabbit and bovine lung may also be due to other pulmonary P450 enzymes, such as CYP2B4 (23). Indeed, a CYP2B4 ortholog has been detected immunochemically in bovine lung (25). Importantly, the anti-CYP4B1 antibody used here detects only a single intense protein band in cow lung microsomes (Figure 2.5). Bovine CYP4B1 is roughly 700 AMU heavier than rabbit CYP4B1 and accordingly the cow lung CYP4B protein detected by the α-CYP4B1 antibody migrates on SDS-PAGE with a higher apparent molecular weight than rabbit CYP4B1. Bovine CYP4B also appears to be an even more prevalent component of pulmonary microsomal P450 than the rabbit ortholog based on the significantly stronger signal probing equal microsomal protein levels with α-CYP4B1 antibody.

The utility of HET0016 as a diagnostic inhibitor for CYP4B1 mediated IPO-activation is further illustrated in Figure 2.6. As mentioned above, CYP4B1 exhibits a gender-specific pattern of expression in mice. Male and female mice have high levels of CYP4B1 expression in lung, but only male mice have detectable levels of CYP4B1 expression in the kidney due to the androgen-dependent expression of renal CYP4B1. This expression pattern seems likely to be responsible for the gender-specific pattern of toxicity seen in mice, in that male mice are subject to renal and pulmonary toxicity when treated with IPO, but female mice are only subject to pulmonary toxicity. As expected, inhibition of *in vitro* IPO activation in mouse microsomes by HET0016 (Figure 2.6) follows a similar pattern to the gender-specific expression of CYP4B1. HET0016 drastically reduces (~90%) the rate of IPO activation in pulmonary microsomes from both male and female mice and the rate of activation in male renal microsomes (~80%). However HET0016 had no effect on the rate of IPO activation in female renal microsomes or in liver microsomes from either species.

We have also assessed IPO activation in animal tissue microsomes from a variety of species including those that feature prominently in preclinal testing of new drug entities (Figure 2.7). With the exceptions of beagle dog and cynomolgus monkey, the lung has the highest rate of IPO activation in all other species examined. In general, *in vitro* activation rates in lung microsomes from each non-canine species correlate well with the observed pulmonary toxicity exhibited by animals dosed with IPO. Figure 2.6 demonstrates that HET0016 eliminates the bioactivation of IPO in those extrahepatic tissues where IPO is readily bioactivated.

IPO toxicity is likely a balance between phase I-mediated bioactivation and phase II-dependent inactivation. To probe the latter, we developed an *in vitro* glucuronidation assay to assess the ability of animal tissue microsomes to form IPO-glucuronide which may play an important role in the elimination of the toxin. Figure 2.8 shows a representative LC/MS/MS chromatogram of an incubation with rabbit liver microsomes along with the fragmentation of IPO-glucuronide which we use to monitor the metabolite. Of note is the fact that the glucuronide peak is absloutely dependent on the cofactor, UDPGA, and can be eliminated by post-incubation treatment with β-glucuronidase. These findings, along with the fragmentation pattern representing the characteristic neutral loss of 176 Da are consistent with the microsomal formation of IPO-glucuronide. Finally, to further establish that the metabolite produced is the IPO-glucuronide, we performed a high-mass accuracy MS analysis. Figure 9 shows that the accurate mass of our metabolite, 367.1016, correlates extremely well with the calculated mass of a sodiated IPO-glucuronide, 367.1005, with an error of only 3 ppm. Collectively, these data provide high confidence this *in vitro* assay does in fact measure formation of IPO-glucuronide.

We have utilized the IPO glucuronide assay to determine if toxicity-susceptible species differentially glucuronidate IPO in target tissue microsomes and to confirm previously reported in vivo glucuronidation from the rat (17). Figure 2.10 indicates that our *in vitro* glucuronidation assay confirms that rat liver microsomes readily glucuronidate IPO in accordance with rat *in vivo* data. It also shows that the liver is the major site of IPO-glucuronidation *in vitro* and that liver microsomes from all tested species produce IPO

glucuronide. In contrast, lung and kidney microsomes from all species tested exhibited very low levels of IPO glucuronidation.

Figure 2.11 shows both activation and glucuronidation of IPO in tissue microsomes from the males of 6 different mouse strains. The LD_{50} of IPO in each strain had previously been established as 20 mg/kg in A/J mice, 20 mg/kg in C57Bl/6 mice, 25 mg/kg in DBA/2J mice, 42 mg/kg in NIH-Swiss mice, 50 mg/kg in C3H-HeJ mice and 60 mg/kg in BALB/Cj mice (26). In all strains, activation rates were highest in kidney followed by lung and glucuronidation of IPO only occurred in liver microsomes. However, activation and elimination rates were not predictive of LD_{50} values in different strains; strains with low LD_{50} values did not exhibit higher rates of activation either in lung or kidney or lower rates of inactivation relative to strains with high LD_{50} values.

2.4 Discussion

Data presented here indicate that CYP4B1 is likely responsible for the bioactivation of IPO in cattle. This is significant because IPO toxicity is a serious hazard to livestock, however, the exposure of cattle to IPO is generally predictable. Ranchers typically feed cattle herds sweet potatoes when other more typical forages have been exhausted, so the exposure of cattle to IPO is generally limited to direct action by ranchers. These data indicate that a potent CYP4B1 inhibitor, while not an efficacious treatment post-IPO exposure, may be a useful prophylactic treatment at times when ranchers rely on sweet potatoes as a food source for their herds. CYP4B1 inhibition may potentially mitigate the

danger inherent in feeding cattle spoiled sweet potatoes and prove a useful agricultural therapeutic.

The data presented here also indicate that our *in vitro* bioactivation assay is generally predictive of the site of IPO toxicity. The high level of IPO activation in pulmonary microsomes in all species compared to activation in renal or liver microsomes (with the notable exception of the dog) correlates well with the observed pulmonary toxicity and edema previously reported in these species. Activation levels are highest in canine liver microsomes, however no hepatotoxicity has been reported in beagle dogs.

To assess non-activating metabolism of IPO we have developed an *in vitro* IPO-glucuronidation assay. This has allowed us to show that dog, cow, monkey, rabbit, rat and mouse liver microsomes are capable of glucuronidating IPO. The existence of a functional IPO elimination pathway in the liver may account for the lack of liver toxicity seen in test animals despite several species (rabbit and mouse in particular) exhibiting relatively high IPO adduction rates in liver microsomes.

Toxicity of a pro-toxin like IPO depends on the relative rate of activation versus the rate of elimination. Viewing liver-mediated glucuronidation as the prime elimination pathway and ene-dial formation as the primary activation pathway, we have attempted to correlate activation/elimination with reported LD_{50} values from various mouse strains. However, mouse strains with a high LD_{50} did not have consistently higher *in vitro* rates of activation or lower rates of glucuronidation relative to strains with a lower LD_{50}.

Differences among strains in the rates of glucuronidation and activation were not predictive of differences in LD_{50} values despite the fact that differences in the rates of glucuronidation and activation between tissues is predictive of the site of toxicity *in vivo*. This could be due in part to the fact that the LD_{50} determinations were performed by different laboratories using slightly different methods and that the range of LD_{50} values spans a relatively narrow range (20-60 mg/kg) (26), making predictions difficult. We may also be underestimating the rates of elimination and activation of IPO using our *in vitro* assays. The current ene-dial trap bioactivation assay is reasonably predictive of the site of organ toxicity, however, it may not capture all potential activated IPO metabolites, for example the unrearranged furan epoxide or γ-diketone. Moreover, IPO glucuronidation is just one of several possible phase II pathways that lead to inativation, e.g. glutathione and sulfate conjugation. Furthermore, IPO itself is relatively water soluble, and may not depend on metabolism and conjugation for its elimination, although we have not had success in detecting unchanged IPO in the urine of mice (see Chapter 3).

It is worth noting that, in the male mouse, activation rates are significantly higher in renal microsomes than in pulmonary microsomes, despite the fact that pulmonary toxicity tends to be the lethal insult in IPO-treated mice with renal toxicity a secondary concern. In male mouse kidney, CYP4B1 is expressed at high levels throughout the cortex which makes up a significant portion of the mass of the kidney, whereas CYP4B1 is localized to the bronchial epithelium in lung which makes up a miniscule portion of the mass of the lung. We attribute the higher activity in male kidney microsomes to the relatively low levels of

CYP4B1 in the whole lung, despite high expression in the bronchial epithelium, which is the ultimate site of murine toxicity.

In summary, the data presented here are the first to identify a CYP4B protein in cow lung microsomes, and show that HET0016 is a potent, nanomolar inhibitor of CYP4B. When combined with the antibody experiments, all bovine data are consistent with a dominant role for CYP4B1 in the pneumotoxicity which arises in cattle that ingest mouldy sweet potatoes. In addition, comparative studies of IPO bioactivation in lung, kidney and liver of toxicity-susceptible species shows that the highest rates of microsomal IPO bioactivation occur in lung tissue (except for male mouse kidney as discussed above), consistent in all cases, except for the dog, with the observed site of organ toxicity. Relatively high rates of IPO bioactivation are also seen in the liver of each species examined, but hepatotoxicity is not an issue, possibly because high rates of liver microsomal glucuronidation (not seen in the lung or kidney) provide an efficient inactivation pathway that limits hepatic exposure to the pro-toxin.

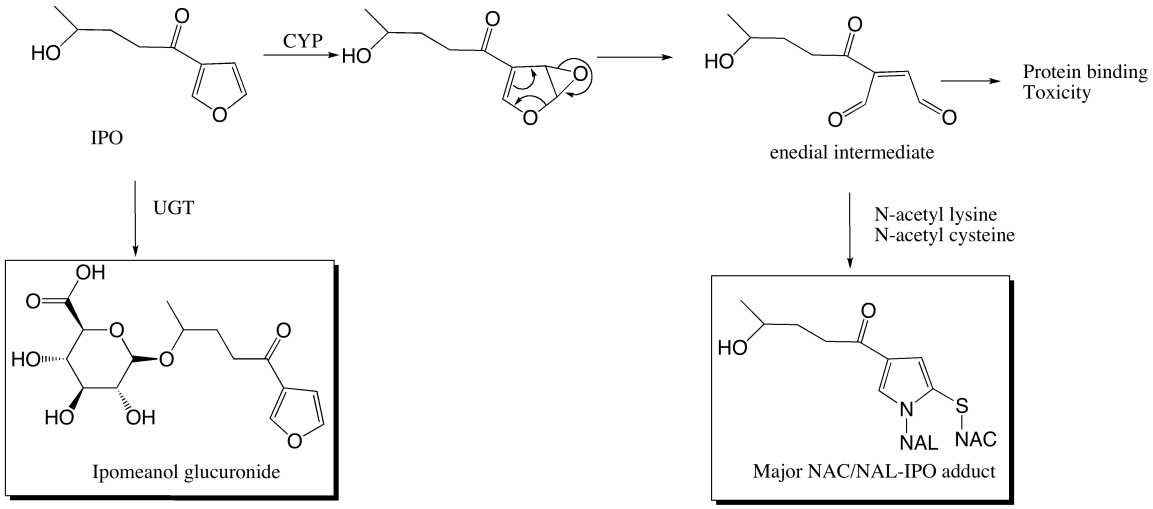

Figure 2.1: Metabolic scheme of IPO metabolism showing elimination *via* direct phase II metabolism (glucuronidation) of IPO and activation via P450-mediated 4-ipomeanol oxidation to the putative reactive ene-dial intermediate. The scheme also highlights the subsequent reaction with nucleophilic trapping agents to yield a stable NAC/NAL-IPO adduct. Formation of this adduct can be monitored by LC/MS/MS and used as an *in vitro* marker of IPO bioactivation.

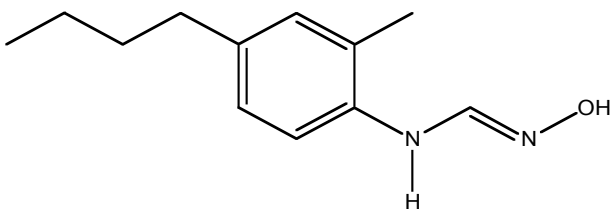

Enzyme	IC_{50} (nM)
CYP4A1	17
CYP4A2	12
CYP4A3	22
CYP4A11	42
CYP4F2	125
CYP4F3	100
CYP2C9	2000
CYP2D6	84000
CYP3A4	71000

Figure 2.2: Inhibition of P450 by HET0016. At concentrations less than 1 uM, HET0016 is a CYP4-selective inhibitor (Miyata et al.).

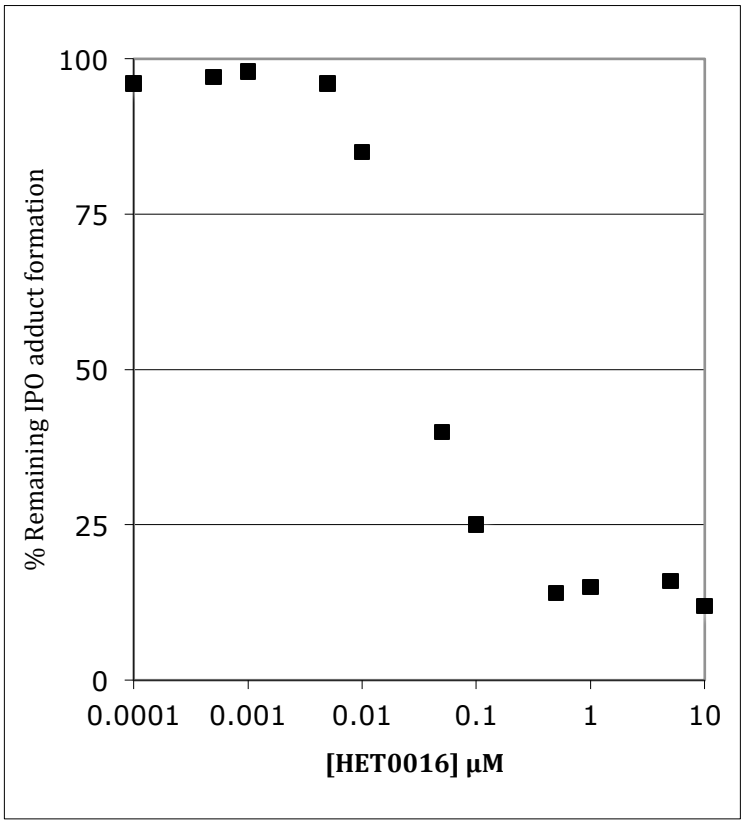

Figure 2.3: *In vitro* inhibition by HET0016 of IPO bioactivation catalyzed by purified rabbit CYP4B1. HET0016 inhibition of CYP4B1-mediated IPO-adduct formation exhibited an IC_{50} of 37 nM.

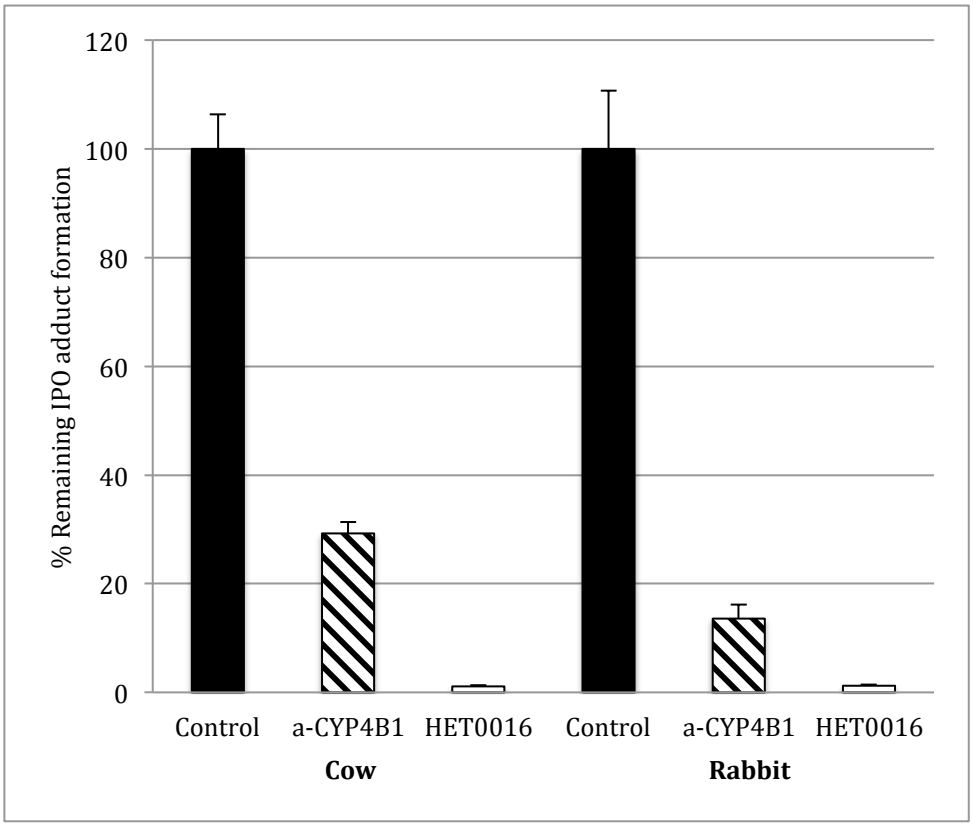

Figure 2.4: *In vitro* inhibition of bioactivation of IPO by HET0016 (300 nM) and α-CYP4B1 antibody (5 mg IgG/mg microsomal protein) in rabbit and bovine pulmonary microsomes. Activity in the presence of the chemical inhibitor and antibody were significantly lower than controls from both species ($p<0.005$; Students t-test).

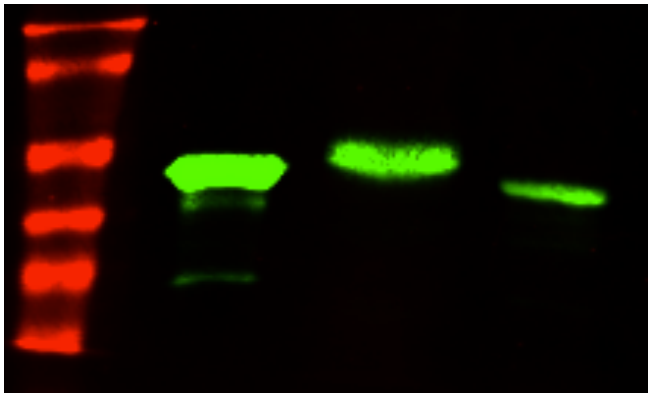

Figure 2.5: Western blot analysis of bovine lung CYP4B1 content. Lane 1: Ladder, Lane 2: Purified rabbit CYP4B1 (2 pmol), Lane 3: Bovine lung microsomes (20 μg), Lane 4: Rabbit lung microsomes (20 μg). Bovine lung expresses a CYP4B protein at high levels comparable to rabbit lung.

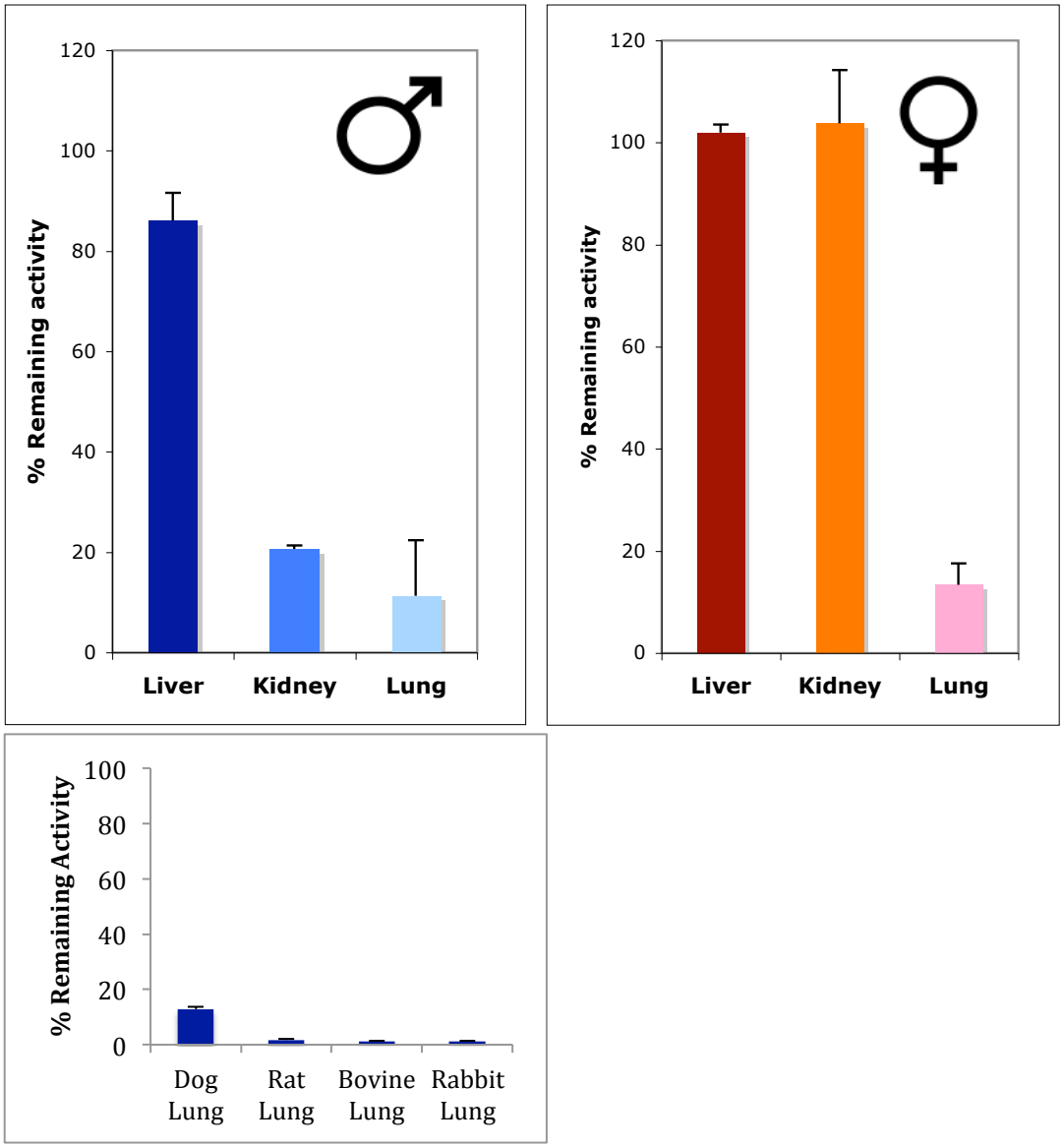

Figure 2.6: *In vitro* inhibition of IPO activation (NAC/NAL adduct formation) in microsomes from male (left) and female (right) mice and pulmonary microsomes from dog, rat, bovine and rabbit (bottom). 300 nM HET0016 significantly reduced IPO activation in pulmonary microsomes in all species and male mouse renal microsomes ($p<0.005$; Students t-test), indicative of CYP4B1 involvement in all species examined.

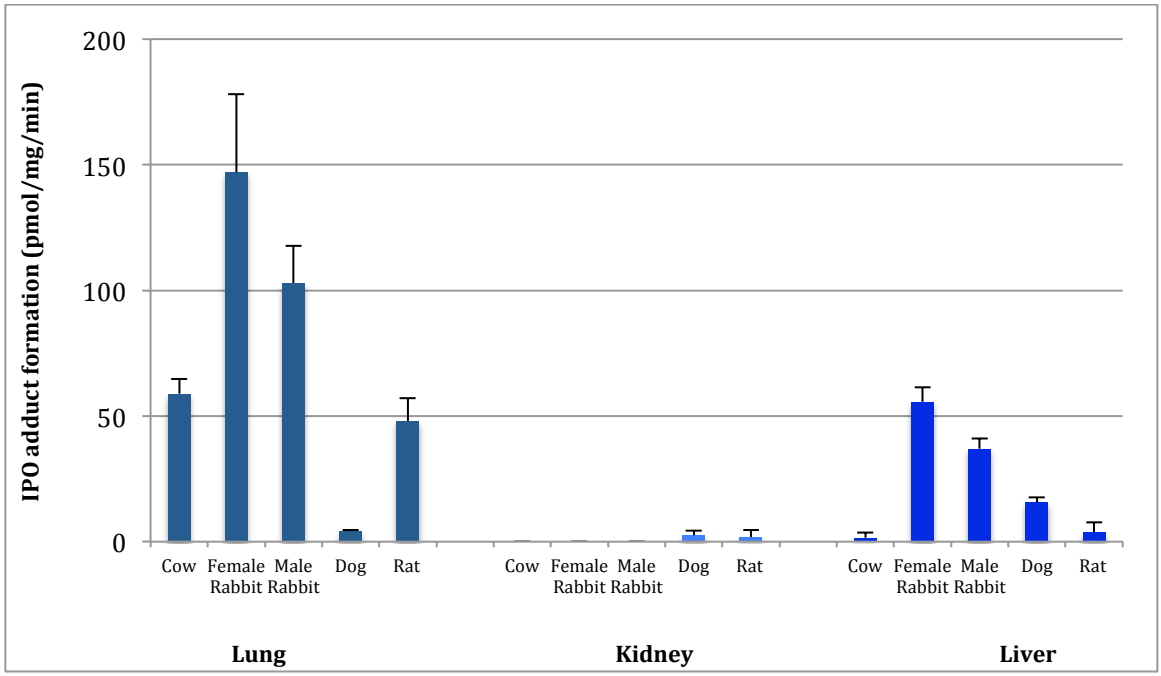

Figure 2.7: *In vitro* activation of IPO by liver, kidney and lung microsomes from various species. In nearly every case, activation rates are highest in pulmonary microsomes and, therefore, in vitro activation to the NAC/NAL adduct alone is predictive of the site of toxicity observed *in vivo*.

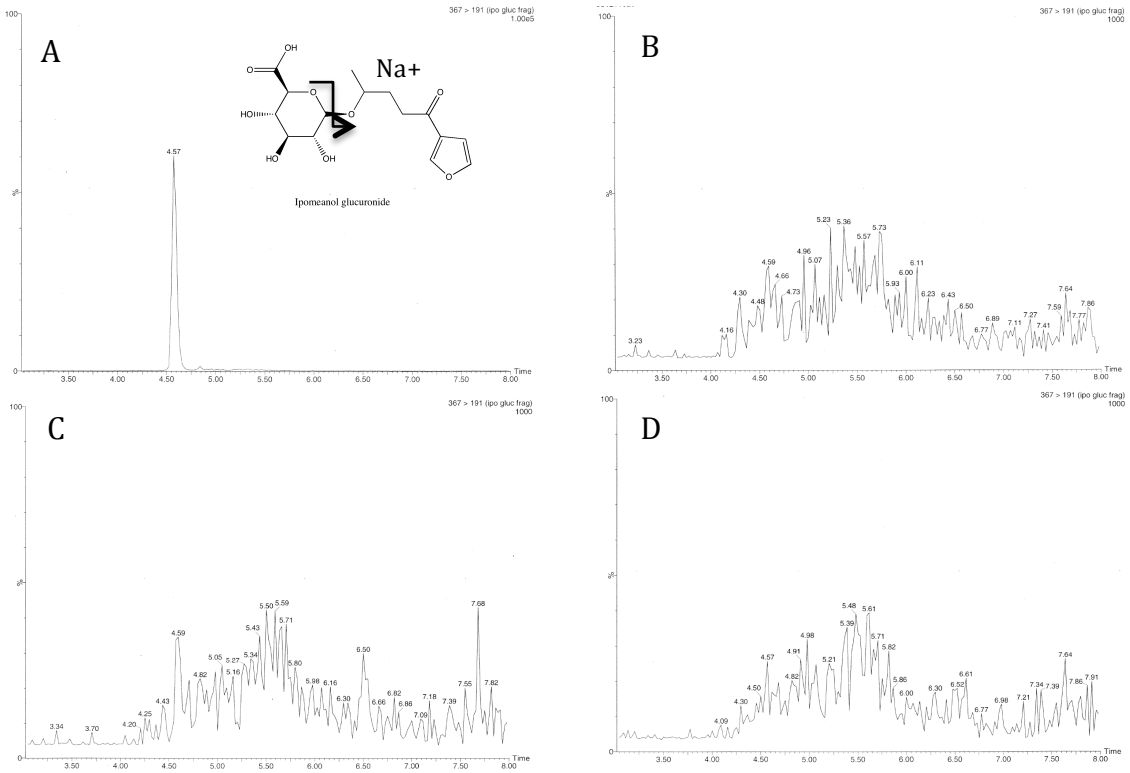

Figure 2.8: Analysis of microsomal IPO-glucuronide formation by LC-MS/MS. IPO-glucuronide was monitored (m/z 367 → 191) as a function of CHAPS, UDPGA and β–glucuronidase inclusion in microsomal incubations. Production of IPO-glucuronide by in mouse liver microsomes coincubated with UDPGA and CHAPS (A), lacking UDPGA (B), lacking CHAPS (C) or following post-incubation treatment with β-glucuronidase. The inlay in panel A shows the fragmentation of IPO-glucuronide during MS/MS analysis.

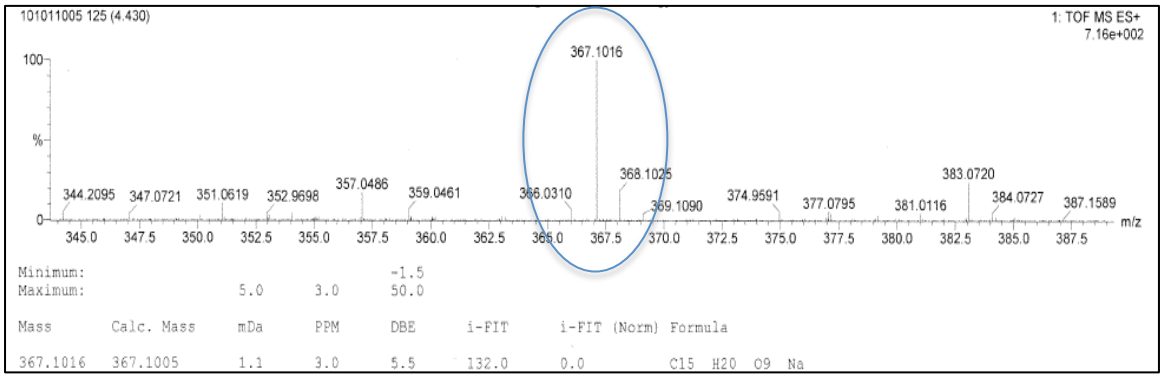

Figure 2.9: High mass accuracy analysis of IPO-glucuronide generated by mouse liver microsomes. Identification of a sodiated adduct of IPO-glucuronide with 3 ppm error. Analysis was performed on a Waters Synapt QTOF.

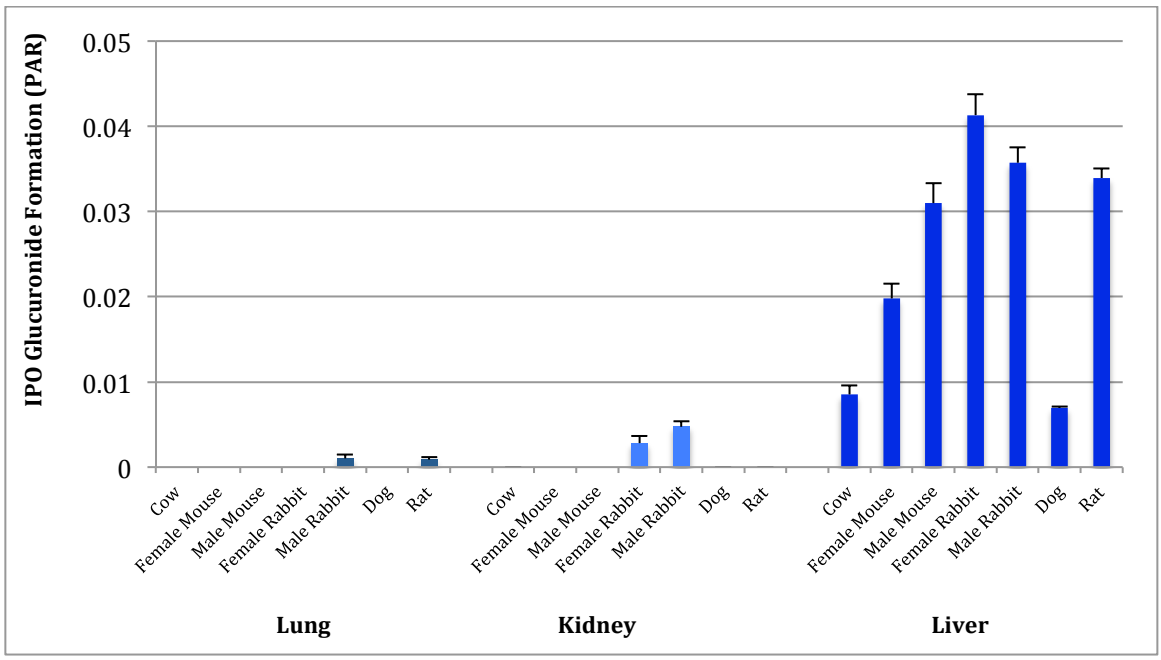

Figure 2.10: *In vitro* glucuronidation of IPO by liver, kidney and lung microsomes from various species. IPO is glucuronidated in the liver of every species examined. The only extrahepatic site of glucuronidation is rabbit kidney, however the rate is roughly 10x lower than the rate of glucuronidation in rabbit liver.

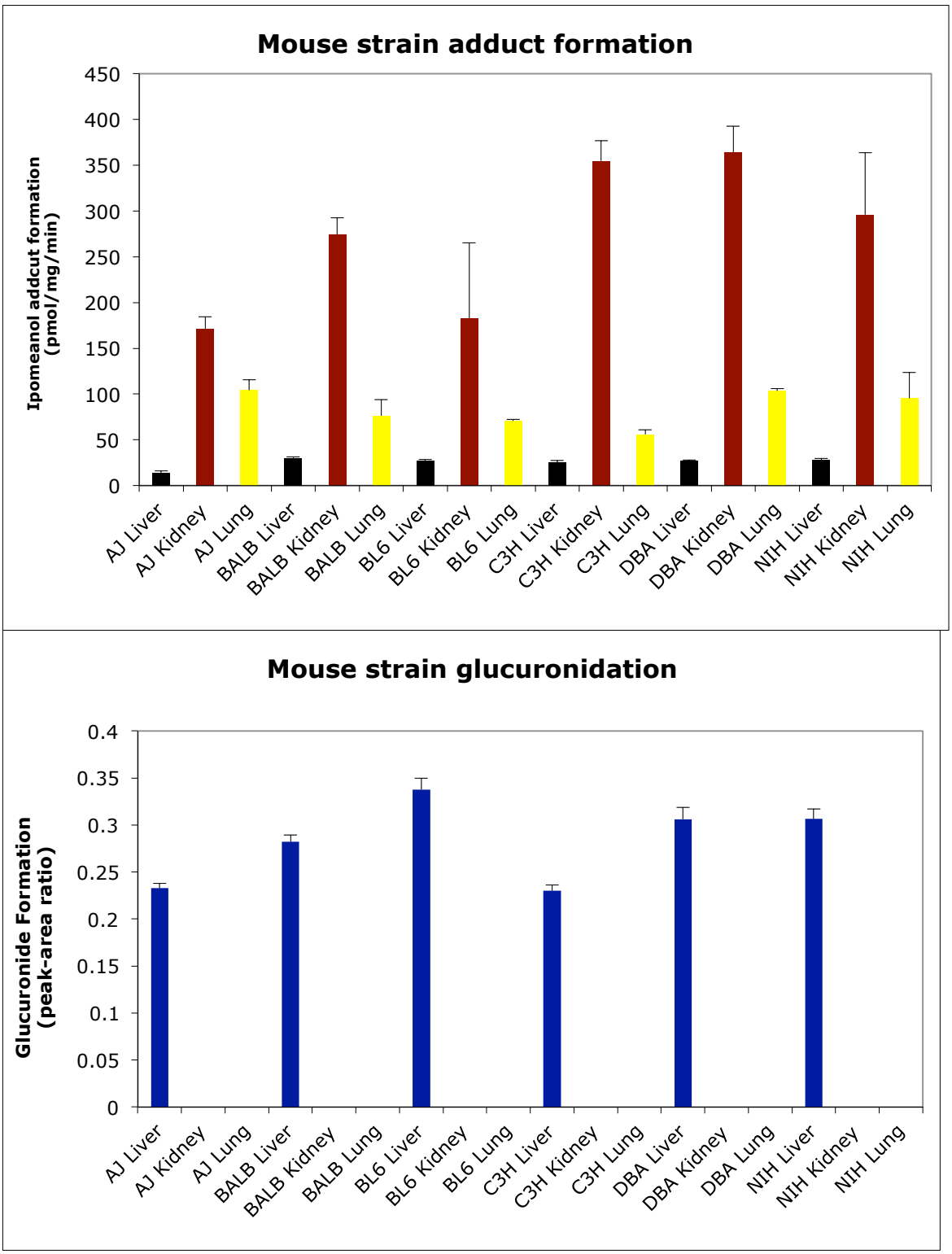

Figure 2.11: Activation measured via NAC/NAL adduct formation (top panel) and elimination measured via IPO-glucuronide formation(lower panel) in male microsomes from various mouse strains and tissues.

2.5 Notes to Chapter 2

1. Doster AR, Mitchell FE, Farrell RL, Wilson BJ. Effects of 4-Ipomeanol, a Product from Mold-Damaged Sweet Potatoes, on the Bovine Lung. Veterinary Pathology. 1978;15:367-75.

2. Monlux W, Fitte J, Kendrick G, Dubuisson H. Progressive Pulmonary Adenomatosis in Cattle. The Southwestern Veterinarian. 1953;6.

3. Spoto C. Moldy Sweet Potatoes Caused 200 Steer Deaths. Wausau Daily Herald. 2011 Jan. 28, 2011.

4. Steckel L, Rhodes N. Perilla Mint. University of Tennessee Agricultural Extension Publication w1352007.

5. Verschoyle RD, Philpot RM, Wolf CR, Dinsdale D. CYP4B1 Activates 4-Ipomeanol in Rat Lung. Toxicology and Applied Pharmacology. 1993;123:193-8.

6. Degawa M, Miura S, Hashimoto Y. Androgen-dependent renal microsomal cytochrome P-450 responsible for N-hydroxylation and mutagenic activation of 3-methoxy-4-aminoazobenzene in the BALB/c mouse. Cancer Res. 1990;50(9):2729-33.

7. Isern J, Meseguer A. Hormonal regulation and characterisation of the mouse Cyp4b1 gene 5'-flanking region. Biochem Biophys Res Commun. 2003;307(1):139-47.

8. Boyd MR, Burka LT. In vivo studies on the relationship between target organ alkylation and the pulmonary toxicity of a chemically reactive metabolite of 4-ipomeanol. The Journal of Pharmacology and Experimental Therapeutics. 1978;207(3):687-97.

9. Boyd MR, Burka LT, Wilson BJ, Sasame HA. In vitro studies on the metabolic activation of the pulmonary toxin, 4-ipomeanol, by rat lung and liver microsomes. The Journal of Pharmacology and Experimental Therapeutics. 1978;207(3):677-86.

10. Devereux TR, Jones KG, Bend JR, Fouts JR, Statham CN, Boyd MR. in Vitro Metabolic Activation of the Pulmonary Toxin, 4-Ipomeanol, in Nonciliated Bronchiolar Epithelial (Clara) and Alveolar Type II Cells Isolated from Rabbit Lung. The Journal of Pharmacology and Experimental Therapeutics. 1982;220:223-7.

11. Baer BR, Rettie AE, Henne KR. Bioactivation of 4-Ipomeanol by CYP4B1: Adduct Characterization and Evidence for an Enedial Intermediate. Chemical Research in Toxicology. 2004;18:855-64.

12. Miyata N, Taniguchi K, Seki T, Ishimoto T, Sato-Watanabe M, Yasuda Y, et al. HET0016, a Potent and Selective Inhibitor of 20-HETE Synthesizing Enzyme. British Journal of Pharmacology. 2001;133(3):325-9.

13. Seki T, Wang MH, Miyata N, Laniado-Schwartzman M. Cytochrome P450 4A isoform inhibitory profile of N-hydroxy-N'-(4-butyl-2-methylphenyl)-formamidine (HET0016), a selective inhibitor of 20-HETE synthesis. Biol Pharm Bull. 2005;28(9):1651-4.

14. Wang MZ, Saulter JY, Usuki E, Cheung YL, Hall M, Bridges AS, et al. CYP4F enzymes are the major enzymes in human liver microsomes that catalyze the O-demethylation of the antiparasitic prodrug DB289 [2,5-bis(4-amidinophenyl)furan-bis-O-methylamidoxime]. Drug Metab Dispos. 2006;34(12):1985-94. PMCID: 2077835.

15. Nakano M, Kelly EJ, Rettie AE. Expression and characterization of CYP4V2 as a fatty acid omega-hydroxylase. Drug Metab Dispos. 2009;37(11):2119-22. PMCID: 2774980.

16. Serabjit-Singh CS, Wolf CR, Philpot RM. The Rabbit Pulmonary Monooxygenase System. The Journal of Biological Chemistry. 1979;254(19):9901-7.

17. Statham CN, Dutcher JS, Kim SH, Boyd MR. Ipomeanol 4-glucuronide, a major urinary metabolite of 4-ipomeanol in the rat. Drug Metab Dispos. 1982;10(3):264-7.

18. Guengerich FP. Analysis and Characterization of Enzymes. In: Hayes AW, editor. Principles and Methods of Toxicology. New York: Raven Press; 1994. p. 1259-313.

19. Gasser R, Philpot RM. Primary structures of cytochrome P-450 isozyme 5 from rabbit and rat and regulation of species-dependent expression and induction in lung and liver: identification of cytochrome P-450 gene subfamily IVB. Mol Pharmacol. 1989;35(5):617-25.

20. Parandoosh Z, Fujita VS, Coon MJ, Philpot RM. Cytochrome P-450 isozymes 2 and 5 in rabbit lung and liver. Comparisons of structure and inducibility. Drug Metab Dispos. 1987;15(1):59-67.

21. Giantin M, Carletti M, Capolongo F, Pegolo S, Lopparelli RM, Gusson F, et al. Effect of breed upon cytochromes P450 and phase II enzyme expression in cattle liver. Drug Metab Dispos. 2008;36(5):885-93.

22. Robertson IG, Serabjit-Singh C, Croft JE, Philpot RM. The relationship between increases in the hepatic content of cytochrome P-450, form 5, and in the metabolism of aromatic amines to mutagenic products following treatment of rabbits with phenobarbital. Mol Pharmacol. 1983;24(1):156-62.

23. Rettie AE, Sheffels PR, Korzekwa KR, Gonzalez FJ, Philpot RM, Baillie TA. CYP4 Isozyme Specificiy and the Relationship between w-Hydroxylation and Terminal Desaturation of Valproic Acid. Biochemistry. 1995;34:7889-95.

24. Vanderslice RR, Domin BA, Carver GT, Philpot RM. Species-dependent expression and induction of homologues of rabbit cytochrome P-450 isozyme 5 in liver and lung. Mol Pharmacol. 1987;31(4):320-5.

25. Arinc E, Hanukoglu I, Sen A, Adali O. Tissue- and Species- Dependent Expression of Sheep Lung Microsomal Cytochrome P4502B(LgM2). Biochemistry and Molecular Biology International. 1995;37(6):1121-6.

26. Dutcher JS, Boyd MR. Species and strain differences in target organ alkylation and toxicity by 4-ipomeanol. Predictive value of covalent binding in studies of target organ toxicities by reactive metabolites. Biochem Pharmacol. 1979;28(23):3367-72.

Chapter 3

In vivo toxicity of 4-Ipomeanol in Wild-Type and *Cyp4b1* null mice

3.1 Introduction

4-Ipomeanol (IPO; 1-(3-Furyl)-4-hydroxy-1-pentanone) is a furanoterpenoid toxin produced by sweet potatoes (*Ipomoea batatas*) in response to infection by the mold *Fusariam solani* (1). IPO was discovered due to the poisoning of bovine livestock that ingested spoiled sweet potatoes and developed severe interstitial pneumonia, and research has shown that IPO is a pulmonary pro-toxin in a number of animals (1, 2). The first evidence that cytochrome P450 was involved in the bioactivation of IPO was provided by Boyd and coworkers at the NIH in 1978, who showed that production of an alkylating metabolite by rat lung and liver microsomes depended upon NADPH and oxygen and was inhibited by carbon monoxide and chemical inhibitors of the P450 system (3). Subsequently, the same group demonstrated protection against covalent binding of IPO to target pulmonary cell types with a similar chemical inhibitor strategy (4). Following the successful purification of multiple pulmonary P450 isoforms from rabbits, Philpot and coworkers demonstrated that covalent binding of electrophilic species derived from IPO to protein and to gluatathione occurred with two lung P450s that they termed P450I and P450II, known today as CYP2B4 and CYP4B1, respectively (5). The first study to investigate IPO bioactivation by human P450s, performed with recombinant enzymes expressed in HepG2 cell lysates; identified several P450 enzyme (CYP1A2, CYP2B7, CYP2F1, CYP3A3 and CYP3A4) as having bioactivating capabilities that were at least 3-fold

above that found with control HepG2 cell lysates (6). Interestingly, in that study, CYP1A2 was by far the most active human P450 in bioactivating IPO to reactive metabolites that bind to calf thymus DNA. More recently, Baer et al (7) reported human CYP1A2, CYP2C19, CYP2D6, CYP2E1 and CYP3A4 were the most active P450s for bioactivation of IPO to the reactive ene-dial that is trapped by NAC/NAL (see Chapter 4). A recurring theme is that, in addition to rabbit CYP4B1, enzymes of the CYP1A, 2B, CYP2C, 2D, 2F and CYP3A subfamilies are capable of IPO bioactivation. However, in terms of drawing conclusions about which of these varied P450 isoforms do, in fact, catalyze IPO bioactivation *in vivo*, there are several limitations. Firstly, it is unclear exactly which P450 isoforms are present in target tissues at sufficiently high levels to cause tissue damage in the intact organism. Secondly, all *in vitro* IPO bioactivation data available to date (except for that provided in Chapters 2 and 4) have been conducted at a single high IPO concentration (usually 0.5 to 1.0 mM) which is unlikely to reflect the physiological concentration of IPO (C_{max} = 50 μM) (8).

Despite these limitations, a plausible hypothesis is that CYP4B1 is primarily responsible for catalyzing IPO bioactivation in the lungs (and likely the kidney) of susceptible animal species. Chapter 2 of this thesis provides considerable support for this view. In addition, rabbit CYP4B1 has been identified as the most catalytically active P450 yet identified for IPO bioactivation *in vitro* (7). Moreover, in an *in vivo* study in rat, a chemical inhibitor of CYP4B1, p-xylene, protected rat lung against damage caused by IPO (9).

In mice, CYP4B1 has been linked to IPO toxicity based on the organ-specific expression pattern of CYP4B1 which correlates with the organ-specific toxicity of IPO (10, 11). CYP4B1 is expressed in both male and female mouse lung but is only expressed in the kidneys of male mice where expression is androgen-regulated (12, 13). This pattern of expression matches the toxicity observed in mice; IPO is a renal and pulmonary toxin in males but only a pulmonary toxin in females (10), indicating that CYP4B1 is potentially responsible for IPO-induced toxicity in mice. Despite the abundant circumstantial evidence, there is no direct link between CYP4B1-mediated activation of IPO and *in vivo* toxicity in mice. Therefore, the main goal of the studies reported in this chapter was to determine the role of murine CYP4B1 in the bioactivation of IPO *in vivo* using *Cyp4b1* knockout mice.

The extent of toxicity caused by a pro-toxin is related to the relationship between the rates of activation and the rates of deactivation/elimination. In the case of IPO, activation is mediated by cytochrome P450, and elimination is likely mediated by phase II metabolism. Statham et al. showed that IPO is extensively glucuronidated in the rat to the extent that 23% of the administered dose of IPO can be recovered in the urine as the glucuronide conjugate (14). Therefore, a secondary goal of this study was to determine if mice produce IPO-glucuronide, *in vitro* and *in vivo*.

3.2 Experimental Procedures

Materials

N-acetylcysteine (NAC), N-acetyllysine (NAL), CHAPS, β-glucuronidase, 4-methylumbelliferone glucuronide (4-MBG), NADPH, UDPGA, $MgCl_2$, EDTA, potassium ferricyanide, potassium ferrocyanide and X-gal were purchased from Sigma Aldrich (St. Louis, MO). IPO was a gift from the National Cancer Institute (Bethesda, MD). HET0016 (N'-hydroxy-N-(4-n-butyl-2-methylphenyl)formamidine) was provided by Kayte Edson (University of Washington).

Goat anti-CYP4B1 IgG (raised against rabbit CYP4B1) was a kind gift of Dr. R.M. Philpot (15). The antibody was used to visualize the presence of CYP4B protein(s) in microsomes by western blotting at a dilution of 1:5000 and visualized using a donkey anti-goat IRDye® 800CW secondary antibody from LI-COR Biosciences (Lincoln, Nebraska USA).

Microsomes were prepared by differential centrifugation according to previously published protocols (16) from frozen tissue pooled from five animals.

Production and characterization of Cyp4b1 -/- mice

Embryonic stem cells (clone G-01) bearing a targeted disruption of the *Cyp4b1* gene were obtained from the KOMP repository (http://www.komp.org/, Univ. CA, Davis). The cells were expanded on mouse embryonic feeder cells and chimeric mice were generated with the assistance of the UW Transgenic Core Facility (Warren Ladiges, DVM, Director). In brief, ES cells (15-20) were injected into host albino C57Bl/6 blastocysts and implanted into pseudopregnant female CD-1 mice obtained from Jackson Laboratories (Bar Harbor,

ME). The resultant offspring (80 to > 95 % coat color chimerism) were back-crossed to albino C57Bl/6 mice to test for germline transmission. Evidence of germline transmission by black coat color was used to select animals for *Cyp4b1* genotyping; heterozygous *Cyp4b1* +/- mice were intercrossed to generate *Cyp4b1* -/- knockouts. The targeting vector designed by CSD/KOMP includes a splice acceptor-beta Galactosidase (*lacZ*) reporter just downstream of exon 1 of the *Cyp4b1* gene (Figure 1). This abolishes CYP4B1 function while placing *lacZ* expression under the control of the mouse *Cyp4b1* gene promoter. To date, >5 generations of knockout mice have been propagated with no overt phenotype and normal viability/fertility. Development of the strategy for the establishment and genotyping of the *Cyp4b1* null mouse colony were performed in the laboratory of our collaborator, Dr. Edward Kelly (Dept. Pharmaceutics, Univ. of Washington).

Cyp4b1 genotyping

Primers were designed to detect the lacZ reporter gene and the disruption of the *Cyp4b1* gene and purchased from Integrated DNA Technologies (San Diego, CA). Specifically, lacZ primers assessed the presence of the beta-galactosidase reporter gene, and *Cyp4b1* primers assessed the presence of wild-type *Cyp4b1*.

lacZ-FOR: 5'TAA TAG CGA AGA GGC CCGC3'

lacZ-REV: 5'CGC CAC ATA TCC TGA TCT TCC3'

Cyp4b1–FOR: 5' GGC AAG GAG CAA AAA TGA TA3'

Cyp4b1-REV: 5'CAC AGA AAT GTG TTG CCA AG3'

DNA was isolated from tail snips and processed using a DNeasy Blood and Tissue Kit (Qiagen, MD). Genes were amplified using hot-start PCR – (95^{o}C for 2 minutes, 94 ^{o}C for 30 seconds, 57^{o}C for 30 seconds, 72^{o}c for 2 minutes) x 35 cycles, 72^{o}C or 5 minutes. Amplicons were resolved using 1% agarose gel electrophoresis.

LacZ staining of CYP4B1 KO tissues

Animals were sacrificed by carbon dioxide narcosis followed by exsanguination and cardiac puncture. Liver and kidney sections were removed and placed in fixative (4% paraformaldehyde/PBS pH 7.0). Lungs were fixed by severing the trachea and injecting fixative through down the airway into the lungs to fill and expand the lungs in order to improve visualization of the airways and to ensure penetration of the staining solution into the terminal bronchioles. Tissues were stored for 1 hour in fixative at 4^{o}C followed by 3x30 minute rinses with PBS at room temperature. Tissues were then stained for 24 hours in staining solution (0.5 M potassium ferricyanide, 0.5 M potassium ferrocyanide, and 1 mg/mL X-gal) at room temperature. Tissues were then rinsed in PBS and fixed overnight in 10% formalin at 4^{o}C.

RT- PCR analysis of CYP4B1 expression

Comparison of *Cyp4b1* gene expression across tissues in wild type male and female C57Bl/6 adult mice (n=3) was determined by Real-Time PCR using the ΔΔCt method with 18S as the housekeeping gene. The Taqman™ primers and probe for each geen were purchased from Applied Biosystems (Foster City, CA). In brief, total RNA was isolated using Tri-reagent (Invitrogen) quantified spectrophotometrically. For cDNA synthesis, 1 μg

RNA was mixed with Applied Biosystem's Taqman reverse transcription kit was used with random hexamer primers and the equivalent of 100 ng total RNA amplified in each RT PCR reaction with triplicates for each gene. Values are normalized to male lung CYP4B1 expression. Genes were amplified using hot-start PCR – (95^{o}C for 10 minutes followed by 40 cycles of 95^{o}C for 15 seconds, 60^{o}C for 60 seconds) cycles, 72^{o}C or 5 minutes.

Western blot analysis of cytochrome P450 expression

To confirm that disruption of the *Cyp4b1* gene eliminated expression of CYP4B1 while not affecting expression of other P450 enzymes, we conducted western blot analysis comparing WT and knockout tissue probed for various P450 enzymes in liver, kidney and lung microsomes. Microsomal samples were diluted in NuPAGE sample reducing agent and sample buffer from Invitrogen (Grand Island, NY). Microsomal protein (20 µg) was separated on a 4-12% Bis-Tris gel and transferred to a nitrocellulose membrane. Membranes were blocked overnight at 4^{o}C in Odyssey™ blocking buffer obtained from Li-Cor (Lincoln, NE) followed by probing with 1^{o} antibody (α-CYP2F2, α-CYP1A, α-CYP3A, α-CYP2B, and α-CYP2A) from Santa-Cruz Biotech (Santa Cruz, CA), (α-CYP2E and α-CYP2D) from Gentest (San Jose, CA) and α-CYP4B1 in blocking buffer and 0.1% Tween at room temperature for 60 minutes. Membranes were washed 3 times for 5 minutes each in PBS followed by incubating with the species-appropriate IRDye 800 CW secondary antibody in blocking buffer and 0.1% Tween for 1 hour. Membranes were washed 3 times for 5 minutes each in PBS and dried followed by visualization on an Odyssey imaging system.

Cyp4b1 KO in vivo study

All protocols involving the use of animals were approved by the Institutional Animal Care and Use Committee at the University of Washington (Seattle, WA) and were performed in accordance with the NIH Guide for the Use and Care of Laboratory Animals. C57/BL6 mice were obtained from Jackson Laboratories (Bar Harbor, ME). Animals were kept on a 12-hour light/dark cycle and provided water and rodent chow ad libitum.

Animals were weighed and given 20 mg/kg ipomeanol IP at hour 0 and moved to metabolic cages for urine collection and monitored hourly for signs of distress. Mice were sacrificed by carbon dioxide narcosis followed by exsanguination at hour 18. Liver, kidney and lung were harvested and fixed in formalin (as described for lacZ staining) for histopathological analysis (analysis performed by Dr. Denny Liggitt in the Department of Comparative Medicine, University of Washington). Heparinized plasma was collected by centrifuging collected blood at 13,000xg for 5 minutes. Urine was prepared for analysis by centrifugation for 10 minutes at 4000xg and filtered through a sterile 0.2 μM PES filter.

In vitro bioactivation

In vitro bioactivation of IPO was assessed by incubating microsomal preparations in triplicate with according to the method described in chapter 2.

Glucuronidation of IPO

In vitro glucuronidation of IPO was assessed by incubating microsomal preparations in triplicate according to the method described in chapter 2.

3.3 Results

Characterization of *Cyp4b1* knockouts.

Genotyping of CYP4B1 mice confirms the presence of the lacZ locus and disruption of the native *Cyp4b1* gene (data not shown) however to further demonstrate targeted site and tissue specific expression of the vector we performed X-gal staining on tissues harvested from *Cyp4b1* null animals. Whole-mount visualization of mouse lung in Figure 3.2 indicates that pulmonary expression of β-galactosidase is limited to the airways; microscopic inspection proves that expression is limited to Clara cell-rich bronchi and bronchioles which is characteristic of CYP4B1 *(9)*. Staining and analysis of kidneys harvested from knockout mice indicates that expression of β-galactosidase follows the same pattern as expression of CYP4B1 in wild-type mice. Expression is restricted to the cortex and expression is significantly higher in male mice than female mice, indicating that renal expression of the reporter is androgen-dependent and localized to the same sites of expression as wild-type CYP4B1. Microscopic localization within the cortex was primarily in proximal convoluted tubules with no evidence for glomeruli staining (data not shown). Lack of staining in the liver is evidence of no β-galactosidase activity, which correlates to a lack of hepatic CYP4B1 expression (data not shown).

Western blot analysis of CYP4B1 expression in the tissues of KO and wild-type mice confirms that incorporation of the lacZ-containing vector results in an absence of CYP4B1 protein in KO mice. As expected, protein expression is high, exhibited by a single strong

band (Figure 3.3) in male wild-type lung and kidney and female wild-type lung in keeping with constitutive expression in male and female lung and androgen-dependent renal CYP4B1 expression. There is no detectable CYP4B1 in female kidney or wild-type livers of either sex. Figure 3.3 also indicates that knockout mice have no immuno-detectable CYP4B1 in any tissue. This confirms targeted disruption of the *Cyp4b1* gene by the targeting vector results in a lack of expression of functional CYP4B1 protein *in vivo*.

Western blot analysis of P450 expression in mouse tissue microsomes from both WT and KO animals indicates that there is no significant compensatory upregulation in the expression of CYP1A, CYP2A, CYP2B, CYP2D, CYP2E, CYP3A or CYP2F enzymes in lung liver or kidney as a result of disruption of the *Cyp4b1* locus (Figure 3.4).

IPO-adduct formation rates in microsomes made from mouse tissue harvested from both *Cyp4b1* null and wild-type mice indicate that CYP4B1 plays a significant role in the bioactivation of IPO. Adduct formation rates are highest in male renal microsososomes followed by male and female pulmonary microsomes; NAC/NAL adduction rates correlate well with the CYP4B1 content of microsomes (Table 3.2). Furthermore, the potent CYP4 inhibitor HET0016 strongly inhibits (80-90% inhibition) IPO-adduct formation in male and female pulmonary and male renal microsomes, tissues with high CYP4B1 expression, but has little affect on adduct formation in hepatic or female renal microsomes (<10% inhibition) where CYP4B1 is poorly expressed (Figure 2.6). These data indicate that *in vitro* bioactivation of IPO is primarily mediated by CYP4B1.

Figure 2.8 shows that in the presense of UDPGA, mouse liver microsomes produce glucuronide-metabolite that can be detected by LC/MS/MS which fragments m/z 367 → 191 corresponding to sodiated IPO-glucuronide undergoing a neutral loss of 176 Da. This is indicative of fragmentation of IPO-glucuronide via loss of the sugar moiety to sodiated IPO. This metabolite can be eliminated by post-incubation treatment with β-glucuronidase, an enzyme that cleaves glucuronide conjugates. High mass-accuracy analysis of this metabolite (Figure 2.9) indicate that the observed mass of 367.1016 corresponds to the calculated mass of $C_{15}H_{20}O_9Na$ 367.1005, the formula of sodiated IPO-glucuronide, with an error of 3 ppm. The dependence on co-incubation with UDPGA, which is a required cofactor for UDP-glucuronosyltransferases (UGTs), of the metabolite, the eradication of the metabolite by β-glucuronidase and the high mass-accuracy correlation with the calculated mass of IPO-glucuronide together indicate that mouse liver microsomes glucuronidate IPO. Table 3.2 demonstrates that IPO is readily glucuronidated in liver microsomes from both male and female mice. There is essentially no production of IPO-glucuronide in renal or pulmonary microsomes harvested from either male or female mice.

An identical metabolite was also found in the urine of mice treated with IPO. This metabolite was readily detectable in urine from both males and females of both genotypes and susceptible to destruction by β-glucuronidase and confirmed by high mass-accuracy mass spectrometry. These data are the first to demonstrate phase II metabolism and elimination of IPO in mice via a glucuronidation pathway.

Results of the *in vivo* study indicate that disruption of the *Cyp4b1* gene is protective in mice exposed to IPO (Figure 3.5). When treated at the LD_{50}, wild-type mice developed pulmonary lesions characterized by significantly widened perivascular/peribronchiolar spaces containing engorged lymphatics and extravascular fluid as well as fibrin strands. Wild-type mice also displayed scattered, focal thickening of alveolar walls and accumulation of mononuclear cells into perivascular spaces. Similar lesions were not evident in *Cyp4b1* KO mice indicating that CYP4B1 is required to activate IPO *in vivo*. Consistent with the androgen-mediated kidney expression, we did observe moderate renal toxicity in two of the four IPO-treated wild-type male mice which was not evident in female mice of either genotype or male knockout mice. The cortices of affected kidneys were characterized histologically by several changes which principally affected renal tubular epithelium (Figure 3.6B). These changes included frequent condensation of renal tubular epithelium sometimes closely adjacent to swollen and vacuolated tubular epithelium. In addition there was widely scattered necrosis and sloughing of tubule lining cells. Occasional accumulation of dark pink proteinaceous fluid within tubule lumens is consistent with some degree of glomerular injury although histologic changes to glomerular tufts were not noticeable.

3.4 Discussion

We have generated a *Cyp4b1* null mouse utilizing a targeting vector designed by CSD/KOMP which includes a splice acceptor-β-balactosidase (*lacZ*) reporter just downstream of exon 1 of the *Cyp4b1* gene (Figure 3.1). This abolishes CYP4B1 function

while placing *lacZ* expression under the control of the mouse *Cyp4b1* gene promoter. We have confirmed disruption of the *Cyp4b1* gene as well as site-specific expression of *lacZ* at the known sites of CYP4B1 expression including pulmonary Clara cells and the cortex of male kidneys. Furthermore there is no evidence of an altered phenotype in *Cyp4b1* null mice relative to WT mice.

Predictably, disruption of *Cyp4b1* eliminates protein expression in microsomes of *Cyp4b1* null mice. In WT mice, CYP4B1 is highly expressed in the kidney and lung of males and the lung of females as evidenced by western blotting and RT PCR (Figure 3.3 and Table 3.1). We see no evidence of CYP4B1 expression in the liver of WT or KO mice of either sex. In *Cyp4b1* null mice there is no detectable CYP4B1 protein in any of the tissues we examined. We conclude that we have successfully produced viable *Cyp4b1* null mice with no detrimental effects resulting from disruption of the gene.

It is possible that elimination of a P450 enzyme can lead to up-regulation of other P450 enzymes to compensate for the disruption of the endogenous functions of the target gene. This possible compensation by other enzymes may mask the loss of the target gene making utilization of the knockout in toxicity studies ineffective if CYP4B1-mediated reaction pathways remain intact. To eliminate this possibility we conducted western blot analysis of IPO target tissues (kidney and lung) and the liver to determine relative levels of expression of the major P450 families in *Cyp4b1* null and WT mice. Our data indicate that expression of CYP enzymes from the 1A, 2A, 2B, 2D, 2E, and 3A families, as well as expression of CYP2F2, is not affected by disruption of the *Cyp4b1* locus. Therefore we can

conclude that differences in activation or metabolism of xenobiotics between knockout and wild-type mice, as well as differences in toxicity in response to pro-toxins, are due to the loss of functional CYP4B1 in the knockout mice and do not result from altered expression of other P450 enzymes as compensation for the lack of CYP4B1 activity.

These data are the first to demonstrate phase II-mediated metabolism of IPO in mice both *in vitro* and *in vivo*. Mouse liver microsomes from both sexes readily produce IPO-glucuronide in the presence of CHAPS and UDPGA. The glucuronide conjugate can be eliminated by β-glucuronidase. This metabolite was analyzed using high mass accuracy mass spectrometry to confirm the accurate mass of 367.1016 which corresponds to a sodiated adduct of IPO-glucuronide. There is no evidence of glucuronidation in extrahepatic tissues. Furthermore we have confirmed the presence of IPO-glucuronide in the urine of both male and female mice. Phase II metabolism of IPO via UGT-mediated glucuronidation may be an important elimination pathway of IPO *in vivo* in the mouse as it is in the rat where half the administered dose of IPO was recovered as the glucuronide conjugate in the urine (14). Indeed glucuronidation rates in mouse liver microsomes are similar to glucuronidation rates in rat liver microsomes (Chapter 2). If *in vitro* glucuronidation rates are predictive of glucuronidation *in vivo*, UGT-mediated glucuronidation is likely to be an important elimination pathway of IPO. The lack of a functional elimination pathway in kidney and lung coupled with high rates of IPO activation in these tissues explains the prevalence of IPO induced toxicity in murine kidney (males) and lung.

The *in vitro* data indicate that IPO adduct formation rates are high in male lung and kidney microsomes and female lung microsomes but are low in female kidney microsomes and liver microsomes of both sexes. This pattern of activation is identical to the pattern of expression of CYP4B1 we have demonstrated via RT PCR and western blotting. As expected, *in vitro* activation rates are significantly decreased in microsomes from *Cyp4b1* null mice in male kidney and lung microsomes as well as female lung microsomes. Activation rates in female lung and all liver microsomes are unaffected by disruption of *Cyp4b1*. These data correlate with HET0016 mediated CYP4 inhibition of IPO activation which follows the identical pattern. Therefore we conclude that CYP4B1 is the enzyme primarily responsible for activating IPO *in vitro* in the primary sites of IPO toxicity in the mouse.

Our *in vitro* data strongly correlate with the data obtained in the *Cyp4b1* KO IPO toxicity study. Based on histopathological analysis of IPO-treated mice, male WT mice experienced both renal and pulmonary toxicity. WT female mice experienced pulmonary toxicity. The sites of toxicity mirror the sites of CYP4B1 expression which is in all murine lungs and high in male kidney where expression is androgen regulated. The sites of toxicity observed indicate that high *in vitro* microsomal activation is predictive of *in vivo* toxicity because the microsomes with the highest activation rates are from the lung and male kidney. No toxicity was observed in any *Cyp4b1* null mice, indicating that CYP4B1 expression and activity is the primary determinant of IPO related toxicity in mice.

We have demonstrated in mice that activation of IPO and its subsequent toxicity is mediated by CYP4B1 and that elimination of IPO occurs, at least in part, *via* glucuronidation. Disruption of *Cyp4b1* mitigates the toxic effects of IPO *in vivo*, and the pattern of toxicity in wild-type mice correlates to the pattern of expression of CYP4B1. This proves that CYP4B1 is integral in the bioactivation of IPO in mice and that IPO-adduct formation *in vitro* is predictive of toxicity *in vivo*.

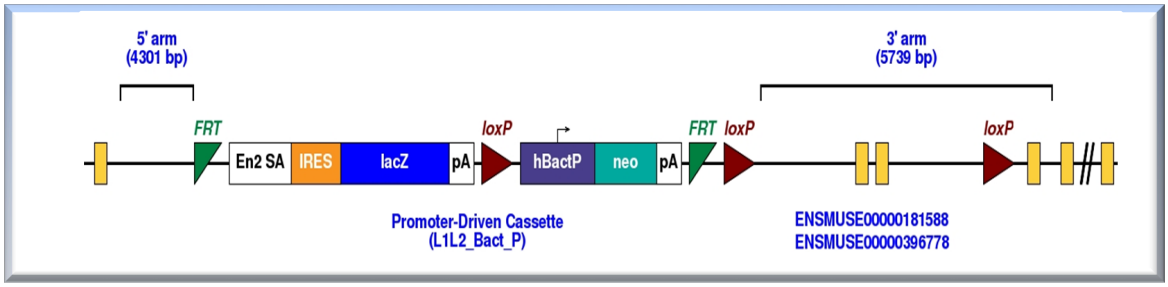

Figure 3.1: Knockout mouse vector. The target vector was constructed by CSD as part of the NIH knockout mouse project (KOMP). The targeting vector design by CSD/KOMP includes a splice acceptor-beta Galactosidase (*lacZ*) reporter just downstream of exon 1 of the *Cyp4b1* gene. This abolishes CYP4B1 expression while placing *lacZ* expression under the control of the mouse *Cyp4b1* gene promoter.
http://www.knockoutmouse.org/martsearch/project/30462

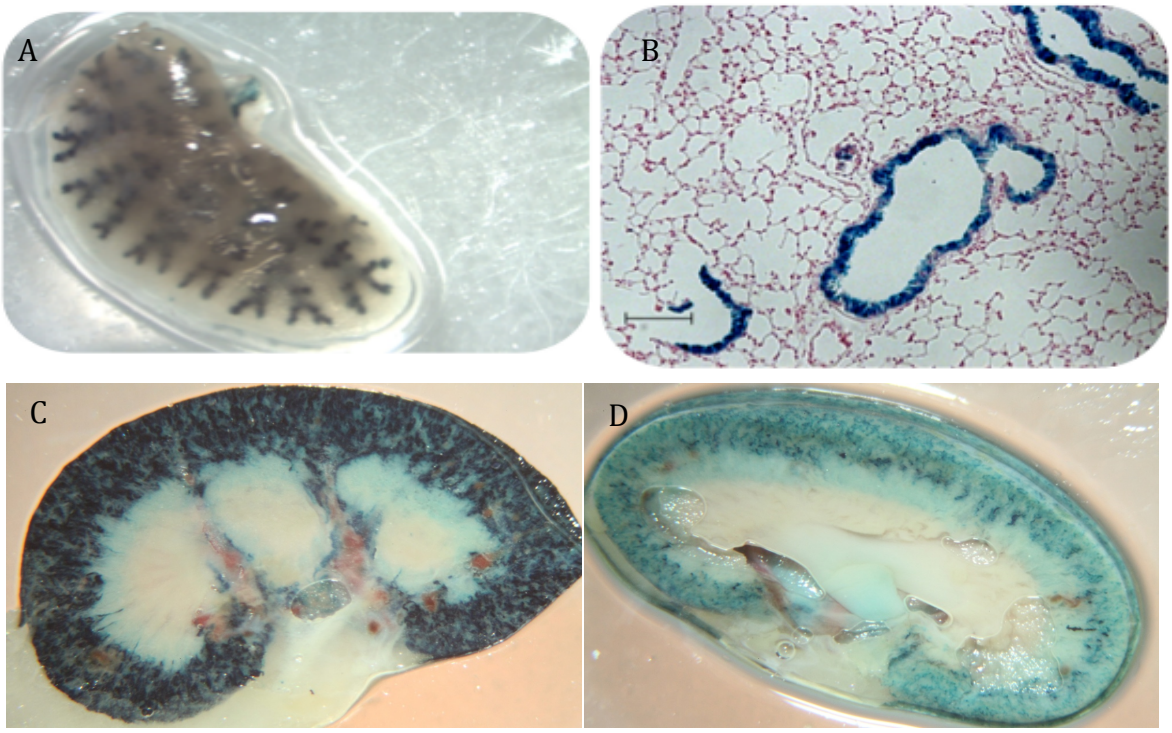

Figure 3.2: (A) Mouse lung lobe from *Cyp4b1* null mice stained with the chromogenic substrate X-Gal. LacZ activity was readily apparent in large airways and terminal bronchioles. **(B)** Microscopic evaluation of mouse lung section from lobe in figure 7 using NuclearFast red counter stain (Bar = 100 μM). Staining/CYP4B1 expression is restricted to bronchioles and absent from alveoli. **(C)** Whole-mount staining of male and female **(D)** mouse kidney showing localization of *lacZ/Cyp4b1* expression in the cortex. Micrscopic evaluation revealed specific localization to the proximal convoluted tubule (data not shown). Expression of *lacZ/Cyp4b1* in male kidney is significantly higher than in female kidney.

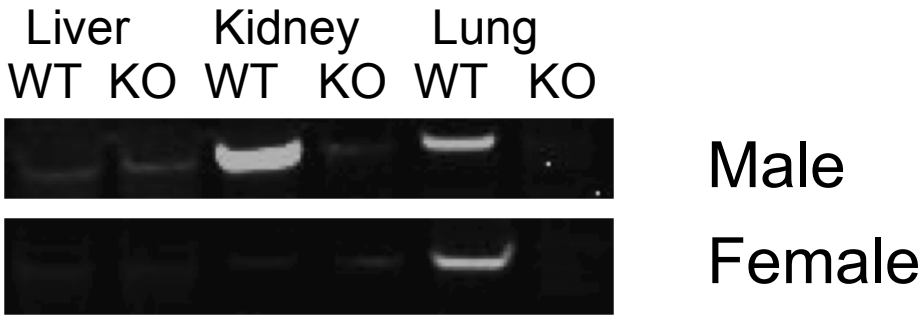

Figure 3.3: Immunoblots of mouse liver, kidney and lung microsomes harvested from wild-type and *Cyp4b1* null mice (pool of 5) probed with goat α–rabbit CYP4B1 antibody (20 μg microsomal protein added per well). CYP4B1 is highly expressed in the lung of male and female wild-type mice and the kidney of wild-type male mice. No CYP4B1 protein is detectable in tissues harvested from *Cyp4b1* null mice.

SEX	Relative *Cyp4b1* Tissue Gene Expression		
	Lung	Kidney	Liver
♂	1.00 (0.63-1.59)	1.32 (1.21-1.43)	0.004 (0.002-0.005)
♀	0.67 (0.57-0.80)	0.16 (0.15-0.17)	0.008 (0.006-0.009)

Table 3.1: *Cyp4b1* gene expression in various tissues in male and female C57Bl/6 mice. RNA was collected from tissues from three eight-week old mice of each sex. Expression levels are reported relative to male lung *Cyp4b1* expression which is set at 1.0 with 18s rRNA as the housekeeping gene.

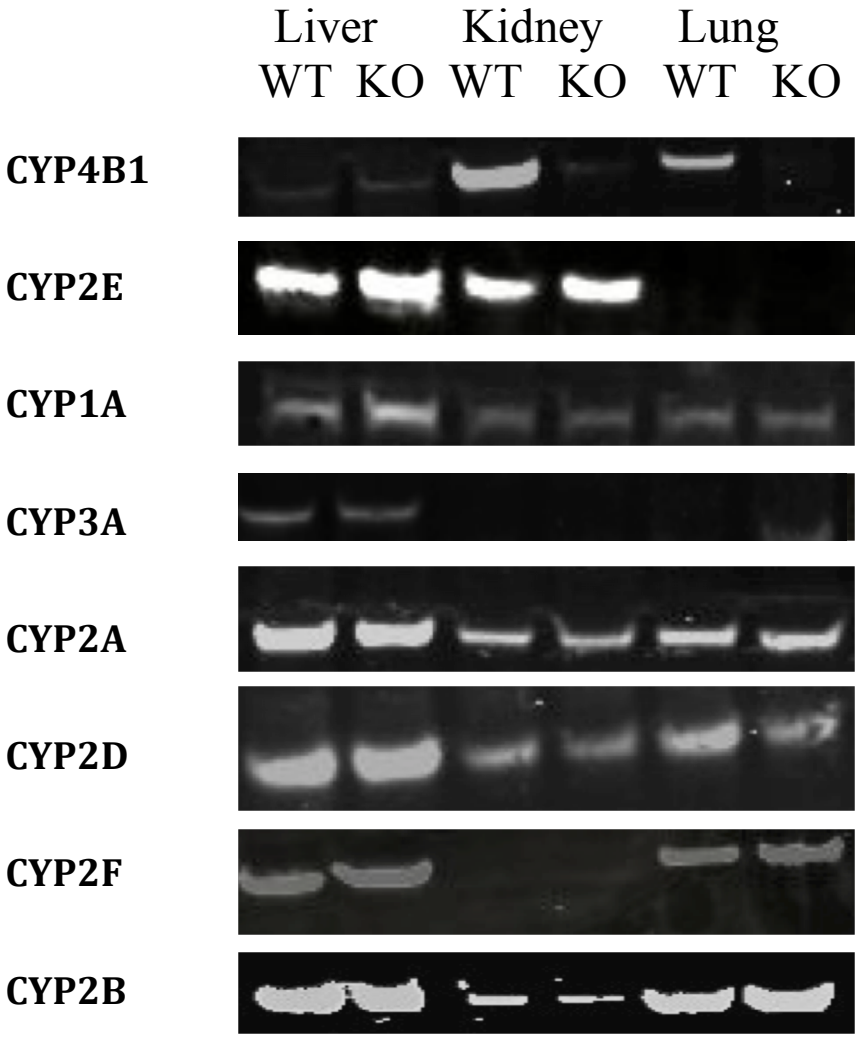

Figure 3.4: Immunoblots of mouse liver, kidney and lung microsomes harvested from wild-type and *Cyp4b1* null mice (20 µg microsomal protein added per well) probed with antibodies against selected P450 enzymes as noted and described in the methods. (20 µg microsomal protein added per well). Disruption of *Cyp4b1* did not lead to significant changes in the expression of other P450 enzymes.

	IPO bioactivation (pmol/mg/min)					
	M Liver	M Kidney	M Lung	F Liver	F Kidney	F Lung
WT	18.1 ± 0.86	230.4 ± 40.2	56.7 ± 5.9	20.7 ± 7.5	1.04 ± 0.19	73.4 ± 7.3
Cyp4b1 KO	13.9 ± 1.8	1.5 ± 0.37	5.8 ± 0.18	22.1 ± 1.4	2.4 ± 1.96	3.3 ± 1.1
	IPO glucuronidation (% male WT liver activity)					
	M Liver	M Kidney	M Lung	F Liver	F Kidney	F Lung
WT	100 ± 6.3	0.82 ± 0.1	1.2 ± 1	57.8 ± 5	0.79 ± 0.2	0.86 ± 0.6
Cyp4b1 KO	105.1 ± 4.8	0.79 ± 0.6	3.6 ± .09	71.2 ± 3.6	0.43 ± 0.2	1.4 ± .7

Table 3.2: *In vitro* activation and glucuronidation of IPO. *Cyp4b1* null mice exhibited >95% decrease in microsomal IPO activation by male and female lung but no change in activation rates in liver where CYP4B1 is not expressed (see Figure 3.3). IPO is glucuronidated only in the liver of both wild-type and *Cyp4b1* null mice. As expected, gene disruption of *Cyp4b1* has no significant effect on the rate of IPO glucuronidation in male or female mice.

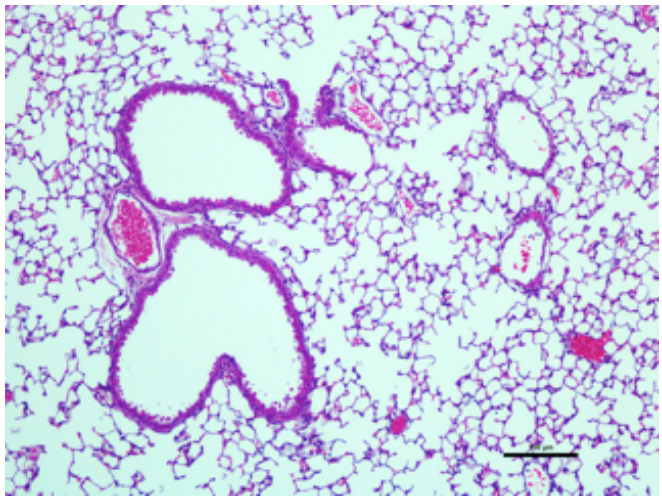

Figure 3.5A: Histology of *Cyp4b1* null mouse lung treated with 20 mg/kg IPO (HE 4x). *Cyp4b1* null mice exhibit no overt signs of toxicity.

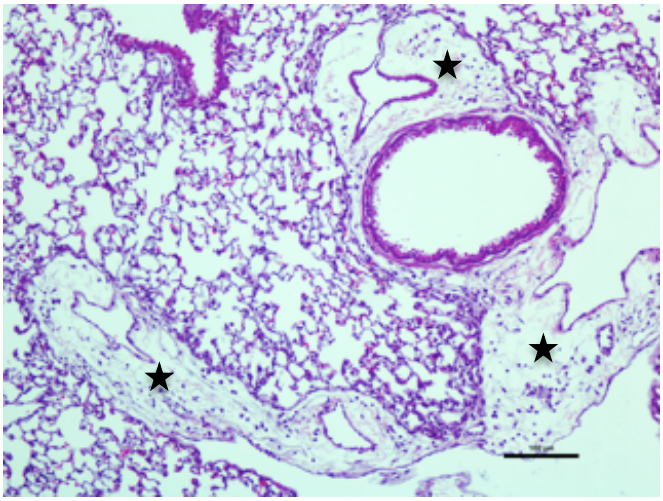

Figure 3.5B: Histology of IPO-treated wild-type mouse lung (HE 10x). The stars indicate significantly widened perivascular spaces. These spaces contain engorged lymphatics and extravascular fluid (washed out in processing) as well as scattered mononuclear inflammatory cells and some fine fibrin strands.

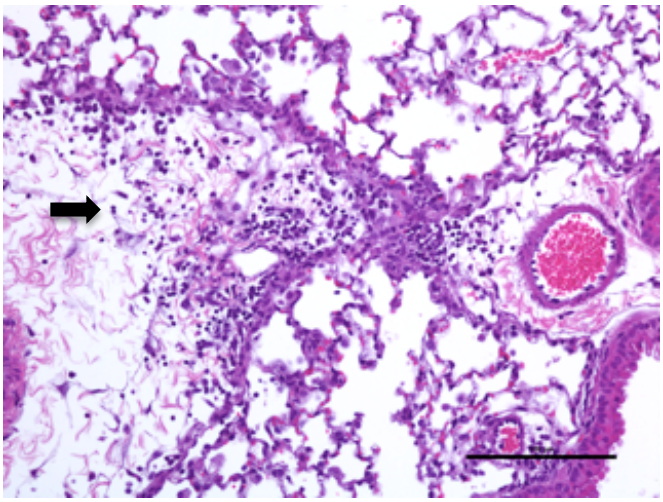

Figure 3.5C: Histology of IPO-treated wild-type mouse lung (HE 20x). The arrow indicates significantly widened perivascular space containing a focal cluster of mononuclear inflammatory cells. Surrounding alveolar walls are also slightly thickened by inflammatory cell and fluid accumulations.

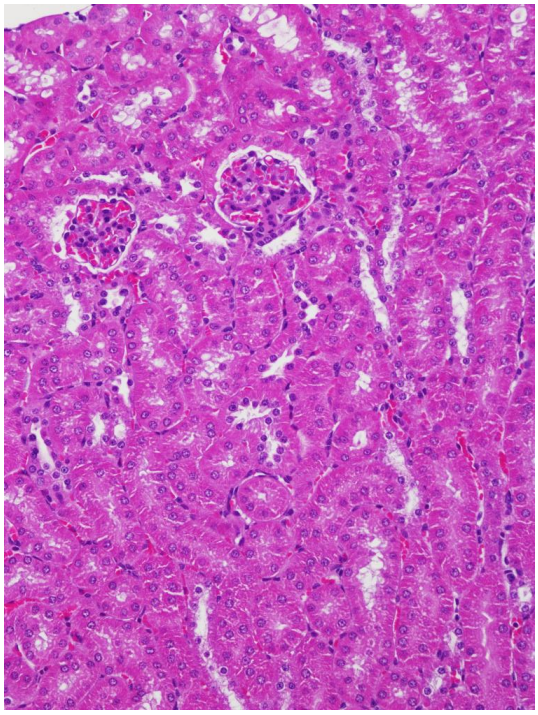

Figure 3.6A: Histology of IPO-treated *Cyp4b1* null mouse male kidney(HE 40x). *Cyp4b1* null mice exhibit no overt signs of toxicity.

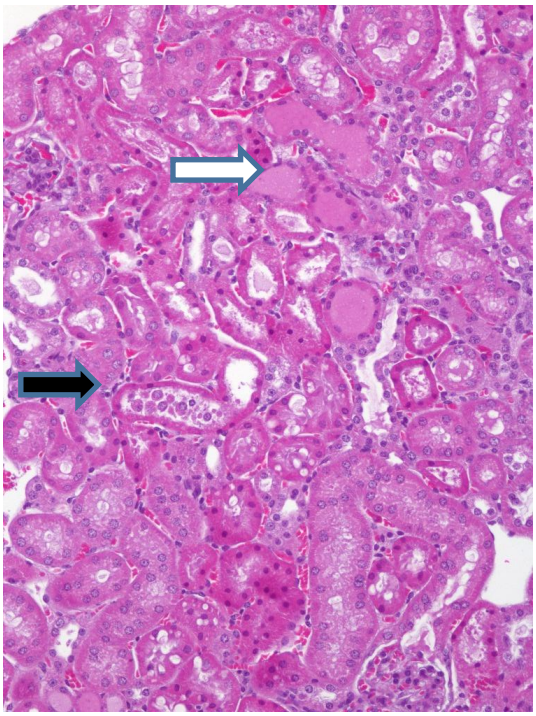

Figure 3.6B: Histology of IPO-treated wild-type mouse male kidney(HE 40x). The kidneys of wild-type male mice showed signs of proteinurea (white arrow) and necrotic and sloughed epithelium (black arrow).

3.5 Notes to Chapter 3

1. Doster AR, Mitchell FE, Farrell RL, & Wilson BJ (1978) Effects of 4-Ipomeanol, a Product from Mold-Damaged Sweet Potatoes, on the Bovine Lung. *Veterinary Pathology* 15:367-375.

2. Garst JE*, et al.* (1985) Species susceptibility to the pulmonary toxicity of 3-furyl isoamyl ketone (perilla ketone): in vivo support for involvement of the lung monooxygenase system. (Translated from eng) *J Anim Sci* 60(1):248-257 (in eng).

3. Boyd MR & Burka LT (1978) In vivo studies on the relationship between target organ alkylation and the pulmonary toxicity of a chemically reactive metabolite of 4-ipomeanol. (Translated from eng) *The Journal of Pharmacology and Experimental Therapeutics* 207(3):687-697 (in eng).

4. Devereux TR*, et al.* (1982) in Vitro Metabolic Activation of the Pulmonary Toxin, 4-Ipomeanol, in Nonciliated Bronchiolar Epithelial (Clara) and Alveolar Type II Cells Isolated from Rabbit Lung. *The Journal of Pharmacology and Experimental Therapeutics* 220:223-227.

5. Wolf CR*, et al.* (1982) The relationship between the catalytic activities of rabbit pulmonary cytochrome P-450 isozymes and the lung-specific toxicity of the furan derivative, 4-ipomeanol. (Translated from eng) *Mol Pharmacol* 22(3):738-744 (in eng).

6. Czerwinski M*, et al.* (1991) Metabolic activation of 4-ipomeanol by complementary DNA-expressed human cytochromes P-450: evidence for species-specific metabolism. (Translated from eng) *Cancer Res* 51(17):4636-4638 (in eng).

7. Baer BR, Rettie AE, & Henne KR (2004) Bioactivation of 4-Ipomeanol by CYP4B1: Adduct Characterization and Evidence for an Enedial Intermediate. *Chemical Research in Toxicology* 18:855-864.

8. Kasturi VK*, et al.* (1998) Phase I study of a five-day dose schedule of 4-Ipomeanol in patients with non-small cell lung cancer. (Translated from eng) *Clin Cancer Res* 4(9):2095-2102 (in eng).

9. Verschoyle RD, Philpot RM, Wolf CR, & Dinsdale D (1993) CYP4B1 Activates 4-Ipomeanol in Rat Lung. *Toxicology and Applied Pharmacology* 123:193-198.

10. Boyd MR & Burka LT (1978) In vivo studies on the relationship between target organ alkylation and the pulmonary toxicity of a chemically reactive metabolite of 4-ipomeanol. (Translated from eng) *J Pharmacol Exp Ther* 207(3):687-697 (in eng).

11. Boyd MR, Burka LT, Wilson BJ, & Sasame HA (1978) In vitro studies on the metabolic activation of the pulmonary toxin, 4-ipomeanol, by rat lung and liver microsomes. (Translated from eng) *J Pharmacol Exp Ther* 207(3):677-686 (in eng).

12. Isern J & Meseguer A (2003) Hormonal regulation and characterisation of the mouse Cyp4b1 gene 5'-flanking region. *Biochemical and Biophysical Research Communications* 307:9.

13. Degawa N, Miura S-i, & Hashimoto Y (1990) Androgen-dependent renal microsomal cytochrome P450 responsible for N-hydroxylation and mutagenic activation of 3-methoxy-4-aminoazobenzene in the BALB/c mouse. *Cancer Research* 50:5.

14. Statham CN, Dutcher JS, Kim SH, & Boyd MR (1982) Ipomeanol 4-glucuronide, a major urinary metabolite of 4-ipomeanol in the rat. (Translated from eng) *Drug Metab Dispos* 10(3):264-267 (in eng).

15. Serabjit-Singh CS, Wolf CR, & Philpot RM (1979) The Rabbit Pulmonary Monooxygenase System. *The Journal of Biological Chemistry* 254(19):9901-9907.

16. Guengerich FP (1994) Analysis and Characterization of Enzymes. *Principles and Methods of Toxicology*, ed Hayes AW (Raven Press, New York), pp 1259-1313.

Chapter 4

The Effect of 3-Methylcholanthrene Mediated CYP1A Induction on 4-Ipomeanol Toxicity in *Cyp1a* Null and Humanized *CYP1A* mice

4.1 Introduction

4-Ipomeanol (IPO) is a furan-containing toxin produced by sweet potatoes (*Ipomoea batatas*) in response to infection by the mold *Fusariam solani* (1). IPO gained notoriety after it was discovered that cattle who consumed mold-infested sweet potatoes developed severe pulmonary lesions and life-threatening edema (2). IPO is an alkylating toxin that forms adducts with cellular proteins following metabolic activation. In the proposed mechanism of activation (Chapter 2), the furan ring of IPO is oxidized to an epoxide that may adduct directly to a protein nucleophile or undergo ring-opening to form a reactive di-aldehyde (a 1,4-enedial) intermediate, which then covalently binds to cellular nucleophiles.

IPO also causes selective pulmonary toxicity in several animal species when given either orally or intra-peritoneally. Interestingly, in the early 1990s, IPO was promoted by the National Cancer Institute for clinical use against lung cancer based, in part, on its pulmonary-selective toxicity profile in animals. McLemore et al. 1990 (3) demonstrated further that IPO is cytotoxic in both primary human pulmonary carcinoma cells and a number of human carcinoma cell lines. Subsequently, IPO was investigated in two phase I clinical trials in patients with non-small cell lung cancer (4, 5). Both trials showed a lack of efficacy towards the disease and dose-limiting hepatotoxicity. The liver toxicity observed

in the phase I trials led to IPO being used in phase II trials in patients with hepatocellular carcinoma (6). The patients in the phase II studies also exhibited hepatotoxicity with no significant anti-tumor effects. Because hepatotoxicity was not observed in pre-clinical test species, these studies raised questions about the physiological mechanisms underlying the species differences in organ toxicity observed in response to IPO administration.

In Chapter 2, we showed that IPO is activated by CYP4B1 in extra-hepatic tissues of cow, rabbit and mouse, and that the murine gender difference in target organ toxicity of IPO (wherein males suffer from lung and kidney toxicity following exposure, but females only suffer from lung toxicity) is likely due to differential tissue distribution of CYP4B1 in male and female mice. Indeed, the lung toxicity observed in most experimental animals species is adequately accounted for by high pulmonary CYP4B1 activity coupled to the low extrahepatic IPO glucuronidation capacity observed in all animal species examined (Chapter 2). What then accounts - in humans - for the absence of IPO-mediated lung toxicity and the presence of toxicity in the liver?

The purpose of the work reported in this chapter is to further explore reasons for the selective toxicity of IPO in human liver. CYP1A2 has emerged as the most likely enzyme to catalyze the bioactivation of IPO in mouse and human liver. CYP1A2's substrate specificity overlaps significantly with that of CYP4B1 as evidenced by the ability of both enzymes to effectively metabolize aromatic amines (7) and IPO (8, 9). It has also been previously shown (10) that aryl-hydrocarbon receptor (AhR) ligands shift the sites of organ toxicity in mice. When treated with IPO, control female mice develop pulmonary

toxicity and male mice experience pulmonary and renal toxicity whereas, 3-methylcholanthrene (3-MC)-induced mice exhibit both pulmonary and hepatic toxicity (11). It is surmised that this shift in organ toxicity is due to the induction of IPO-bioactivating enzymes in the liver (12).

At first glance, human CYP1A2 is a good candidate for bioactivation of IPO in the human liver *in vivo* based on the high (84%) sequence homology and substrate overlap with murine CYP1A2. Furthermore, Czerwinski et al (9) and Baer et al (8) have shown that of the major human hepatic P450 isoforms, CYP1A2 has the highest IPO-activation rate based on adduct formation in both HepG2 cells over-expressing specific P450 enzymes and *in vitro* using recombinant P450 enzymes. If activation of IPO is the primary determinant of organ toxicity in humans, one possible explanation for the liver selective toxicity in humans compared to (untreated) mice is that hCYP1A2 produces reactive species from IPO *in vivo* at a higher rate than the mouse ortholog (assuming equal levels of expression). While the microsomal studies described in Chapters 2 and 5 do not provide strong support for this view, there are a number of limitations inherent in using *in vitro* methodologies alone to evaluate *in vivo* toxicities.

Firstly, the *in vitro* IPO bioactivation assay developed by Baer et al (8) and used in earlier chapters to measure the IPO-NAC/NAL adduct (Figure 2.1), has the limitation that it uses only ene-dial production as a measure of IPO activation, so it monitors only the production of a single reactive species. However, the ene-dial is one of multiple possible reactive metabolites generated by activation of IPO, for example the unrearranged furan

epoxide or the putative γ-diketone that could be formed by side-chain oxidation. It is possible that different P450 enzymes produce varying levels of several reactive metabolites; in this case the *in vitro* assay may under-predict the contribution of certain enzymes to toxicity because the production of all reactive species is not monitored. Another limitation is that *in vitro* test systems (microsomes and recombinant enzymes) may not accurately represent the *in vivo* environment especially with respect to P450/CPR ratios (see Chapter 5), so results relying on *in vitro* detection of ene-dial formation may not be representative of activation *in vivo*. Finally, by monitoring only P450-mediated bioactivation of IPO *in vitro*, we neglect its potential inactivation and elimination *via* phase II metabolism. These limitations highlight the potential benefits of *in vivo* toxicity studies in mice in which we can directly measure toxicity in a system with all phase I and II enzymes intact instead of looking for indirect markers of IPO activation. Therefore, induction and toxicity studies in CYP1A knockout and human CYP1A knock-in (13) mice were pursued in order to help elucidate the basis for the different sites of IPO-mediated organ toxicity in mice and humans.

4.2 Experimental Procedures

Materials

Ethoxyresorufin (EROD), methoxyresorufin (MROD), 3-methylcholanthrene (3-MC), N-acetylcysteine (NAC), N-acetyllysine (NAL), CHAPS, DMSO, β-glucuronidase and 4-methylumbelliferone glucuronide were purchased from Sigma Aldrich (St. Louis, MO). 4-

Ipomeanol was a gift from the National Cancer Institute (Bethesda, MD). Goat anti-CYP1A1/1A2 and rabbit anti-goat IgG-HRP were purchased from Oxford Biomedical Research (Oxford, MI) and Santa Cruz Biotechnology, Inc. (Santa Cruz, CA), respectively. Furafylline was obtained from Dr. Kent Kunze (University of Washington, Seattle, WA).

Animals and Treatments

All protocols involving the use of animals were approved by the Institutional Animal Care and Use Committee at the University of Washington (Seattle, WA) and were performed in accordance with the NIH Guide for the Use and Care of Laboratory Animals. C57/BL6 mice (WT), *Cyp1a1/1a2(-/-)_hCYP1A1/1A2(-)* (KO) mice, and *hCYP1A1_1A2_Cyp1a1/1a2(-/-)-Ahr*^{b1} transgenic humanized (H) mice were obtained from Jackson Laboratories (Bar Harbor, ME). Animals were kept on a 12-hour light/dark cycle and provided water and rodent chow ad libitum.

Animals were weighed, randomly assigned to treatment groups and dosed intra-peritoneally (IP) with 60 mg/kg 3-MC or corn oil vehicle control at hour 0 and hour 24. Animals were given 20 mg/kg IPO *via* IP injection at 48 hours and moved to metabolic cages for urine collection and monitored hourly for signs of distress. At 66 hours, mice were sacrificed by carbon dioxide narcosis followed by cervical dislocation and exsanguination. Liver, kidney and lung were harvested and fixed in formalin for histopathological analysis (analysis performed by Dr. Denny Liggitt in the Department of Comparative Medicine, University of Washington). Plasma was obtained by centrifuging blood collected by cardiac puncture at 1300g for 5 minutes. Plasma analysis was

performed by Phoenix Central Laboratories (Everett, WA). Urine was prepared for LC/MS/MS analysis by centrifugation for at 4000g for 10 minutes and filtration through a sterile 0.2 μM PES filter.

For tissue harvesting, female animals were weighed and randomly assigned to treatment groups and dosed IP with 60 mg/kg 3-MC or corn oil vehicle control at hour 0 and 24 hours. Mice were sacrificed by carbon dioxide narcosis followed by cervical dislocation and exsanguination at 48 hours. Livers, kidneys and lungs were harvested and frozen in liquid nitrogen. Frozen organs were ground up and homogenized in 2 to 3 mL of resuspension buffer consisting of 50 mM Tris HCl pH 7.4, 150 mM KCl and 2 mM EDTA per gram of tissue. Homogenate was centrifuged at 12,000 g for 20 minutes at 4 degrees to remove cellular debris. Microsomes were pelleted by centrifuging at 105,000 g for 60 minutes at 4^{o}C, resuspended in 0.5 to 1 mL 250 mM sucrose per gram of tissue and stored at -80^{o}C until use.

CYP1A Genotyping

Primers listed below, designed to determine the presence of the intact wild-type mouse *Cyp1a* locus (WT), the *Cyp1a2/Cyp1a1(-)* targeted allele (KO), *hCYP1A1* (H1A1) or *hCYP1A2* (H1A2) were purchased from Integrated DNA Technologies (San Diego, CA).

WT-FOR: 5’ TCG ACA CGG CAC TCT GAG 3’

WT-REV: 5’ GGC TAA CCA TCT CGT CAG C 3’

KO–FOR: 5’ GAC ATA GGA GCT ACC TAC AC 3’

KO-REV: 5’ GTC AAA GTA ACC AGA CAC ATC CTG C 3’

H1A1-FOR: 5’ AGG CTG GCC TAT GTG GTC TA 3’

H1A1-REV: 5’ GCA GCC CTG TTT GTT CCT G 3’

H1A2–FOR: 5’ AGG ATT GGC ATT GTT GAA GG 3’

H1A2-REV: 5’ GGG CAC TGG CCA TAG TAT TC 3’

Specifically, amplification with WT primers indicates an intact functional murine *Cyp1a* gene and amplification of KO primers indicates insertion of the *Cyp1a* targeting vector which leads to deletion of the section of murine chromosome 9 that contains the *Cyp1A2* and *Cyp1a1* genes. H1A1 and H1A2 primers are used to verify the presence of the 180-kb human *CYP1A1_CYP1A2* locus-containing bacterial artificial chromosome (Human CTB clone 31H21) which consists of the 23.3 kb spacer region, 90 kb of *CYP1A2* 3'-flanking region and 53 kb of *CYP1A1* 3' flanking region by specifically targeting both *CYP1A1* and *CYP1A2*.

DNA was isolated from tail snips and processed using a DNeasy Blood and Tissue Kit (Qiagen, MD). Genes were amplified using hot-start PCR – (95^{o}C for 2 minutes, 94 ^{o}C for 30 seconds, 57^{o}C for 30 seconds, 72^{o}c for 2 minutes) x 35 cycles, 72^{o}C or 5 minutes. Amplicons were resolved using 1% agarose gel electrophoresis.

In vitro metabolism of IPO

In vitro bioactivation and glucuronidation of IPO was assessed by incubating 50 μM IPO in microsomal preparations in triplicate according to the protocol described in Chapter

2. Inhibition experiments using the diagnostic CYP1A2 inhibitor, furafylline (10 μM) included a 15 minute preincubation before addition of IPO. Rates were compared to activation rates in control incubations containing DMSO and no inhibitor. Total organic content was 0.5 % v/v.

Characterization of 3MC-induced mice

Induction of CYP1A was confirmed by Western blot and activity assays. EROD and MROD were utilized as diagnostic substrates for CYP1A activity (14). These enzyme activities were measured by incubating 5 μM substrate in DMSO (final organic content 0.5% v/v) in potassium phosphate buffer (100 mM pH 7.4), NADPH (1 mM), EDTA (1 mM), and $MgCL_2$ (3 mM) with a final incubation volume of 200 μL with 0.2 mg/mL protein for 5 min at 37 ^{o}C. Generation of the fluorescent product, resorufin, was monitored at an excitation wavelength of 530 nm and an emission wavelength of 585 nm in a Synergy HTTR spectrophotometer.

Western blot analysis of 3MC-induced and control liver microsomes from wild-type and humanized CYP1A mice was performed by the following procedure. Microsomal proteins (30 μg) were separated by SDS-PAGE for 1.5 hr at 130V. Proteins were then transferred to PVDF membranes overnight. Membranes were incubated with blocking buffer (5% milk in 1X TBS-T) for 1 hour at room temperature (RT) and then washed 3 times with 1X TBS-T. Membranes were then incubated with primary antibody (goat anti-CYP1A1/1A2) diluted 1:1000 in 2.5% milk in 1X-TBST for 1 hour at RT. Membranes were washed again in 1X TBS-T and then incubated with the secondary antibody (rabbit anti-

goat IgG-HRP) diluted 1:5000 in 2.5% milk. Antibodies were detected by chemilluminescence using an Odyssey system for visualization. Membranes were probed a second time with an antibody to β-actin to assess consistency of protein loading.

4.3 Results

Western blot analysis of microsomes from 3-MC treated animals indicated that both Cyp1a (mouse CYP1A1 and CYP1A2) and hCYP1A (human CYP1A1 and CYP1A2) were inducible in the mouse (Figure 4.1). CYP1A was induced ~4.25 fold versus vehicle control, whereas hCYP1A was induced ~2.6 fold versus vehicle control.

The specific genotypes of the mice used in this study were confirmed by PCR amplification of the *mCyp1a* gene (WT), the knockout transgene (KO), and in the case of humanized CYP1A mice, both hCYP1A1 and hCYP1A2 (Figure 4.2).

MROD and EROD are diagnostic markers of CYP1A1 and CYP1A2 activities, respectively (14). Using these probes, CYP1A activities were found to be highly inducible in both WT and CYP1A humanized mice (Figure 4.3). However, consistent with the Western blot data, MROD and EROD activity in liver microsomes from humanized CYP1A mice was induced to a lesser extent than murine CYP1A. MROD activity was increased 24-fold in WT mice compared to 5-fold in humanized CYP1A mice. EROD activity was increased 32-fold in WT mice compared to 4.8-fold in humanized CYP1A mice.

IPO activation was induced to a much lesser extent by 3-MC than the resorufin-based markers of CYP1A activity. Activation was increased less than 2-fold in WT mice and is not induced under these conditions in humanized CYP1A mice (Figure 4.4).

To probe the contribution of *Cyp1a* enzymes to IPO activation *in vitro*, we conducted activation assays utilizing mouse liver microsomes in the presence of the CYP1A inhibitor, furafylline. Figure 4.5 shows that co-incubation with furafylline eliminated 28% of IPO activation in WT microsomes. IPO bioactivation in *Cyp1a* null mice shows a corresponding 27% decline relative to metabolism in WT mouse liver microsomes.

We have previously demonstrated that IPO is subject to phase II metabolism *via* glucuronidation in mouse liver microsomes (Chapter 2) and is subject to glucuronidation in the mouse *in vivo* (Chapter 3). Figure 4.6 shows the induction by 3MC of IPO glucuronide formation in both WT and hCYP1A mice. In both genotypes, *in vitro* glucuronidation increases by ~50% in liver microsomes from induced mice relative to glucuronidation in microsomes from mice treated with corn oil vehicle.

Table 1 depicts the average histopathological scores (Dr. Denny Liggitfor each treatment group relative to genotype, sex and 3-MC induction. As expected, there is no evidence of renal damage in female mice from any treatment group. We do see moderate to severe nephrosis and proteinurea in the kidneys of un-induced male mice of every genotype (Figure 5.8). Somewhat surprisingly, both control transgenic mouse groups exhibited more severe kidney toxicity than WT mice. 3-MC induction reduced the severity

of kidney damage relative to vehicle control to very mild in *Cyp1a* null mice and to no evidence of renal toxicity in WT and hCYP1A mice.

In general, lung toxicity was less severe than expected based on observation of the IPO-treated mice prior to sacrifice. All non-induced mice exhibited signs of pulmonary impairment including accelerated respiration rates and lethargy compared to induced animals. Histopathological scoring indicated that pulmonary toxicity in all animals was only mild to moderate (Figure 4.7 and Table 4.1). There was an expected decrease in the severity of pulmonary toxicity in both male and female mice of all genotypes following 3-MC induction with the exception of male *Cyp1a* null mice, where both un-induced and induced mice suffered from mild lung toxicity. These data are less stark than the difference in toxicity observed between control and induced male kidney, but they follow the same trend of 3-MC induction ameliorating the toxic effects of IPO. There was no histopathological evidence for liver damage in any treatment group.

We conducted a screen of plasma markers of both hepatic and renal toxicity (glucose, BUN, creatinine, calcium, phosphorous, total protein, albumin, globulin, bilirubin, ALP, GGT, ALT, AST and cholesterol) in plasma collected from all animals. There were no indications of impaired hepatic function detected; however, we did find elevated blood urea nitrogen (BUN) levels in male mice (Figure 4.9). Normal values range from 8-30 mg/dl, and values above 30 are considered indicative of impaired kidney function. BUN values for all female mice fell within the normal range and were not affected by genotype or 3-MC induction (data not shown) which correlates with the lack of renal injury seen in

female kidney sections. In male mice, however, BUN levels were elevated above the normal range in both *Cyp1a* null and hCYP1A mice. In all three male genotypes, induction by 3-MC lowered BUN levels in the plasma of male mice, however, this decrease was only statistically significant in *Cyp1a* null and hCYP1A mice.

4.4 Discussion

The main goal of this study was to determine whether CYP1A-humanized mice could serve as a model for the liver toxicity of IPO that has been observed in humans, in contrast to the lung toxicity that dominates in animal species, and by extension determine if human liver toxicity is due to enhance IPO activation by human CYP1A2 relative to mouse CYP1A2. CYP1A transgenic mice were chosen for the reasons outlined in the introduction coupled with the key observation that 3MC induction in mice appeared to 'unmask' liver damage by IPO (11) Based upon IPO bioactivation studies conducted with recombinant human P450s that highlighted a potential role for hCYP1A2, we took advantage of the availability of a CYP1A null and humanized CYP1A mouse line that has proven useful for the study of CYP1A involvement in aromatic amine activation (15).

If the hepatic toxicity of IPO observed in humans is due to increased bioactivation by hCYP1A2 relative to mCYP1A2, we might expect that humanized mice would experience liver toxicity regardless of 3-MC induction. Nonetheless, we felt it was important to include an induction arm in the study and so firstly, we evaluated the hepatic P450 response of wild-type and humanized CYP1A mice to 3MC induction. This study

demonstrated that both Cyp1a in WT and CYP1A in humanized CYP1A mice was readily induced by 3-MC. However, the magnitude of induction was markedly higher in WT mice compared to humanized mice, based on both enzyme activity assays and immunoquantification of CYP1A content.

We next evaluated 'induction' of IPO bioactivation in the same liver microsomal samples as above. An approximate 2-fold increase in IPO bioactivation was observed which is very much lower than the induction of EROD and MROD activities (~30 fold increase). Furthermore, both inhibition of CYP1A by furafylline and elimination of CYP1A in *Cyp1a* null mice decreased IPO activation rates in mouse liver by less than 30%, These data suggest that bioactivation of IPO in mouse liver *in vivo* is unlikely to be mediated predominantly by CYP1A. We have also shown that control liver microsomes from hCYP1A mice do not have significantly different IPO activation rates compared to WT mice, which suggests that human CYP1A enzymes may not have markedly higher capacity for catalyzing the activation of IPO relative to mouse CYP1A enzymes.

In vivo toxicity studies demonstrated that hCYP1A mice experienced pulmonary and renal toxicity and female hCYP1A mice demonstrated only pulmonary toxicity. These observations are consistent with the maintenance of constitutive murine CYP4B1 in the transgenic animals models. However, neither male nor female hCYP1A mice showed any evidence of liver toxicity assessed either by histopathology or plasma markers of hepatic dysfunction.. Collectively, these data indicate that human and mouse CYP1A enzymes show essentially equal propensity to activate IPO and that the hepatic toxicity observed in

humans is not predicated upon an increased rate of IPO activation by human CYP1A2 relative to murine CYP1A2. This was a disappointing result, but may reflect, at least in part, IACUC regulations that restricted IPO doses to the published murine LD_{50}, which is an order of magnitude lower than the dose at which humans develop hepatotoxicity (16, 17).

Induction with the AhR ligand, 3-MC, *did* alleviate pulmonary and renal toxicity in mice treated with IPO in WT and humanized CYP1A, but also surprisingly in *Cyp1a* null mice. The latter finding suggests strongly that these changes in the severity of IPO-mediated extra-hepatic organ damage are unrelated to murine (hepatic) CYP1A content. Previous studies had shown a decrease in covalent binding of IPO of up to 75% in 3-MC induced rats (18). While one interpretation is that increased hepatic CYP1A enzymes may reduce pulmonary exposure to IPO in induced animals, treatment with 3-MC may also lead to induction of other member(s) of the Ah battery (19, 20) that either contribute to IPO clearance or detoxify reactive IPO metabolites. 3-MC is a known inducer both of epoxide hydrolase (21) and GSTA1 (22), which may contribute to detoxification of ipomeanol epoxide or the ene-dial, respectively. Moreover, at least at the transcript level, several UGT genes (primarily from the Ugt1a family) are significantly induced by AhR ligands (23). Indeed our data show that mouse liver microsomes readily glucuronidate IPO (at levels similar to the rat, Chapter 2) and the rates of glucuronidation are increased following 3-MC induction. Since phase II metabolism generally leads to excretion and, in the case of IPO, might diminish the levels of pro-toxin available for bioactivation, the 5-fold increase in the LD_{50} of IPO following 3-MC treatment reported earlier, (11), may have been be due in part to induction of this UGT-mediated elimination of IPO.

In summary, we conclude that the mouse-human species difference resulting in pulmonary/renal toxicity in mice versus liver toxicity in humans is not due to an enhanced ability of human CYP1A to bioactivate IPO relative to murine CYP1A. The failure of the 3-MC induced *hCYP1A1/1A2* knock-in mice to serve as a model for human liver toxicity of IPO in these studies may reflect (i) IACUC-imposed restrictions on dosing, (ii) the maintenance of hepatic glucuronidation of IPO which proceeds at a much higher level in mouse liver than it does in human liver (Chapter 5), and/or (iii) the presence of functional mCYP4B1 in the kidneys and lungs of the *CYP1A* transgenic animals. Furthermore enzyme induction by 3-MC is not limited to P450s, and it is possible that induction UGT enzymes involved in the metabolism elimination of IPO or of reactive-intermediate detoxifying enzymes (epoxide hydrolase and GSTA1) by 3-MC could account for the lack pulmonary and renal toxicity observed in this study as well as the increase in IPO LD_{50} previously observed in 3-MC induced mice.

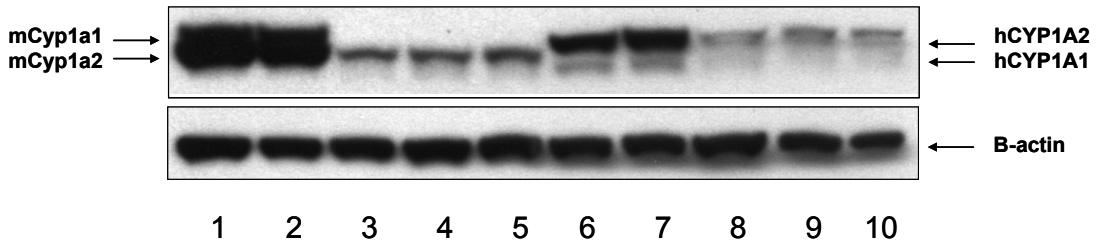

Figure 4.1 Immunoblots of mouse liver microsomal proteins after 3-methylcholanthrene induction probed with goat anti-CYP1A1/1A2 and mouse anti-β-actin. Lane contents are as follows: 1-2: 3-methylcholanthrene-treated wild-type; 3-5: vehicle-treated wild-type; 6-7: 3-methylcholanthrene treated humanized CYP1A; 8-10: vehicle-treated humanized CYP1A (30 μg microsomal protein added per well). Fold induction by 3MC of CYP1A2 over corn oil control was 4.25 and 2.60 for wild-type and humanized, respectively.

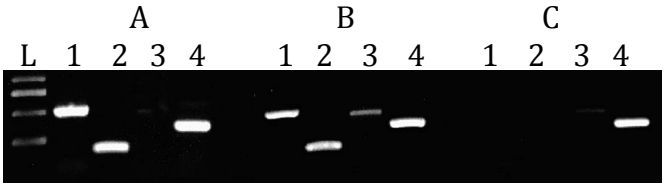

Figure 4.2 Northern blot for the 3 different genotypes of mice studied. Lane contents are as follows: L: MW ladder, 1: human CYP1A1 (H1A1) – 490 bp; 2: human CYP1A2 (H1A2) – 176 bp; 3: mouse Cyp1a (WT) – 417 bp; 4: knockout transgene (KO) – 353 bp. Gel A contains PCR products from a humanized *CYP1A* mouse on a *mCyp1a* null background evidenced by amplification of H1A1, H1A2 and the KO transgene. Gel B contains PCR products from a humanized *CYP1A* mouse heterozygous for WT *mCyp1A* and the knockout transgene evidenced by amplification of H1A1, H1A2, WT and KO. Gel C contains PCR products from a *mCyp1a* knockout animal evidenced by amplification of the KO transgene but no human or mouse *CYP1A* genes. Amplification with WT primers (lane 3) indicates an intact functional murine *Cyp1a* gene and amplification of KO primers (lane 4) indicates insertion of the *Cyp1a* targeting vector which leads to deletion of the section of murine chromosome 9 that contains the *Cyp1A2* and *Cyp1a1* genes. H1A1 and H1A2 primers (lanes 1 and 2) are used to verify the presence of the 180-kb human *CYP1A1_CYP1A2* locus-containing bacterial artificial chromosome.

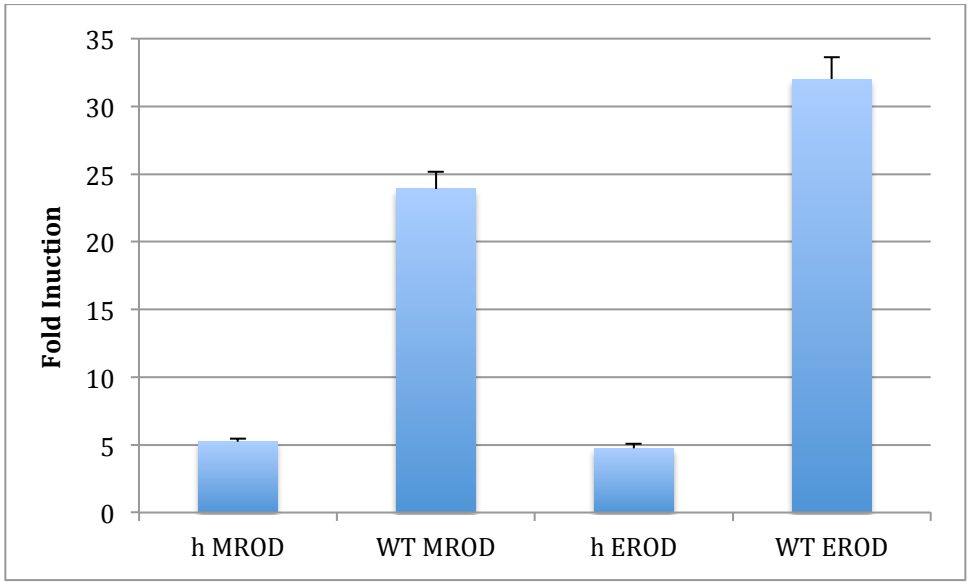

Figure 4.3 Induction by 3-methylcholanthrene relative to corn oil control of CYP1A activity measured by methoxyresorufin O-dealkylation (MROD) and ethoxyresorufin O-dealkylation (EROD) in microsomes harvested from wild-type (WT) and humanized CYP1A (h) mice. CYP1A activity is significantly induced ($P < 0.05$ compared to corresponding control value) in both genotypes however mouse CYP1A activity is induced 25-30 fold and human CYP1A activity is induced 5 fold.

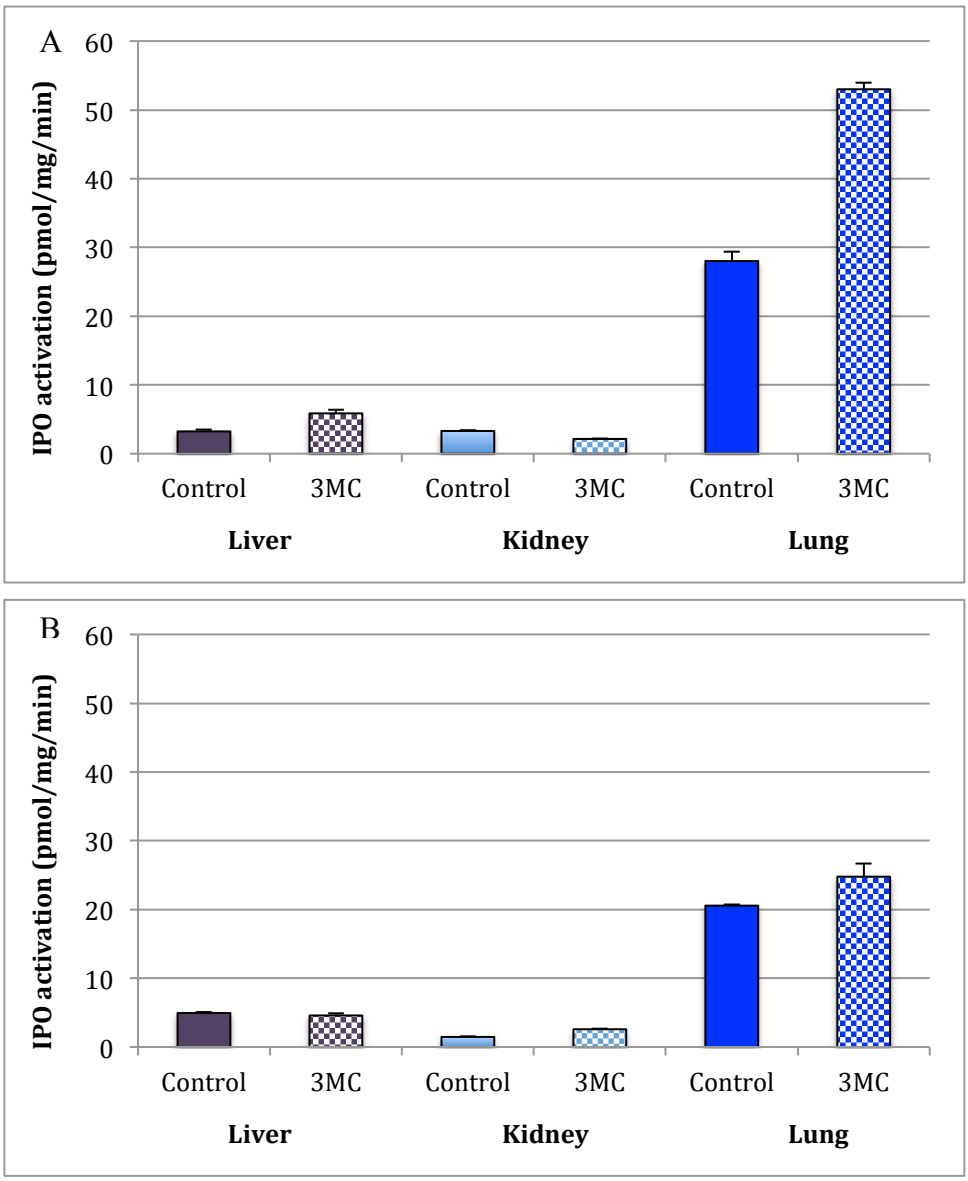

Figure 4.4 IPO activation in wild-type (A) and humanized CYP1A (B) by control and 3-methylcholanthrene induced female mouse microsomes. IPO activation is significantly induced (~2 fold) in liver and lung microsomes from wild-type animals ($P < 0.05$ compared to corresponding control value) but not induced in livers or lungs from humanized mice.

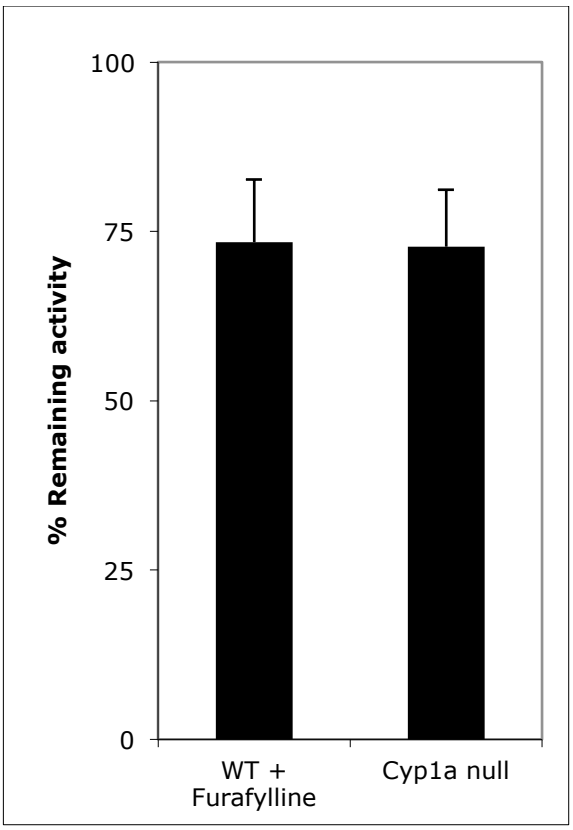

Figure 4.5 Inhibition of IPO activation in wild-type mouse liver microsomes by furafylline (compared to DMSO vehicle control) and activation of IPO in liver microsomes from Cyp1a knockout mice (compared to activation in liver microsomes from wild-type mice). Elimination of CYP1A activity reduces IPO activation in mouse liver microsomes by roughly 25%.

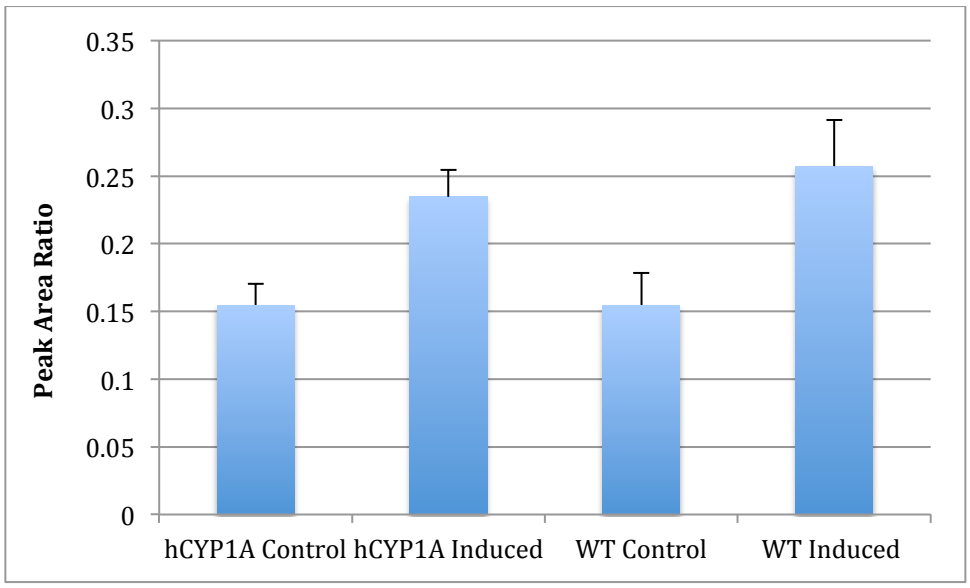

Figure 4.6 Glucuronidation of IPO in microsomes from induced and un-induced livers from wild-type (WT) and humanized CYP1A mice. Induction with 3-methylcholanthrene increases glucuronidation rates by ~50% in liver microsomes made from mice of both genotypes relative to corn oil control.

		Male	Female
Kidney	WT Control	NP/P 2	None
	WT Induced	None	None
	Cyp1a KO Control	NP/P 4	None
	Cyp1a KO Induced	NP/P 1	None
	hCYP1A Control	NP/P 4	None
	hCYP1A Induced	None	None
Lung	WT Control	Moderate	Moderate
	WT Induced	Minimal	Minimal
	Cyp1a KO Control	Mild	Moderate
	Cyp1a KO Induced	Mild	Mild
	hCYP1A Control	Mild	Moderate
	hCYP1A Induced	None	Mild

Table 4.1 Histopathological scoring for each treatment group. 3-Methylcholanthrene induction almost completely alleviates IPO-caused nephrotoxicity in male mice. Nephrotoxicity is completely absent in female mice. 3-Methylcholanthrene induction tends to decrease the extent of pulmonary toxicity in all mice regardless of genotype. (NP – nephrosis (renal tubular injury); P-proteinuria scored on a scale from 1 to 5 with 1 indicating very mild injury and 5 indicating severe injury). Scoring performed by Dr. Denny Liggitt in the Department of Comparative Medicine, University of Washington.

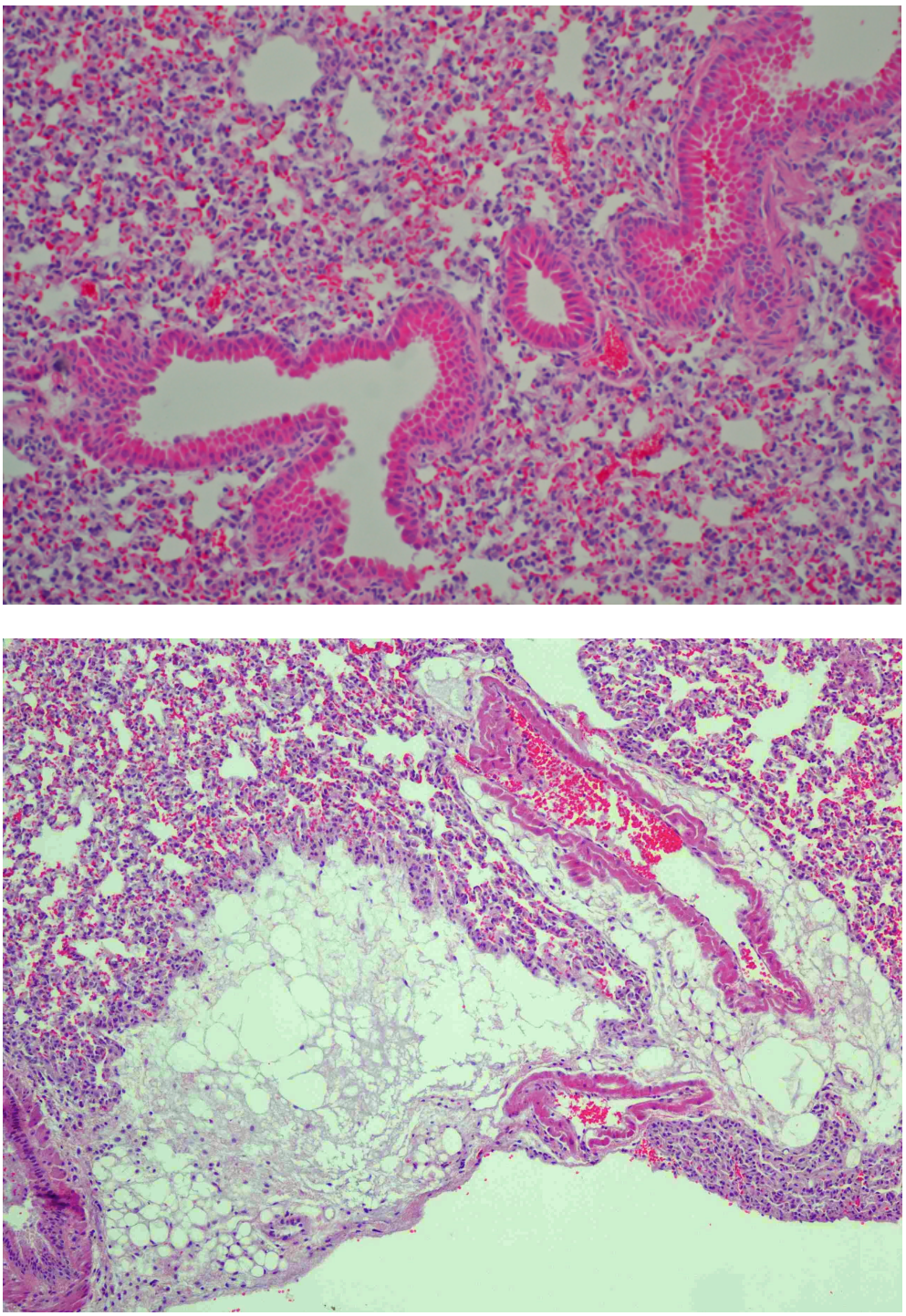

Figure 4.7 Lung histopathology. The top panel shows a healthy lung from an induced wild-type female mouse. The bottom panel shows an injured lung from a control female wild-type mouse.

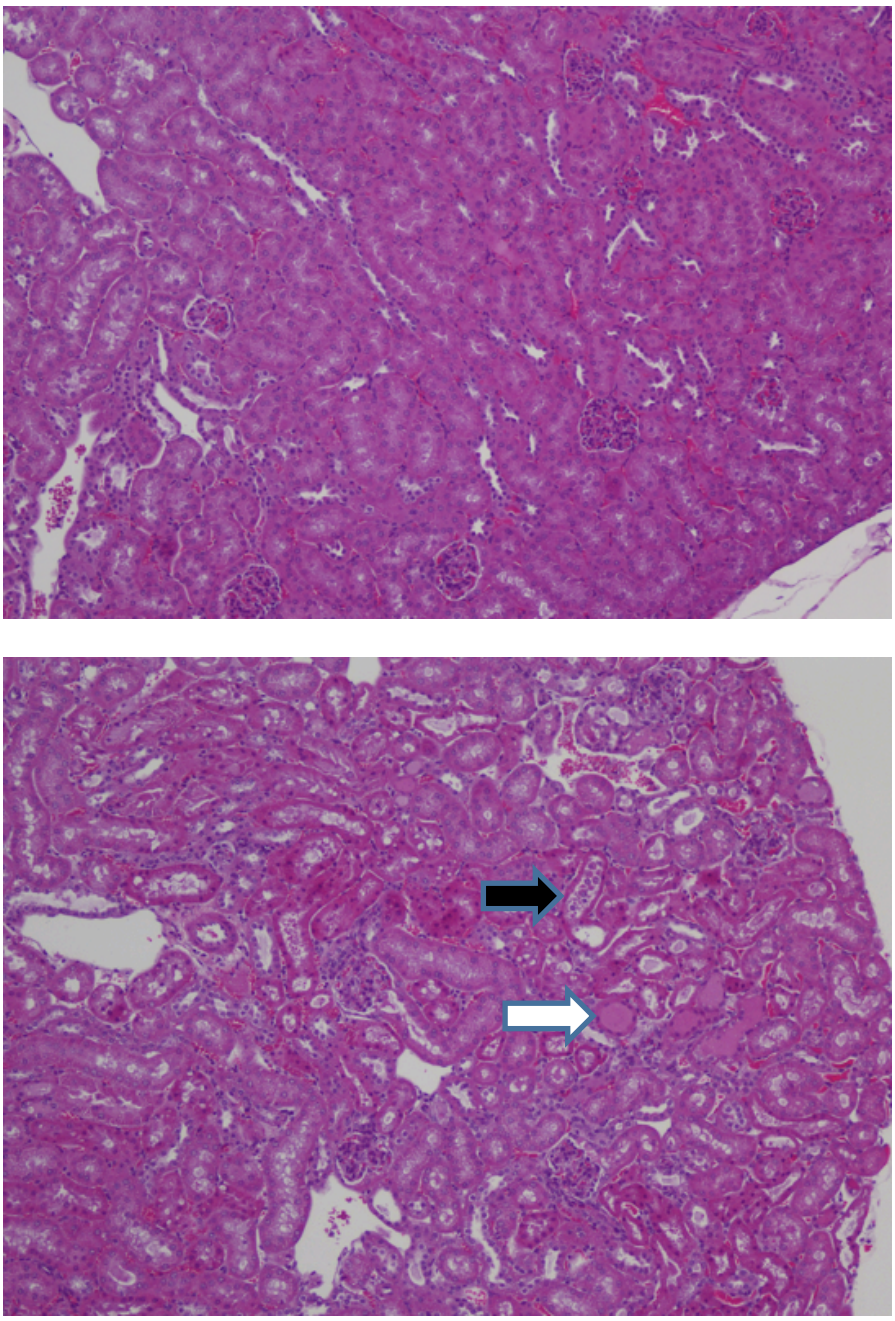

Figure 4.8 Kidney histopathology. The top panel shows a healthy kidney from an induced The bottom panel shows an injured kidney from a control male *Cyp1a* null mouse. The kidneys of uninduced male mice showed signs of proteinurea (white arrow) and necrotic and sloughed epithelium (black arrow).

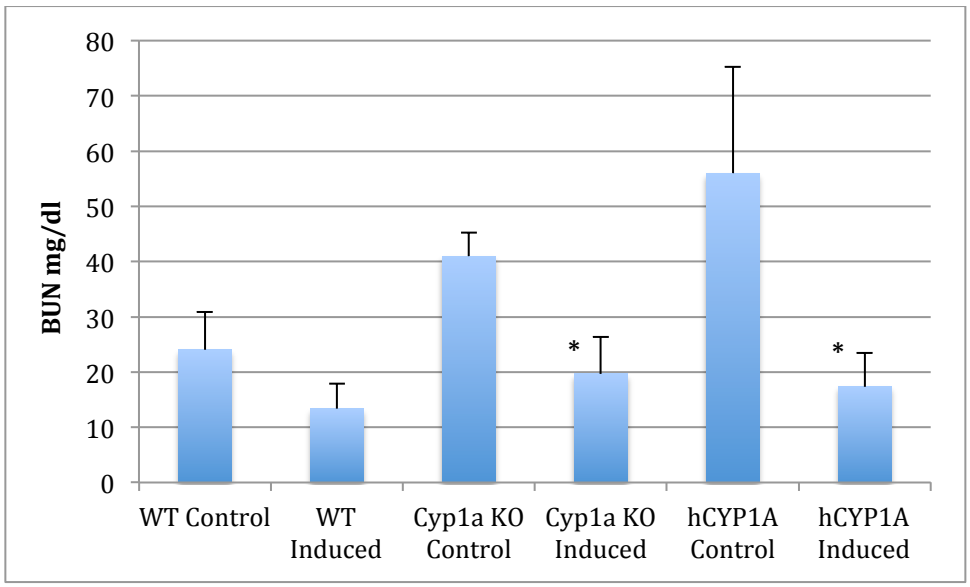

Figure 4.9 Average blood urea nitrogen levels in plasma from male mice with respect to induction. Values above 30 are considered to be elevated and indicative of impaired kidney function. In all cases, induction with 3-methylcholanthrene decreased blood urea nitrogen to within normal levels (* $P < 0.05$ compared to corresponding control value).

4.5 Notes to Chapter 4

1. Boyd MR & Wilson BJ (1972) Isolation and characterization of 4-ipomeanol, a lung-toxic furanoterpenoid produced by sweet potatoes (Ipomoea batatas). (Translated from eng) *J Agric Food Chem* 20(2):428-430 (in eng).

2. Doster AR, Mitchell FE, Farrell RL, & Wilson BJ (1978) Effects of 4-ipomeanol, a product from mold-damaged sweet potatoes, on the bovine lung. (Translated from eng) *Vet Pathol* 15(3):367-375 (in eng).

3. McLemore TL*, et al.* (1990) Metabolic activation of 4-ipomeanol in human lung, primary pulmonary carcinomas, and established human pulmonary carcinoma cell lines. (Translated from eng) *J Natl Cancer Inst* 82(17):1420-1426 (in eng).

4. Rowinsky E*, et al.* (1993) Phase I and pharmacological stuy of the pulmonary cytotoxin 4-ipomeanol on a single dose schedule in lung cancer patients: Hepatotoxicity is dose limiting in humans. *Cancer Research* 53:8.

5. Kasturi VK*, et al.* (1998) Phase I study of a five-day dose schedule of 4-Ipomeanol in patients with non-small cell lung cancer. (Translated from eng) *Clin Cancer Res* 4(9):2095-2102 (in eng).

6. Lakhanpal S, Donehower RC, & Rowinsky EK (2001) Phase II study of 4-ipomeanol, a naturally occurring alkylating furan, in patients with advanced hepatocellular carcinoma. (Translated from eng) *Invest New Drugs* 19(1):69-76 (in eng).

7. Imaoka S*, et al.* (1995) Mutagenic activation of 3-methoxy-4-aminoazobenzene by mouse renal cytochrome P450 CYP4B1: Cloning and characterization of mouse CYP4B1. *Archives of Biochemistry and Biophysics* 321(1):8.

8. Baer BR, Rettie AE, & Henne KR (2004) Bioactivation of 4-Ipomeanol by CYP4B1: Adduct Characterization and Evidence for an Enedial Intermediate. *Chemical Research in Toxicology* 18:855-864.

9. Czerwinski M*, et al.* (1991) Metabolic activation of 4-ipomeanol by complementary DNA-expressed human cytochromes P-450: evidence for species-specific metabolism. (Translated from eng) *Cancer Res* 51(17):4636-4638 (in eng).

10. Boyd MR & Dutcher JS (1981) Renal toxicity due to reactive metabolites formed in situ in the kidney: investigations with 4-ipomeanol in the mouse. (Translated from eng) *J Pharmacol Exp Ther* 216(3):640-646 (in eng).

11. Boyd MR & Dutcher JS (1981) Renal toxicity due to reactive metabolites formed in situ in the kidney: investigations with 4-ipomeanol in the mouse. (Translated from eng) *The Journal of Pharmacology and Experimental Therapeutics* 216(3):640-646 (in eng).

12. Boyd MR & Burka LT (1978) In vivo studies on the relationship between target organ alkylation and the pulmonary toxicity of a chemically reactive metabolite of 4-ipomeanol. (Translated from eng) *The Journal of Pharmacology and Experimental Therapeutics* 207(3):687-697 (in eng).

13. Dragin N, Uno S, Wang B, Dalton TP, & Nebert DW (2007) Generation of 'humanized' hCYP1A1_1A2_Cyp1a1/1a2(-/-) mouse line. (Translated from eng) *Biochem Biophys Res Commun* 359(3):635-642 (in eng).

14. Burke MD, Thompson S, Weaver RJ, Wolf CR, & Mayer RT (1994) Cytochrome P450 specificities of alkoxyresorufin O-dealkylation in human and rat liver. (Translated from eng) *Biochem Pharmacol* 48(5):923-936 (in eng).

15. Kimura S*, et al.* (1999) CYP1A2 is not the primary enzyme responsible for 4-aminobiphenyl-induced hepatocarcinogenesis in mice. *Carcinogenesis* 20(9):6.

16. Kasturi VK*, et al.* (1998) Phase I study of a five-day dose schedule of 4-Ipomeanol in patients with non-small cell lung cancer. (Translated from eng) *Clin Cancer Res* 4(9):2095-2102 (in eng).

17. Lakhanpal S, Donehower RC, & Rowinsky EK (2001) Phase II study of 4-ipomeanol, a naturally occurring alkylating furan, in patients with advanced hepatocellular carcinoma. (Translated from eng) *Invest New Drugs* 19(1):69-76 (in eng).

18. Statham CN & Boyd MR (1982) Effects of phenobarbital and 3-methylcholanthrene on the in vivo distribution, metabolism and covalent binding of 4-ipomeanol in the rat; implications for target organ toxicity. (Translated from eng) *Biochem Pharmacol* 31(24):3973-3977 (in eng).

19. Kohle C & Bock KW (2007) Coordinate regulation of Phase I and II xenobiotic metabolisms by the Ah recepter and Nrf2. *Biochem Pharmacol* 73:10.

20. Nebert DW*, et al.* (2000) Role of the aromatic hydrocarbon receptor and [Ah] gene battery in the oxidative stress response, cell cycle control, and apoptosis. *Biochem Pharmacol* 39:23.

21. Meijer J & DePierre JW (1987) Hepatic levels of cytosolic, microsomal and 'mitochondrial' epoxide hydrolases and other drug-metabolizing enzymes after treatment of mice with various xenobiotics and endogenous compounds. (Translated from eng) *Chem Biol Interact* 62(3):249-269 (in eng).

22. Yeager RL, Reisman SA, Aleksunes LM, & Klaassen CD (2009) Introducing the "TCDD-inducible AhR-Nrf2 gene battery". (Translated from eng) *Toxicol Sci* 111(2):238-246 (in eng).

23. Buckley DB & Klaassen CD (2009) Induction of mouse UDP-glucuronosyltransferase mRNA expression in liver and intestine by activators of aryl-hydrocarbon receptor, constitutive androstane receptor, pregnane X receptor, peroxisome proliferator-activated

receptor alpha, and nuclear factor erythroid 2-related factor 2. (Translated from eng) *Drug Metab Dispos* 37(4):847-856 (in eng).

Chapter 5

Bioactivation of 4-Ipomeanol by Human P450s

5.1 Introduction

The pulmonary damage caused by IPO in both livestock and laboratory animals is localized to the terminal bronchial epithelium, notably Clara cells (*1, 2*). These are ciliated secretory cells that are involved in the metabolism of inhaled xenobiotics and, therefore, not surprisingly have relatively high levels of cytochrome P450 expression relative to other areas of the lung. As noted in Chapter 4, this site-specific toxicity prompted the National Cancer Institute (NCI) to assess the utility of IPO as an anti-lung cancer therapy in humans with terminal diagnoses (*3*). However, IPO showed no ability to reduce tumor size or halt tumorigenesis in non-small cell lung carcinoma in humans (*4, 5*).

Unpredictably, the dose-limiting toxicity observed in clinical treatment with IPO was hepatotoxicity. This liver toxicity, which was observed in the Phase I trials, prompted the use of IPO in a Phase II trial conducted in patients with hepatocellular carcinoma (*6*). The cancer patients in this study also exhibited hepatotoxicity, and as with lung cancer patients, no chemotherapeutic efficacy. Because no mammalian species treated with IPO exhibited liver toxicity, even at lethal doses of the pro-toxin, the basis for the species differences in pulmonary versus hepatic toxicity seen with IPO is an important unresolved question.

We have previously shown that IPO is bioactivated in the lung of multiple species by CYP4B1 (Chapters 2 and 3) (*7*). The pattern of expression of *CYP4B1/4b1* in humans and mice is similar. In both species, CYP4B1 mRNA is expressed predominantly in the lung. Therefore, the species differences in target organ toxicity of IPO between mice and humans is not due to a differential tissue distribution of the enzyme, although this does seem to account for the gender difference in IPO-mediated renal toxicity in mice (Chapter 3).

The lack of CYP4B1-mediated activation of IPO in humans and, therefore, the lack of efficacy regarding pulmonary cancer treatment and clinical pulmonary toxicity, is likely linked to the 'aberrant' *CYP4B1* gene that encodes a non-functional enzyme in humans. Previous studies have shown that the *CYP4B1* gene across all species examined encodes an evolutionarily-conserved proline residue in the meander region of the protein. Furthermore, the meander proline is conserved in practically all human P450 enzymes (Chapter 1). Indeed, only the human *CYP4B1* gene does not code for this conserved proline; instead translation of the wild-type human gene results in a serine variant (S427P). Introduction of the corresponding S427P mutation into rabbit *CYP4B1* interfered with heme incorporation, and reversion of S427 to the conserved proline in human *CYP4B1* yielded a functional enzyme that incorporated heme (Chapter 1) (*8*). Therefore, the species difference between mice and humans for IPO-mediated lung damage is likely due, at least in part, to human CYP4B1 being unable to activate IPO.

There is, however, some evidence that humans can express functional CYP4B1. Human bladder microsomes activate 2-acetylaminofluorene, a pro-carcinogen and a known

CYP4B1 substrate (*9*). This activity was inhibited by an anti-CYP4B1 antibody. Imaoka et al. were able to express an active fusion protein of human CYP4B1 and CPR in yeast (*10*). Unusually, the active protein utilized in this study incorporated a serine residue inserted at a new amino acid position, S207. This insertion was predicted from cDNA clones isolated from seminal vesicles of multiple donors. The S207 insertion might conceivably stabilize incorporation of the heme, however, Imaoka et al. (*9, 10*) were unable to express functional non-fusion CYP4B1 even with the S207 insertion. Therefore, expression of human CYP4B1 as a P450-CPR fusion protein may stabilize the enzyme to allow incorporation of heme and production of a functional enzyme and the S207 insertion could be incidental. However, the functional consequences of the S207 insertion in native (non-fusion) CYP4B1 are unknown. This will be explored here.

There is some evidence that P450 enzymes other than CYP4B1, notably the hepatic-expressed CYP1A2, can activate IPO. CYP1 enzymes have been implicated in the hepatic bioactivation of IPO in mice due to the change in IPO-induced organ toxicity after treatment with 3-methylcholanthrene (3-MC); an aryl-hydrocarbon receptor (AhR) ligand that induces CYP1A2 (and other CYP1 enzymes) in mice (*11*). 3-MC-treated mice were reported to suffer from pulmonary and hepatic toxicity following IPO exposure, whereas untreated mice experienced pulmonary and renal toxicity.

In Chapter 4, we hypothesized that this change in the pattern of organ toxicity might be attributable to the increase in hepatic murine CYP1A2 caused by polycyclic aromatic hydrocarbon induction, but the experimental results did not support this view. We also reported in Chapter 4 that the species difference in liver toxicity between humans and

experimental animals is not due to an increase the activity of human CYP1A2 towards IPO relative to murine CYP1A2. Instead, liver toxicity in humans might result from a decrease in the activity of human CYP4B1 relative to murine CYP4B1 coupled with a lack of IPO glucuronidation in human liver (Chapter 2 and 4). Regardless, CYP1A2 remains an attractive candidate for the IPO bioactivating enzyme in human liver.

The basis for the above argument is compelling evidence demonstrating that human CYP1A2 has the highest activity for bioactivation of IPO among the major hepatic drug-metabolizing P450 enzymes. Czerwinski et al. (*12*) established a panel of HepG2 cells expressing various human and rodent P450 enzymes and incubated these cells with radiolabeled IPO. Of the recombinantly expressed P450s examined, human CYP1A2-containing cells exhibited the highest level of adducts to calf thymus DNA, suggesting that under the experimental conditions used, CYP1A2 has the highest activity of the major hepatic P450 enzymes for generation of reactive intermediates of IPO. It is worth noting that, in the same studies, cells expressing murine *Cyp1a1* produced very low levels of DNA-adducts, which may suggest that it is induction of CYP1A2, and not CYP1A1, that leads to IPO-mediated hepatotoxicity in 3-MC treated mice. However, murine CYP1A2 was not included in the studies by Czerwinski et al. (*12*)

Baer et al. (*13*) conducted a separate screen of IPO toxicity potential by human P450 enzymes utilizing commercially available recombinant enzymes and formation of the NAC/NAL adduct described in Chapter 2 as the measure of IPO bioactivation. Again, CYP1A2 exhibited the highest IPO activation rates among the enzymes examined. However,

this screen was conducted at 1 mM IPO substrate concentration, which greatly exceeds the maximum plasma concentration observed in the clinic (*5*), and so may not be representative of enzymatic activation of IPO at physiologically relevant doses.

The primary focus of this chapter is identify the enzyme(s) responsible for activating IPO in human liver microsomes under conditions that are more relevant to the physiological situation experienced by Phase II patients that experience liver toxicity with the investigational drug. Additionally, because compromised CYP4B1 activity may protect humans from pulmonary toxicity, we also assessed the functional implications of the S207 insertion with regard to IPO activation and cytotoxicity in an engineered cell line.

5.2 Experimental Procedures

Materials.

Human tissue microsomes were obtained from XenoTech LLC (Kansas City, KS). N-acetyl-cysteine, N-acetly-lysine, methanol, itraconazole, diethyldithiocarbamate, aminobenzotriazole and potassium phosphate were obtained from Sigma-Aldrich (St. Louis, MO). IPO was a gift from the National Cancer Institute (Bethesda, MD). Recombinant human P450 Supersomes were obtained from BD Gentest (Bedford, MA). HepG2 cells expressing various CYP4B1 constructs were a gift from Dr. Helmut Hannenberg at the University of Dusseldorf (Dusseldorf, Germany). Furafylline was obtained from Dr. Kent Kunze at the University of Washington (Seattle, WA). (+)-N-3-benzyl-nirvanol was

obtained as previously described (*14*). Human liver microsomes were purchased from XenoTech LLC (Kansas City, KS).

Bioactivation of IPO

In vitro bioactivation of IPO was assessed by incubating microsomal or recombinant enzyme preparations in triplicate with IPO, potassium phosphate buffer (100 mM pH 7.4), NADPH (1 mM), EDTA (1 mM), MgCl2 (3 mM) and NAC and NAL (20 mM each). All reactions were terminated by the addition of an equal volume of ice-cold methanol containing the internal standard furafylline and centrifuged for 10 min at 4000 rpm to remove protein. Activation rates were assessed by monitoring fragmentation of the NAC/NAL adduct according to the method described in Chapter 2.

The screen of recombinant enzymes was conducted at 50 μM IPO using 100 pmol/mL P450 at a final reaction volume of 500 μL. Incubations were allowed to proceed for 10 minutes at 37°C in a shaking water bath.

Kinetic analysis of IPO activation by recombinant P450 enzymes was conducted at 50 pmol/mL P450 at a final reaction volume of 200 μL with IPO concentrations ranging from 25 μM to 10 mM. Incubations were allowed to proceed for 15 minutes at 37°C in a shaking water bath. Kinetic parameters were determined using Prism graph software.

Chemical inhibition of IPO activation was performed in pooled human liver microsomal incubations at a protein concentration of 0.2 mg/mL and IPO concentration of

50 μM for 30 minutes at an incubation volume of 500 μL. All inhibitors were dissolved in DMSO and incubations were conducted at 0.5% organic. a, itraconazole 0.4 μM, (+)-N-3-benzyl-nirvanol 0.8 μM and diethyldithiocarbamate 20 μM. Incubations with furafylline and diethyldithiocarbamate included a 15 minute pre-incubation prior to addition of IPO.

Reaction phenotyping was performed using a reaction phenotyping kit (XenoTech) containing liver microsomes from 16 individuals previously characterized for activity towards a panel of diagnostic P450 substrates. Individual livers were selected to ensure the kit contained a broad range of enzymatic activities towards each substrate. Incubations were performed as described above with 0.1 mg microsomal protein in a 500 μL reaction volume for 30 minutes at 37°C. Statistical significance of the correlation of IPO activation with P450 activity was performed using a non-directional t-test on the Vassar University vassarstats.net.

Glucuronidation of IPO

In vitro glucuronidation of IPO was assessed according to the method described in Chapter 2.

HepG2 cells stably expressing different CYP4B1 isoforms were produced by Dr. Hanenberg's group as previously described (*15*). Briefly, PCR amplicons of rabbit *CYP4B1* and three human *CYP4B1* gene variants were cloned into the puc2CL6IN lentiviral vector using *Xho1* and *BamH1* cloning sites. HEK293T cells were transfected using polethyleneimine transfection reagent with 6 μg each of HIV1 helper plasmid pCD-NL-BH,

expression construct for HIV1 gag/pol/rev (*16*), envelope vector (pczVSV-G) (*17*), and the vector plasmid. Viral supernatants were harvested 48 hours post transfection, filtered through a 0.45 μm filter and used to transduce HepG2 cells. After 24 hours, transduced cells were selected with 1 mg/ml Genticin for 7-10 days and passaged >4 times before exposure to 29 μM IPO and assessment of resulting cell viability.

5.3 Results

The requirement of the meander region proline at amino acid position 427 for bioactivation of IPO by human CYP4B1 expressed in HepG2 cells is demonstrated in Figure 5.1. HepG2 cells overexpressing various human CYP4B1 variants were subjected to treatment with 29 μM IPO and assessed for cell survival (red line). Cell survival is contrasted to *in vitro* bioactivation of IPO by membranes harvested from the same cells (blue bars). The data demonstrate that IPO is not cytotoxic to HepG2 cells that express wild-type (S427) human CYP4B1 and membranes from these cells do not catalyze the bioactivation of IPO to the NAC/NAL adduct. However, reversion of the wild-type serine to the evolutionarily conserved proline encodes an active protein which can activate IPO both in cells (shown by cytotoxicity) and *in vitro* (shown by NAC/NAL adduct formation).

A screen of the available recombinant human P450 enzymes demonstrates that human CYP1A2 has the highest activity towards IPO bioactivation at the physiologically relevant concentration of 50 μM *in vitro* (Figure 5.2). These findings agree with the screen that was conducted earlier at 1 mM IPO by Baer and coworkers (*13*), and with previously

reported data which showed that, from a panel of HepG2 cells expressing various human P450 enzymes treated with radiolabeled IPO, cells which expressed CYP1A2 showed the highest level of IPO-DNA adducts (*12*).

Next, we performed a kinetic analysis of human liver microsomal bioactivation of IPO and compared the data to that obtained with recombinant enzymes identified as IPO activators in the Supersomes™ screen (Table 5.1). Human liver microsomal metabolism of IPO appeared to be a low-affinity, monophasic process with a Km of approximately 2 mM. Recombinant human CYP1A2, CYP2C19 and CYP2E1 were all a low-affinity enzymes for IPO with Km values similar to that of 1A2. CYP3A4 was the highest-affinity bioactivator of IPO, exhibiting both Km and Vmax values that were substantially lower than those of the other three enzymes. When considered in terms of catalytic efficiency, the rank order of IPO bioactivating human P450s was; CYP1A2 ~ CYP3A4 > CYP2C19 ~ CYP2E1.

A screen of chemical inhibitors that are diagnostic for specific human liver P450 isoforms indicated that no single enzyme is responsible for IPO activation in human liver microsomes (Figure 5.3). Inhibitors against CYP1A2 (furafylline), CYP2C19 (benzylnirvanol), CYP2D6 (quinidine), CYP2E1 (diethyldithiocarbamate) and CYP3A4 (itraconazole), used at double the IC_{50} concentrations, did not greatly reduce IPO bioactivation activity in human liver microsomes. Of the inhibitors tested, only furafylline significantly inhibited IPO activation, but only to the extent of a 25% reduction in rate.

Next, we performed a correlation analysis of IPO activation at high (1 mM) and low (50 μM) IPO concentration by comparing the rate of IPO activation in a panel of liver microsomes from 16 individual donors with the reaction rates for several diagnostic P450 substrates (Table 5.2). The panel was specifically chosen to incorporate a broad range of P450 activities for all the major hepatic enzymes, and IPO activation rates varied up to 25 fold between individuals. Both CYP1A2 (phenacetin-O-deethylation and ethoxyresorufin-O-dealkylation) and CYP3A4 (testosterone 6β-hydroxylation and midazolam 1'-hydroxylation) are represented by two different probes, but in neither case does IPO activation correlate well with enzyme activity. At both high and low IPO concentration, the enzyme with the highest correlation to IPO activation is CYP2E1, as measured by chlorzoxasone 6-hydroxylation. However, the R^2 in both cases is lower than 0.6 indicating a poor albeit statistically significant ($p < 0.05$) correlation.

To assess non-P450 mediated activation of IPO, the pan-P450 inhibitor aminobenzotriazole was used to eradicate P450 activity in human liver microsomes After pre-incubation with 2 mM ABT and NADPH, followed by washing, re-pelleting and re-suspending the microsomes, P450-inactivated (based on lack of a CO-binding spectrum) microsomes lost 75% of IPO activation (Figure 5.4). This indicates that IPO-activation is largely P450-mediated, however, there may exist a small (25%) non-P450 component to IPO-activation in human liver microsomes.

We have attributed much of the the species differences in organ toxicities of IPO toxicity to differences in P450-mediated biactivation, and we have also shown that liver

microsomes from nearly all animal species tested can form IPO-glucuronide at significant rates (Chapter 2). Human liver microsomes catalyzed formation of IPO-glucuronide at low, but detectable rates, when a substrate concentration of 1 mM IPO was used (Chapter 2). However, no detectable IPO-glucuronide was formed by human liver microsomes at 50 μM IPO.

5.4 Discussion

Human CYP4B1 has been shown to be inactive *in vitro (8)*, however, there has been some speculation that it may be active either *in vivo* or in whole cell systems (*9, 10*). In the current studies, we tested this in an engineered cell line which was shown to be highly sensitive to IPO cytotoxicity at relevant substrate concentrations. Based on the activity of the S427P mutant both in whole cells and cell membranes, we conclude that the meander proline is indeed essential for CYP4B1 activity. Furthermore, human CYP4B1 incorporating the insertion of a serine at amino acid position 207 did not salvage enzyme activity. The inability CYP4B1 containing the S207 insert to activate IPO in whole cells or *in vitro* indicates that the serine insert does not compensate for the inactivating S427 background. These data demonstrate conclusively that human wild-type CYP4B1 activity is severely compromised by the presence of the meander serine residue. This lack of enzyme activity in the lung is likely the basis for the protection against pulmonary toxicity in human lung and the lack of efficacy in using IPO as a therapeutic for pulmonary carcinoma.

As discussed above, there are abundant data in the literature suggesting that CYP1A2 is an important enzyme for IPO bioactivation in human liver, but no kinetic evaluation had been performed. In the current studies, we find that human CYP1A2-mediated bioactivation of IPO is a low affinity process (Km = 2.3 mM), but with the highest turnover number (~1/min). If human CYP1A2 is the dominant catalyst for the bioactivation of IPO, we would expect that furafylline would eliminate IPO activation *in vitro.* However, we found that no specific P450 inhibitor, including furafylline, eliminated IPO activation in human liver microsomes. Inhibition with furafylline resulted in only a 25% reduction of IPO activation in human liver microsomes. We conclude that CYP1A2 plays a significant role (~25-30%) in the activation of IPO in human liver at low substrate concentration, similar to the contribution of mouse CYP1A2 (Chapter 4).

CYP3A4 is a higher affinity activator of IPO than CYP1A2; however, its low Vmax may partially explain why itraconazole does not inhibit IPO activation in human liver microsomes. Furthermore IPO has recently been shown to be a mechanism-based inactivator of CYP3A4 (*18*). IPO-mediated destruction of CYP3A4 may explain our observation that IPO activation rates do not correlate with testosterone 6-β-hydroxylation or midazolam 1'-hydroxylation rates in human liver microsomes.

Because inhibitor studies and kinetic analysis of IPO did not clearly implicate any one P450 enzyme in the human liver bioactivation of IPO, we performed reaction phenotyping on a panel of human liver microsomes characterized for CYP activity in an attempt to is determine whether bioactivation of IPO correlated with enzyme activity of

any particular P450 enzyme, by this method. However, reaction phenotyping provided no indication that IPO activation rates correlated with CYP1A2 activity, although it did highlight a potential contribution by CYP2E1 in that there was a a significant correlation between IPO bioactivation and chlorzoxazone 6-hydroxylation as evidenced by an r^2 value of 0.58 ($p < 0.05$). CYP2E1 has recently been reported to catalyze furan bioactivation in human liver microsomes (*19*), so a role for this enzyme in IPO bioactivation is not unexpected. However, inhibition of CYP2E1 by diethyldithiocarbamate had no effect on IPO activation rates. Therefore, it appears neither CYP1A2, nor any one of the other four enzymes shown to activate IPO in the screen of recombinant enzymes, catalyzes the bulk of IPO activation.

IPO activation does not appear to be mediated by any single P450 enzyme and the lack of correlation with P450 isoform activity and lack of inhibition of activation by P450 inhibitors raises the possibility that IPO activation in human liver microsomes could be mediated, at least in part, by an NADPH-dependent non-P450 enzyme(s). Inactivation of total human liver microsomal P450 by ABT resulted in a 75% reduction of IPO activation. Therefore, we conclude that IPO is bioactivated in human liver by multiple P450 enzymes and that up to a quarter of ene-dial formation occurs *via* non-P450 mediated enzymatic activation.

In conclusion toxicity of a pro-toxin can be viewed as a balance between activation and elimination. If activation rates exceed elimination rates in a given tissue, the pro-toxin is likely to lead to toxicity. Unlike the phase II activity that we observed in multiple other

non-primate species, human liver microsomes do not readily glucuronidate IPO. Based on this observation it is reasonable to conclude that the hepatic toxicity seen in humans dosed with IPO is based, in part, on the lack of CYP4B1-mediated bioactivation in extra-hepatic tissues and in part, on the lack of phase II-mediated elimination of parent IPO by human liver.

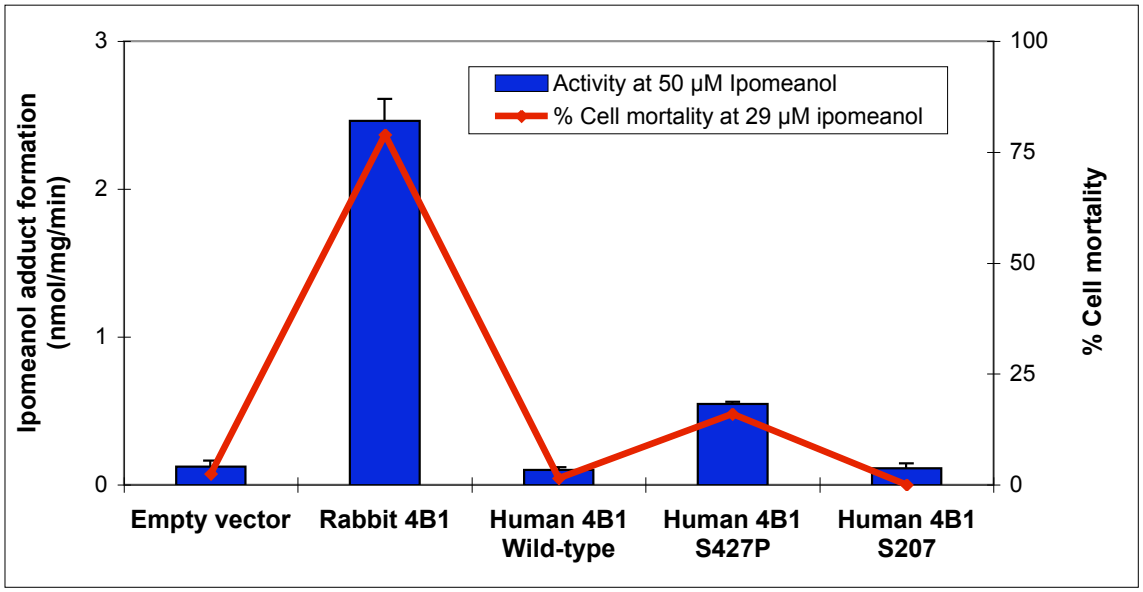

Figure 5.1: In vitro bioactivation of IPO (left axis, blue columns) by membranes from HepG2 cells overexpressing CYP4B1 and cytotoxicity in the presence of IPO (right column, red line). As expected, IPO is not toxic to cells expressing wild-type human CYP4B1, nor do membranes from these cells catalyze the bioactivation of IPO. However, when the meander serine is reverted to the evolutionarily conserved proline, IPO becomes cytotoxic and membranes from these cells bioactivate IPO in vitro. The S207 insertion variant does not 'rescue' loss of CYP4B1 enzyme activity due to the presence of S427.

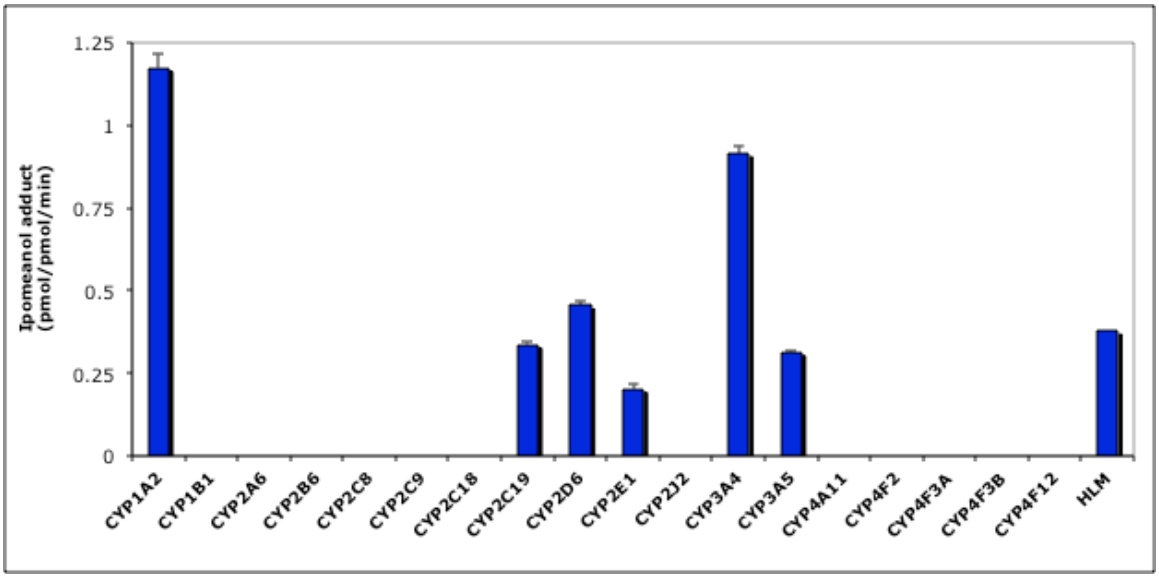

Figure 5.2: *In vitro* bioactivation of IPO (50 μM) by recombinant human liver P450 Supersomes™ and pooled human liver microsomes. 50 μM IPO is the relevant physiological concentration of IPO based on clinical trials of IPO as an anti-cancer therapy.

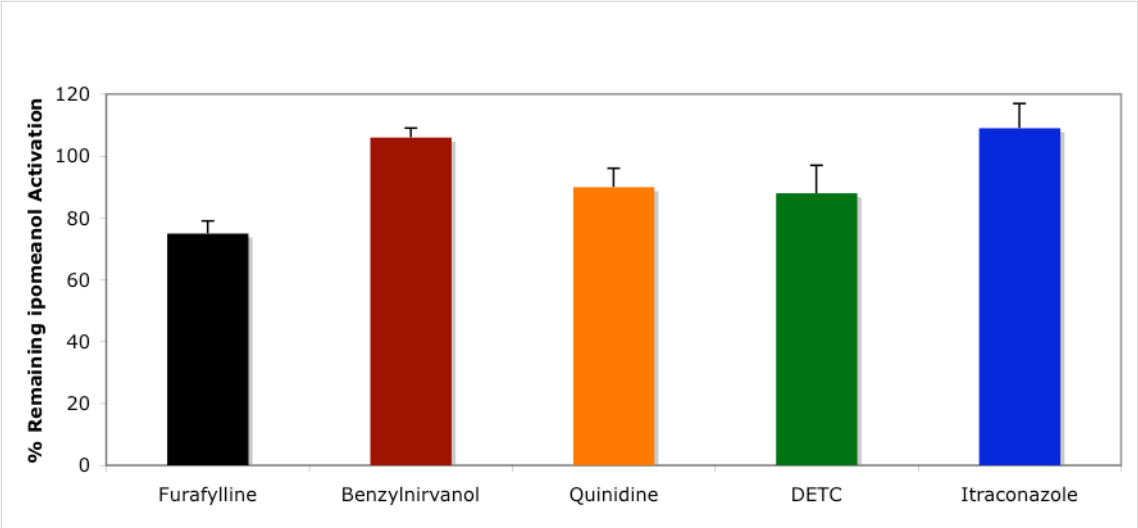

Figure 5.3: Inhibition of IPO (50 μM) bioactivation in pooled human liver microsomes by diagnostic P450 inhibitors (at 2x the IC_{50} concentration) towards the enzymes known to activate IPO *in vitro*. No enzyme-specific inhibitor eliminates IPO bioactivation in human liver microsomes which indicates that no single enzyme is primarily responsible for activating IPO. Furafylline (CYP1A2) has the greatest inhibitory effect on IPO activation, but only reduces bioactivation rates by ~25%.

Enzyme	Km (μM)	Vmax (nmol/pmol/min)	Vmax/Km
HLM	2313	245	0.106
CYP1A2	3000	820	0.273
CYP3A4	376.5	93.4	0.248
CYP2C19	2945	416	0.141
CYP2D6	ND	ND	ND
CYP2E1	3300	380	0.115

Table 5.1: Kinetic characterization of IPO bioactivation by human P450s and human liver microsomes (HLM). The presence of a high-affinity, low-capacity component catalyzed by CYP3A4 and a low-affinity, high-capacity component catalyzed by CYP1A2 indicate that the activation of IPO in human liver may be catalyzed by a minimum of two enzymes. Kinetic parameters for CYP2D6 were not determined because activation was not saturable.

Enzyme	Substrate	R^2 at 50 μM	R^2 at 1 mM
CYP2E1	Chlorzoxazone	0.5816	0.4909
CYP2C9	Diclofenac	0.4122	0.1893
CYP3A4	Midazolam	0.3424	0.3634
CYP2C8	Paclitaxel	0.3177	0.4608
CYP3A4	Testosterone	0.2303	0.2226
CYP1A2	Phenacetin	0.2184	0.2287
CYP4A11	Lauric Acid	0.1741	0.0254
CYP1A2	Ethoxyresorufin	0.1502	0.0986
CYP2B6	Bupropion	0.0404	0.1971
CPR	Cytochrome C	0.022	0.2072
CYP2A6	Coumarin	0.0096	0.0549
FMO	Benzydamine	0.009	0.0899
CYP2B6	Mephenytoin	0.0065	0.0065
CYP2D6	Dextromethorphan	0.0057	0.0635
CYP2C19	Mephenytoin	0.0003	0.161

Table 5.2: Correlation analysis of P450 activity with IPO bioactivation in a panel of human liver microsomes from 16 individuals at 50 μM and 1 mM IPO. There is significant correlation between IPO activation and CYP2E1 activity measured by chlorzoxazone-6-hydroxylation utilizing a non-directional student's t-test ($p < 0.05$).

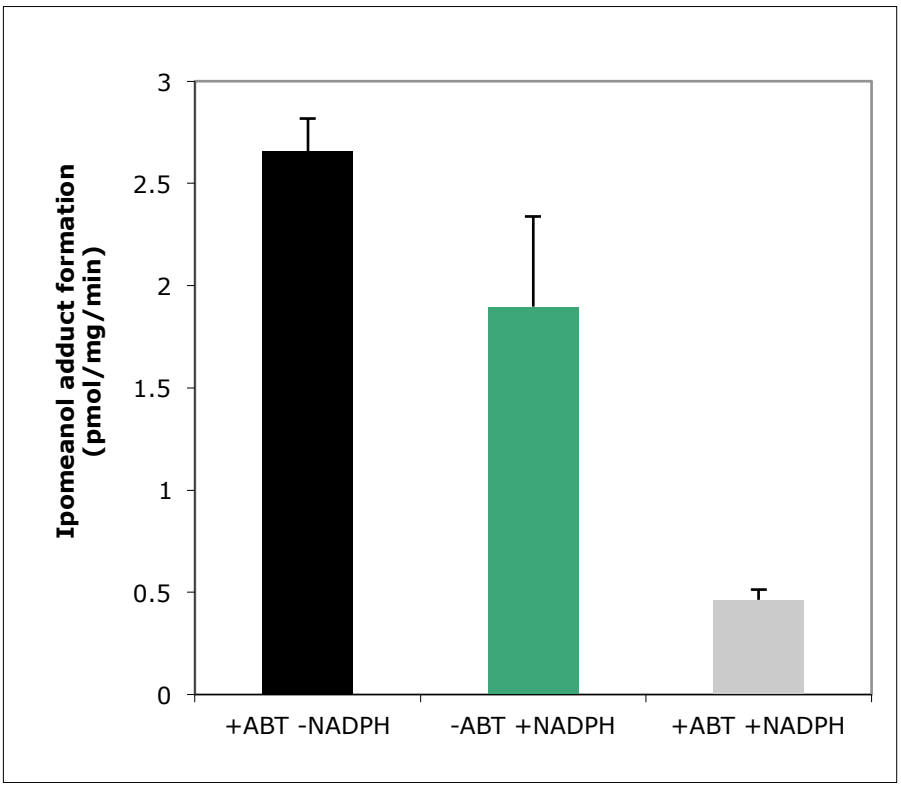

Figure 5.4: Inhibition of IPO activation by the pan-P450 inhibitor, ABT (2 mM). The ~75% inhibition of IPO adduct formation rate by ABT indicates that IPO activation is largely, but perhaps not exclusively, P450-mediated.

5.5 Notes to Chapter 5

1. Boyd, M. R. (1977) Evidence for the Clara cell as a site of cytochrome P450-dependent mixed-function oxidase activity in lung, *Nature 269*, 713-715.

2. Devereux, T. R., Jones, K. G., Bend, J. R., Fouts, J. R., Statham, C. N., and Boyd, M. R. (1982) in Vitro Metabolic Activation of the Pulmonary Toxin, 4-Ipomeanol, in Nonciliated Bronchiolar Epithelial (Clara) and Alveolar Type II Cells Isolated from Rabbit Lung, *The Journal of Pharmacology and Experimental Therapeutics 220*, 223-227.

3. McLemore, T. L., Litterst, C. L., Coudert, B. P., Liu, M. C., Hubbard, W. C., Adelberg, S., Czerwinski, M., McMahon, N. A., Eggleston, J. C., and Boyd, M. R. (1990) Metabolic activation of 4-ipomeanol in human lung, primary pulmonary carcinomas, and established human pulmonary carcinoma cell lines, *J Natl Cancer Inst 82*, 1420-1426.

4. Rowinsky, E. K., Noe, D. A., Ettinger, D. S., Christian, M. C., Lubejko, B. G., Fishman, E. K., Sartorius, S. E., Boyd, M. R., and Donehower, R. C. (1993) Phase I and pharmacological study of the pulmonary cytotoxin 4-ipomeanol on a single dose schedule in lung cancer patients: hepatotoxicity is dose limiting in humans, *Cancer Res 53*, 1794-1801.

5. Kasturi, V. K., Dearing, M. P., Piscitelli, S. C., Russell, E. K., Sladek, G. G., O'Neil, K., Turner, G. A., Morton, T. L., Christian, M. C., Johnson, B. E., and Kelley, M. J. (1998) Phase I study of a five-day dose schedule of 4-Ipomeanol in patients with non-small cell lung cancer, *Clin Cancer Res 4*, 2095-2102.

6. Lakhanpal, S., Donehower, R. C., and Rowinsky, E. K. (2001) Phase II study of 4-ipomeanol, a naturally occurring alkylating furan, in patients with advanced hepatocellular carcinoma, *Invest New Drugs 19*, 69-76.

7. Parkinson, O. T., Kelly, E. J., Bezabih, E., Whittington, D., and Rettie, A. E. (2011) Bioactivation of 4-Ipomeanol by a CYP4B enzyme in bovine lung and inhibition by HET0016, *J Vet Pharmacol Ther*.

8. Zheng, Y. M., Fisher, M. B., Yokotani, N., Fujii-Kuriyama, Y., and Rettie, A. E. (1998) Identification of a meander region proline residue critical for heme binding to cytochrome P450: implications for the catalytic function of human CYP4B1, *Biochemistry 37*, 12847-12851.

9. Imaoka, S., Yoneda, Y., Sugimoto, T., Hiroi, T., Yamamoto, K., Nakatani, T., and Funae, Y. (2000) CYP4B1 is a possible risk factor for bladder cancer in humans, *Biochem Biophys Res Commun 277*, 776-780.

10. Imaoka, S., Hayashi, K., Hiroi, T., Yabusaki, Y., Kamataki, T., and Funae, Y. (2001) A transgenic mouse expressing human CYP4B1 in the liver, *Biochem Biophys Res Commun 284*, 757-762.

11. Boyd, M. R., and Dutcher, J. S. (1981) Renal toxicity due to reactive metabolites formed in situ in the kidney: investigations with 4-ipomeanol in the mouse, *The Journal of Pharmacology and Experimental Therapeutics 216*, 640-646.

12. Czerwinski, M., McLemore, T. L., Philpot, R. M., Nhamburo, P. T., Korzekwa, K., Gelboin, H. V., and Gonzalez, F. J. (1991) Metabolic activation of 4-ipomeanol by complementary DNA-expressed human cytochromes P-450: evidence for species-specific metabolism, *Cancer Res 51*, 4636-4638.

13. Baer, B. R., Rettie, A. E., and Henne, K. R. (2004) Bioactivation of 4-Ipomeanol by CYP4B1: Adduct Characterization and Evidence for an Enedial Intermediate, *Chemical Research in Toxicology 18*, 855-864.

14. Suzuki, H., Kneller, M. B., Haining, R. L., Trager, W. F., and Rettie, A. E. (2002) (+)-N-3-Benzyl-nirvanol and (-)-N-3-benzyl-phenobarbital: new potent and selective in vitro inhibitors of CYP2C19, *Drug Metab Dispos 30*, 235-239.

15. Nakano, M., Kelly, E. J., Wiek, C., Hanenberg, H., and Rettie, A. E. (2012) CYP4V2 in Bietti's Crystalline Dystrophy: Ocular Localization, Metabolism of omega-3 Polyunsaturated Fatty Acids and Functional Deficit of the p.H331P Variant, *Mol Pharmacol*.

16. Mochizuki, H., Schwartz, J. P., Tanaka, K., Brady, R. O., and Reiser, J. (1998) High-titer human immunodeficiency virus type 1-based vector systems for gene delivery into nondividing cells, *J Virol 72*, 8873-8883.

17. Pietschmann, T., Heinkelein, M., Heldmann, M., Zentgraf, H., Rethwilm, A., and Lindemann, D. (1999) Foamy virus capsids require the cognate envelope protein for particle export, *J Virol 73*, 2613-2621.

18. Alvarez-Diez, T. M., and Zheng, J. (2004) Mechanism-based inactivation of cytochrome P450 3A4 by 4-ipomeanol, *Chemical Research in Toxicology 17*, 150-157.

19. Gates, L. A., Lu, D., and Peterson, L. A. (2012) Trapping of cis-2-butene-1,4-dial to measure furan metabolism in human liver microsomes by cytochrome P450 enzymes, *Drug Metab Dispos 40*, 596-601.

Chapter 6

General Conclusions and Future Directions

6.1 Conclusions

We have shown that CYP4B1 is responsible for the bioactivation of IPO in lung microsomes harvested from species (dog, rat, cow, rabbit and mouse) that are highly susceptible to IPO-induced pulmonary toxicity. *In vitro* activation was eliminated by co-incubation with a CYP4 chemical inhibitor or α-CYP4B1 antibody. Furthermore, both target organ toxicity and *in vitro* bioactivation correlated with tissue CYP4B1 content in rabbit, cow and mouse. We have also shown that liver microsomes from all experimental species examined produce IPO-glucuronide.

To probe the role of CYP4B1 in IPO toxicity *in vivo*, we have characterized *Cyp4b1* null mice (produced by Dr. Ed Kelly) with respect to P450 expression and IPO toxicity. *Cyp4b1* null mice did not exhibit an overt phenotype, and expression of other P450 enzymes was not up-regulated in response to disruption of the gene. Disruption of murine *Cyp4b1* was protective against IPO-induced lung and kidney toxicity. Wild-type mice treated with a single, LD_{50} dose of IPO (20 mg/kg) developed severe pulmonary edema (males and females) as well as nephrotic lesions (males). Histopathological analysis of tissues from *Cyp4b1* null mice treated with IPO (20 mg/kg) showed no signs of toxicity. Therefore, it is clear that CYP4B1 is responsible for catalyzing the bioactivation of IPO which leads to pneumo- and nephrotoxicity *in vivo* in the mouse.

In humans exposed to IPO, liver toxicity has been reported. We hypothesized that human hepatotoxicity might occur due to increased activity of human CYP1A2 towards IPO activation relative to the orthologous mouse enzyme. To this end we assessed IPO toxicity in wild-type, *Cyp1a* null and humanized CYP1A mice. Humanized mice did not experience liver toxicity when administered IPO; instead they developed pulmonary and renal toxicity (males) that was identical to the pattern of toxicity found in wild-type and *Cyp1a* null mice. We then attempted to determine if CYP1A2 was the primary mediator of IPO activation in human liver microsomes. However, bioactivation rates did not correlate well with any P450 enayme activity, including CYP1A2, and activation was not inhibited by any specific P450 inhibitor other than modestly by furafylline. Therefore we conclude that IPO activation in human liver is catalyzed primarily by P450 enzymes, but no single enzyme is responsible for the majority of the bioactivation. Therefore, the lack of pulmonary toxicity in humans is due to the absence of catalytically active CYP4B1 in human lung, as assessed both *in vitro* and *ex vivo*.

Lastly, we have shown that IPO is glucuronidated *in vivo* in the mouse and *in vitro* in cow, dog, rat, rabbit and mouse liver. However, IPO is not readily glucuronidated in the human liver (or in human lung, intestine or kidney). Therefore, we conclude that IPO glucuronidation is likely to be, at least partially, protective against IPO toxicity. This fits with the observations of liver toxicity due to IPO in humans - hepatic bioactivation in the absence of hepatic glucuronidation - and with the absence of liver toxicity in IPO-treated rabbits - relatively high levels of IPO bioactivation in rabbit liver microsomes coupled with

rapid glucuronidation rates. Taken together, the lack of IPO bioactivation in human lung and lack of IPO glucuronidation in human liver likely accounts for the species differences in liver versus lung toxicity observed between humans and experimental animals.

6.2 Future Directions

Although we have demonstrated that IPO is glucuronidated readily *in vitro* in dog, rat, cow, rabbit and mouse liver and *in vivo* in mice, we lack an IPO-glucuronide chemical standard for absolute quantification of this Phase II metabolite. Because mice excrete large amounts of IPO glucuronide in the urine, facile approaches to obtaining a chemical standard could be to purify IPO-glucuronide from IPO-treated mouse urine or use rabbit liver microsomes as a bioreactor from which to isolate sufficient material for NMR analysis (to confirm the identity of the metabolite) and use as a chemical standard to determine the rates of glucuronidation *in vitro* as well as the fraction of administered dose that is recovered in the urine from IPO-treated mice.

Due to IACUC regulations, the *in vivo* studies that were undertaken were limited to IPO doses of 20 mg/kg, the LD_{50} in mice. However, disruption of *Cyp4b1* is protective in mice, so we saw no signs of toxicity in the knockout animals. It would be worthwhile to establish an LD_{50} for IPO in *Cyp4b1* null mice to characterize the degree of protection, and to determine if, at higher IPO doses, the site of toxicity eventually shifts to the liver when CYP4B1-mediated pulmonary and renal bioactivation are eliminated.

With regard to the humanized CYP1A study, like *Cyp4b1* disruption, 3-MC treatment protected against pulmonary toxicity in IPO-treated mice. While the LD_{50} and site(s) of IPO-mediated toxicity are known in 3MC-induced mice, it would also be desirable to have information on these parameters for *Cyp1a* null and humanized CYP1A mice. Furthermore, the initial scope of the CYP1A transgenic mouse project included only female mice of the three genotypes, due to the simplicity of the single site of toxicity in female mice (lung) compared to two sites in male mice (lung and kidney), as well as difficulty in procuring sufficient numbers of animals of both sexes. To complete the study we would ideally extend it to include males and assess potential shifts in target organ toxicity in a setting that includes both nephrotoxicity and pneumotoxicity of IPO.

Due to the lack of active CYP4B1 in humans and the possibility that human IPO activation is catalyzed by CYP1A2, crossing the *Cyp4b1* null mice with humanized CYP1A mice may result in a mouse model that approximates human IPO activation. However these mice would be expected to eliminate IPO *via* glucuronidation, a pathway that is not present in humans, so this model may not result in hepatotoxicity similar to that observed in humans.

Finally, perilla ketone (PK) is a structural analog of IPO that (similar to IPO) is known to cause lethal interstitial pneumonia in cattle as well as preclinical test species. We have conducted initial *in vitro* studies towards determining the role of CYP4B1 in the bioactivation of PK, however, further studies are needed including PK toxicity in the *Cyp4b1*

null mice to determine if *Cyp4b1* disruption is protective from PK poisoning as it is for IPO, and to examine if PK undergoes phase II metabolism in mice.

Because agricultural IPO/PK poisoning is generally predictable, it may be reasonable to develop a CYP4B1 chemical inhibitor as a prophylactic treatment for cattle at times when IPO/PK poisoning risk is high. We have demonstrated in vitro that HET0016 is a potent inhibitor of CYP4B1 and eliminates IPO activation in bovine lung microsomes, however, it's utility as a CYP4B1 inhibitor *in vivo* is not known. Studies to determine if pre-treatment of mice with HET0016 is protective from IPO/PK toxicity, as well as to determine if HET0016 has any deleterious effects on mice which may preclude it from being used as a veterinary therapeutic are needed. This could be a useful future direction that might ultimately yield a drug therapy useful to the dairy and livestock industries.

List of References

(1992). "Toxicology and Carcinogenesis Studies of Naphthalene (CAS No. 91-20-3) in B6C3F1 Mice (Inhalation Studies)." National Toxicology Program technical report series **410**: 1-172.

(1993). "Toxicology and Carcinogenesis Studies of Furan (CAS No. 110-00-9) in F344 Rats and B6C3F1 Mice(Gavage Studies)." National Toxicology Program technical report series **402**: 1-286.

(2000). "Toxicology and carcinogenesis studies of naphthalene (cas no. 91-20-3) in F344/N rats (inhalation studies)." National Toxicology Program technical report series(500): 1-173.

(2002). "Furan." Report on carcinogens : carcinogen profiles / U.S. Dept. of Health and Human Services, Public Health Service, National Toxicology Program **10**: 130-131.

(2011). "Furan." Report on carcinogens : carcinogen profiles / U.S. Dept. of Health and Human Services, Public Health Service, National Toxicology Program **12**: 205-207.

Alvarez-Diez, T. M. and J. Zheng (2004). "Mechanism-based inactivation of cytochrome P450 3A4 by 4-ipomeanol." Chemical Research in Toxicology **17**(2): 150-157.

Arinc, E., I. Hanukoglu, et al. (1995). "Tissue- and Species- Dependent Expression of Sheep Lung Microsomal Cytochrome P4502B(LgM2)." Biochemistry and Molecular Biology International **37**(6): 1121-1126.

Armbrecht, B. H., F. A. Hodges, et al. (1963). "Mycotoxins. I. Studies on aflatoxin derived from contaminated peanut meal and certain strains of Aspergillus flavus." J. Assoc. Offic. Agr. Chemists **16**: 13.

Asao, T., G. Buechi, et al. (1965). "The Structures of Aflatoxins B and G." Journal of the American Chemical Society **87**: 882-886.

Baer, B. R., A. E. Rettie, et al. (2004). "Bioactivation of 4-Ipomeanol by CYP4B1: Adduct Characterization and Evidence for an Enedial Intermediate." Chemical Research in Toxicology **18**: 855-864.

Baldwin, R. M., W. T. Jewell, et al. (2004). "Comparison of pulmonary/nasal CYP2F expression levels in rodents and rhesus macaque." The Journal of Pharmacology and Experimental Therapeutics **309**(1): 127-136.

Baldwin, R. M., M. A. Shultz, et al. (2005). "Bioactivation of the pulmonary toxicants naphthalene and 1-nitronaphthalene by rat CYP2F4." The Journal of Pharmacology and Experimental Therapeutics **312**(2): 857-865.

Boyd, M. R. (1977). "Evidence for the Clara cell as a site of cytochrome P450-dependent mixed-function oxidase activity in lung." Nature **269**(5630): 713-715.

Boyd, M. R. and L. T. Burka (1978). "In vivo studies on the relationship between target organ alkylation and the pulmonary toxicity of a chemically reactive metabolite of 4-ipomeanol." The Journal of Pharmacology and Experimental Therapeutics **207**(3): 687-697.

Boyd, M. R., L. T. Burka, et al. (1978). "In vitro studies on the metabolic activation of the pulmonary toxin, 4-ipomeanol, by rat lung and liver microsomes." The Journal of Pharmacology and Experimental Therapeutics **207**(3): 677-686.

Boyd, M. R. and J. S. Dutcher (1981). "Renal toxicity due to reactive metabolites formed in situ in the kidney: investigations with 4-ipomeanol in the mouse." The Journal of Pharmacology and Experimental Therapeutics **216**(3): 640-646.

Boyd, M. R. and B. J. Wilson (1972). "Isolation and characterization of 4-ipomeanol, a lung-toxic furanoterpenoid produced by sweet potatoes (Ipomoea batatas)." Journal of agricultural and food chemistry **20**(2): 428-430.

Buckley, D. B. and C. D. Klaassen (2009). "Induction of mouse UDP-glucuronosyltransferase mRNA expression in liver and intestine by activators of aryl-hydrocarbon receptor, constitutive androstane receptor, pregnane X receptor, peroxisome proliferator-activated receptor alpha, and nuclear factor erythroid 2-related factor 2." Drug metabolism and disposition: the biological fate of chemicals **37**(4): 847-856.

Buckpitt, A. R. and M. R. Boyd (1978). "Xenobiotic metabolism in birds, species lacking pulmonary Clara cells." Pharmacologist **20**.

Buckpitt, A. R., C. N. Statham, et al. (1982). "In vivo studies on the target tissue metabolism, covalent binding, glutathione depletion, and toxicity of 4-ipomeanol in birds, species deficient in pulmonary enzymes for metabolic activation." Toxicology and Applied Pharmacology **65**(1): 38-52.

Burka, L. T., L. Kuhnert, et al. (1977). "Biogenesis of lung-toxic furans produced during microbial infection of sweet potatoes (Ipomoea batatas)." Journal of the American Chemical Society **99**(7): 2302-2305.

Burka, L. T., K. D. Washburn, et al. (1991). "Disposition of [14C]furan in the male F344 rat." Journal of toxicology and environmental health **34**(2): 245-257.

Burke, M. D., S. Thompson, et al. (1994). "Cytochrome P450 specificities of alkoxyresorufin O-dealkylation in human and rat liver." Biochemical pharmacology **48**(5): 923-936.

Byrns, M. C., D. P. Predecki, et al. (2002). "Characterization of nucleoside adducts of cis-2-butene-1,4-dial, a reactive metabolite of furan." Chemical Research in Toxicology **15**(3): 373-379.

Byrns, M. C., C. C. Vu, et al. (2006). "Detection of DNA adducts derived from the reactive metabolite of furan, cis-2-butene-1,4-dial." Chemical Research in Toxicology **19**(3): 414-420.

Byrns, M. C., C. C. Vu, et al. (2004). "The formation of substituted 1,N6-etheno-2'-deoxyadenosine and 1,N2-etheno-2'-deoxyguanosine adducts by cis-2-butene-1,4-dial, a reactive metabolite of furan." Chemical Research in Toxicology **17**(12): 1607-1613.

Chen, L. J., S. S. Hecht, et al. (1995). "Identification of cis-2-butene-1,4-dial as a microsomal metabolite of furan." Chemical Research in Toxicology **8**(7): 903-906.

Chen, L. J., S. S. Hecht, et al. (1997). "Characterization of amino acid and glutathione adducts of cis-2-butene-1,4-dial, a reactive metabolite of furan." Chemical Research in Toxicology **10**(8): 866-874.

Chen, Z. R., A. A. Somogyi, et al. (1991). "Disposition and metabolism of codeine after single and chronic doses in one poor and seven extensive metabolisers." British journal of clinical pharmacology **31**(4): 381-390.

Christian, M. C., R. E. Wittes, et al. (1989). "4-Ipomeanol: a novel investigational new drug for lung cancer." Journal of the National Cancer Institute **81**(15): 1133-1143.

Czerwinski, M., T. L. McLemore, et al. (1991). "Metabolic activation of 4-ipomeanol by complementary DNA-expressed human cytochromes P-450: evidence for species-specific metabolism." Cancer research **51**(17): 4636-4638.

Degawa, M., S. Miura, et al. (1990). "Androgen-dependent renal microsomal cytochrome P-450 responsible for N-hydroxylation and mutagenic activation of 3-methoxy-4-aminoazobenzene in the BALB/c mouse." Cancer research **50**(9): 2729-2733.

Degawa, N., S.-i. Miura, et al. (1990). "Androgen-dependent renal microsomal cytochrome P450 responsible for N-hydroxylation and mutagenic activation of 3-methoxy-4-aminoazobenzene in the BALB/c mouse." Cancer Research **50**: 5.

Degen, G. H. and H. G. Neumann (1981). "Differences in aflatoxin B1-susceptibility of rat and mouse are correlated with the capability in vitro to inactivate aflatoxin B1-epoxide." Carcinogenesis **2**(4): 299-306.

Desmeules, J., M. P. Gascon, et al. (1991). "Impact of environmental and genetic factors on codeine analgesia." European journal of clinical pharmacology **41**(1): 23-26.

Devereux, T. R., K. G. Jones, et al. (1982). "In vitro metabolic activation of the pulmonary toxin, 4-ipomeanol, in nonciliated bronchiolar epithelial (Clara) and alveolar type II cells isolated from rabbit lung." The Journal of Pharmacology and Experimental Therapeutics **220**(1): 223-227.

Doster, A. R., F. E. Mitchell, et al. (1978). "Effects of 4-ipomeanol, a product from mold-damaged sweet potatoes, on the bovine lung." Veterinary Pathology **15**(3): 367-375.

Dragin, N., S. Uno, et al. (2007). "Generation of 'humanized' hCYP1A1_1A2_Cyp1a1/1a2(-/-) mouse line." Biochemical and biophysical research communications **359**(3): 635-642.

Dutcher, J. S. and M. R. Boyd (1979). "Species and strain differences in target organ alkylation and toxicity by 4-ipomeanol. Predictive value of covalent binding in studies of target organ toxicities by reactive metabolites." Biochemical pharmacology **28**(23): 3367-3372.

Fahmy, M. J., O. G. Fahmy, et al. (1978). "Aflatoxin B1-2,3-dichloride as a model of the active metabolite of aflatoxin B1 in mutagenesis and carcinogenesis." Cancer research **38**(8): 2608-2616.

Falzon, M., J. B. McMahon, et al. (1986). "Metabolic activation and cytotoxicity of 4-ipomeanol in human non-small cell lung cancer lines." Cancer research **46**(7): 3484-3489.

Garst, J. E., W. C. Wilson, et al. (1985). "Species susceptibility to the pulmonary toxicity of 3-furyl isoamyl ketone (perilla ketone): in vivo support for involvement of the lung monooxygenase system." Journal of animal science **60**(1): 248-257.

Gasser, R. and R. M. Philpot (1989). "Primary structures of cytochrome P-450 isozyme 5 from rabbit and rat and regulation of species-dependent expression and induction in lung and liver: identification of cytochrome P-450 gene subfamily IVB." Molecular pharmacology **35**(5): 617-625.

Gates, L. A., D. Lu, et al. (2012). "Trapping of cis-2-butene-1,4-dial to measure furan metabolism in human liver microsomes by cytochrome P450 enzymes." Drug metabolism and disposition: the biological fate of chemicals **40**(3): 596-601.

Giantin, M., M. Carletti, et al. (2008). "Effect of breed upon cytochromes P450 and phase II enzyme expression in cattle liver." Drug metabolism and disposition: the biological fate of chemicals **36**(5): 885-893.

Guengerich, F. P. (1994). Analysis and Characterization of Enzymes. Principles and Methods of Toxicology. A. W. Hayes. New York, Raven Press**:** 1259-1313.

Hansen, A. A. (1925). "Two Fatal Cases of Potato Poisoning." Science **61**(1578): 340-341.

Hansen, A. A. (1928). "Potato poisoning." N. Am. Vet. **9**: 4.

Heppner, C. W. and J. R. Schlatter (2007). "Data requirements for risk assessment of furan in food." Food additives and contaminants **24 Suppl 1**: 114-121.

Hiura, M. (1943). "Studies on storage and rot of sweet potato." Rep. Gifu Agric. Coll. **50**: 5.

Hukkanen, J., O. Pelkonen, et al. (2002). "Expression and regulation of xenobiotic-metabolizing cytochrome P450 (CYP) enzymes in human lung." Critical reviews in toxicology **32**(5): 391-411.

Imaoka, S., K. Hayashi, et al. (2001). "A transgenic mouse expressing human CYP4B1 in the liver." Biochemical and biophysical research communications **284**(3): 757-762.

Imaoka, S., T. Hiroi, et al. (1995). "Mutagenic activation of 3-methoxy-4-aminoazobenzene by mouse renal cytochrome P450 CYP4B1: Cloning and characterization of mouse CYP4B1." Archives of Biochemistry and Biophysics **321**(1): 8.

Imaoka, S., Y. Yoneda, et al. (2000). "CYP4B1 is a possible risk factor for bladder cancer in humans." Biochemical and biophysical research communications **277**(3): 776-780.

Ingelman-Sundberg, M. (2005). "Genetic polymorphisms of cytochrome P450 2D6 (CYP2D6): clinical consequences, evolutionary aspects and functional diversity." The pharmacogenomics journal **5**(1): 6-13.

Isern, J. and A. Meseguer (2003). "Hormonal regulation and characterisation of the mouse Cyp4b1 gene 5'-flanking region." Biochemical and biophysical research communications **307**(1): 139-147.

Kasturi, V. K., M. P. Dearing, et al. (1998). "Phase I study of a five-day dose schedule of 4-Ipomeanol in patients with non-small cell lung cancer." Clinical cancer research : an official journal of the American Association for Cancer Research **4**(9): 2095-2102.

Kimura, S., M. Kawabe, et al. (1999). "CYP1A2 is not the primary enzyme responsible for 4-aminobiphenyl-induced hepatocarcinogenesis in mice." Carcinogenesis **20**(9): 6.

Kirchheiner, J., H. Schmidt, et al. (2007). "Pharmacokinetics of codeine and its metabolite morphine in ultra-rapid metabolizers due to CYP2D6 duplication." The pharmacogenomics journal **7**(4): 257-265.

Kohle, C. and K. W. Bock (2007). "Coordinate regulation of Phase I and II xenobiotic metabolisms by the Ah recepter and Nrf2." Biochemical pharmacology **73**: 10.

Kubota, M. and T. Matsuura (1952). J. Chem. Soc. Japan **74**.

Lakhanpal, S., R. C. Donehower, et al. (2001). "Phase II study of 4-ipomeanol, a naturally occurring alkylating furan, in patients with advanced hepatocellular carcinoma." Investigational new drugs **19**(1): 69-76.

Lancaster, M. C., F. P. Jenkins, et al. (1961). "Toxicity associated with Certain Samples of Groundnuts." Nature **192**(4807): 1095-1096.

Martin, C. N. and R. C. Garner (1977). "Aflatoxin B -oxide generated by chemical or enzymic oxidation of aflatoxin B1 causes guanine substitution in nucleic acids." Nature **267**(5614): 863-865.

McLemore, T. L., C. L. Litterst, et al. (1990). "Metabolic activation of 4-ipomeanol in human lung, primary pulmonary carcinomas, and established human pulmonary carcinoma cell lines." Journal of the National Cancer Institute **82**(17): 1420-1426.

Meijer, J. and J. W. DePierre (1987). "Hepatic levels of cytosolic, microsomal and 'mitochondrial' epoxide hydrolases and other drug-metabolizing enzymes after treatment of mice with various xenobiotics and endogenous compounds." Chemico-biological interactions **62**(3): 249-269.

Miyata, N., K. Taniguchi, et al. (2001). "HET0016, a Potent and Selective Inhibitor of 20-HETE Synthesizing Enzyme." British Journal of Pharmacology **133**(3): 325-329.

Mochizuki, H., J. P. Schwartz, et al. (1998). "High-titer human immunodeficiency virus type 1-based vector systems for gene delivery into nondividing cells." Journal of virology **72**(11): 8873-8883.

Monlux, W., J. Fitte, et al. (1953). "Progressive Pulmonary Adenomatosis in Cattle." The Southwestern Veterinarian **6**.

Monroe, D. H. and D. L. Eaton (1988). "Effects of modulation of hepatic glutathione on biotransformation and covalent binding of aflatoxin B1 to DNA in the mouse." Toxicology and Applied Pharmacology **94**(1): 118-127.

Morehouse, K. M., P. J. Nyman, et al. (2008). "Survey of furan in heat processed foods by headspace gas chromatography/mass spectrometry and estimated adult exposure." Food additives & contaminants. Part A, Chemistry, analysis, control, exposure & risk assessment **25**(3): 259-264.

Nakano, M., E. J. Kelly, et al. (2009). "Expression and characterization of CYP4V2 as a fatty acid omega-hydroxylase." Drug metabolism and disposition: the biological fate of chemicals **37**(11): 2119-2122.

Nakano, M., E. J. Kelly, et al. (2012). "CYP4V2 in Bietti's Crystalline Dystrophy: Ocular Localization, Metabolism of omega-3 Polyunsaturated Fatty Acids and Functional Deficit of the p.H331P Variant." Molecular pharmacology.

Nebert, D. W., A. L. Roe, et al. (2000). "Role of the aromatic hydrocarbon receptor and [Ah] gene battery in the oxidative stress response, cell cycle control, and apoptosis." Biochemical pharmacology **39**: 23.

Newberne, P. M. and G. N. Wogan (1968). "Sequential morphologic changes in aflatoxin B carcinogenesis in the rat." Cancer research **28**(4): 770-781.

Nichols, W. K., R. Mehta, et al. (2003). "3-methylindole-induced toxicity to human bronchial epithelial cell lines." Toxicological sciences : an official journal of the Society of Toxicology **71**(2): 229-236.

O'Brien, K., E. Moss, et al. (1983). "Metabolic basis of the species difference to aflatoxin B1 induced hepatotoxicity." Biochemical and biophysical research communications **114**(2): 813-821.

Parandoosh, Z., V. S. Fujita, et al. (1987). "Cytochrome P-450 isozymes 2 and 5 in rabbit lung and liver. Comparisons of structure and inducibility." Drug metabolism and disposition: the biological fate of chemicals **15**(1): 59-67.

Parkinson, O. T., E. J. Kelly, et al. (2011). "Bioactivation of 4-Ipomeanol by a CYP4B enzyme in bovine lung and inhibition by HET0016." Journal of veterinary pharmacology and therapeutics.

Peterson, L. A., K. C. Naruko, et al. (2000). "A reactive metabolite of furan, cis-2-butene-1,4-dial, is mutagenic in the Ames assay." Chemical Research in Toxicology **13**(7): 531-534.

Pietschmann, T., M. Heinkelein, et al. (1999). "Foamy virus capsids require the cognate envelope protein for particle export." Journal of virology **73**(4): 2613-2621.

Ramsdell, H. S. and D. L. Eaton (1990). "Species susceptibility to aflatoxin B1 carcinogenesis: comparative kinetics of microsomal biotransformation." Cancer research **50**(3): 615-620.

Regal, K. A., G. M. Laws, et al. (2001). "Detection and characterization of DNA adducts of 3-methylindole." Chemical Research in Toxicology **14**(8): 1014-1024.

Rettie, A. E., P. R. Sheffels, et al. (1995). "CYP4 Isozyme Specificiy and the Relationship between w-Hydroxylation and Terminal Desaturation of Valproic Acid." Biochemistry **34**: 7889-7895.

Robertson, I. G., C. Serabjit-Singh, et al. (1983). "The relationship between increases in the hepatic content of cytochrome P-450, form 5, and in the metabolism of aromatic amines to mutagenic products following treatment of rabbits with phenobarbital." Molecular pharmacology **24**(1): 156-162.

Roebuck, B. D. and G. N. Wogan (1977). "Species comparison of in vitro metabolism of aflatoxin B1." Cancer research **37**(6): 1649-1656.

Rowinsky, E., D. Noe, et al. (1993). "Phase I and pharmacological stuy of the pulmonary cytotoxin 4-ipomeanol on a single dose schedule in lung cancer patients: Hepatotoxicity is dose limiting in humans." Cancer Research **53**: 8.

Rowinsky, E. K., D. A. Noe, et al. (1993). "Phase I and pharmacological study of the pulmonary cytotoxin 4-ipomeanol on a single dose schedule in lung cancer patients: hepatotoxicity is dose limiting in humans." Cancer research **53**(8): 1794-1801.

Sabbioni, G., P. L. Skipper, et al. (1987). "Isolation and characterization of the major serum albumin adduct formed by aflatoxin B1 in vivo in rats." Carcinogenesis **8**(6): 819-824.

Seki, T., M. H. Wang, et al. (2005). "Cytochrome P450 4A isoform inhibitory profile of N-hydroxy-N'-(4-butyl-2-methylphenyl)-formamidine (HET0016), a selective inhibitor of 20-HETE synthesis." Biological & pharmaceutical bulletin **28**(9): 1651-1654.

Serabjit-Singh, C. S., C. R. Wolf, et al. (1979). "The Rabbit Pulmonary Monooxygenase System." The Journal of Biological Chemistry **254**(19): 9901-9907.

Slaughter, S. R., C. N. Statham, et al. (1983). "Covalent binding of metabolites of 4-ipomeanol to rabbit pulmonary and hepatic microsomal proteins and to the enzymes of the pulmonary cytochrome P-450-dependent monooxygenase system." The Journal of Pharmacology and Experimental Therapeutics **224**(1): 252-257.

Spoto, C. (2011). Moldy Sweet Potatoes Caused 200 Steer Deaths. Wausau Daily Herald. Wausau Wisconsin.

Statham, C. N. and M. R. Boyd (1982). "Effects of phenobarbital and 3-methylcholanthrene on the in vivo distribution, metabolism and covalent binding of 4-ipomeanol in the rat; implications for target organ toxicity." Biochemical pharmacology **31**(24): 3973-3977.

Statham, C. N., J. S. Dutcher, et al. (1982). "Ipomeanol 4-glucuronide, a major urinary metabolite of 4-ipomeanol in the rat." Drug metabolism and disposition: the biological fate of chemicals **10**(3): 264-267.

Steckel, L. and N. Rhodes (2007). Perilla Mint. University of Tennessee Agricultural Extension Publication w135.

Suzuki, H., M. B. Kneller, et al. (2002). "(+)-N-3-Benzyl-nirvanol and (-)-N-3-benzyl-phenobarbital: new potent and selective in vitro inhibitors of CYP2C19." Drug metabolism and disposition: the biological fate of chemicals **30**(3): 235-239.

Swenson, D. H., J. K. Lin, et al. (1977). "Aflatoxin B1-2,3-oxide as a probable intermediate in the covalent binding of aflatoxins B1 and B2 to rat liver DNA and ribosomal RNA in vivo." Cancer research **37**(1): 172-181.

Vanderslice, R. R., B. A. Domin, et al. (1987). "Species-dependent expression and induction of homologues of rabbit cytochrome P-450 isozyme 5 in liver and lung." Molecular pharmacology **31**(4): 320-325.

Verschoyle, R. D., R. M. Philpot, et al. (1993). "CYP4B1 Activates 4-Ipomeanol in Rat Lung." Toxicology and Applied Pharmacology **123**: 193-198.

Wang, M. Z., J. Y. Saulter, et al. (2006). "CYP4F enzymes are the major enzymes in human liver microsomes that catalyze the O-demethylation of the antiparasitic prodrug DB289 [2,5-bis(4-amidinophenyl)furan-bis-O-methylamidoxime]." Drug metabolism and disposition: the biological fate of chemicals **34**(12): 1985-1994.

Weems, J. M., N. S. Cutler, et al. (2009). "3-Methylindole is mutagenic and a possible pulmonary carcinogen." Toxicological sciences : an official journal of the Society of Toxicology **112**(1): 59-67.

Weems, J. M., J. G. Lamb, et al. (2010). "Potent mutagenicity of 3-methylindole requires pulmonary cytochrome P450-mediated bioactivation: a comparison to the prototype cigarette smoke mutagens B(a)P and NNK." Chemical Research in Toxicology **23**(11): 1682-1690.

Wilson, B. J., M. R. Boyd, et al. (1971). "A lung oedema factor from mouldy sweet potatoes (Ipomoea batatas)." Nature **231**(5297): 52-53.

Wilson, B. J. and L. T. Burka (1979). "Toxicity of novel sequiterpenoids from the stressed sweet potato (Ipomoea batatas)." Food and cosmetics toxicology **17**(4): 353-355.

Wilson, B. J., D. T. Yang, et al. (1970). "Toxicity of mould-damaged sweet potatoes (Ipomoea batatas)." Nature **227**(5257): 521-522.

Wogan, G. N. and P. M. Newberne (1967). "Dose-response characteristics of aflatoxin B1 carcinogenesis in the rat." Cancer research **27**(12): 2370-2376.

Wolf, C. R., C. N. Statham, et al. (1982). "The relationship between the catalytic activities of rabbit pulmonary cytochrome P-450 isozymes and the lung-specific toxicity of the furan derivative, 4-ipomeanol." Molecular pharmacology **22**(3): 738-744.

Yeager, R. L., S. A. Reisman, et al. (2009). "Introducing the "TCDD-inducible AhR-Nrf2 gene battery"." Toxicological sciences : an official journal of the Society of Toxicology **111**(2): 238-246.

Yue, Q. Y., J. Hasselstrom, et al. (1991). "Pharmacokinetics of codeine and its metabolites in Caucasian healthy volunteers: comparisons between extensive and poor hydroxylators of debrisoquine." British journal of clinical pharmacology **31**(6): 635-642.

Yue, Q. Y., J. O. Svensson, et al. (1991). "A comparison of the pharmacokinetics of codeine and its metabolites in healthy Chinese and Caucasian extensive hydroxylators of debrisoquine." British journal of clinical pharmacology **31**(6): 643-647.

Zheng, Y. M., M. B. Fisher, et al. (1998). "Identification of a meander region proline residue critical for heme binding to cytochrome P450: implications for the catalytic function of human CYP4B1." Biochemistry **37**(37): 12847-12851.

Zheng, Y. M., K. R. Henne, et al. (2003). "Genotyping and site-directed mutagenesis of a cytochrome P450 meander Pro-X-Arg motif critical to CYP4B1 catalysis." Toxicology and Applied Pharmacology **186**(2): 119-126.

Zhou, X., J. D'Agostino, et al. (2012). "Respective roles of CYP2A5 and CYP2F2 in the bioactivation of 3-methylindole in mouse olfactory mucosa and lung: studies using Cyp2a5-null and Cyp2f2-null mouse models." Drug metabolism and disposition: the biological fate of chemicals **40**(4): 642-647.

Vita

Oliver Thomas Parkinson was born on December 18, 1980 to Andrew and Kay Parkinson. He graduated from Shawnee Mission East High School in 1998 after which he enrolled at the University of Kansas where he earned a Bachelor of Science degree in Biochemistry in December of 2002. After graduation he spent a year working in Dr. Elizabeth Gillam's lab at the University of Queensland, where he developed his predisposition for catastrophic knee failure. He returned to the United States to work in the research and development department at XenoTech. In September 2005, he enrolled in the graduate program of Medicinal Chemistry at the University of Washington. During his enrollment, he followed the traditional path from rugby to science to circus, where he founded Duo Idiotica, a highly acclaimed duo trapeze act. He is also the reigning Sudden Impact light heavyweight mixed martial arts champion. Oliver received the Doctor of Philosophy degree in Medicinal Chemistry in the summer of 2012.